

# NAVAL POSTGRADUATE SCHOOL MONTEREY, CALIFORNIA



## THESIS

A COMPARISON OF DDS AND DRFM  
TECHNIQUES IN THE GENERATION OF  
"SMART NOISE" JAMMING WAVEFORMS

by

Charles Joffery Watson

September 1996

Co- Advisors:

Phillip E. Pace  
D. Curtis Schleher

Thesis  
W23575

Approved for public release; distribution is unlimited.

DUDLEY KNOX LIBRARY  
NAVAL POSTGRADUATE SCHOOL  
MONTEREY CA 93943-5101

REPORT DOCUMENTATION PAGE			Form Approved OMB No. 0704-0188
Public reporting burden for this collection of information is estimated to average 1 hour per response, including the time for reviewing instruction, searching existing data sources, gathering and maintaining the data needed, and completing and reviewing the collection of information. Send comments regarding this burden estimate or any other aspect of this collection of information, including suggestions for reducing this burden, to Washington Headquarters Services, Directorate for Information Operations and Reports, 1215 Jefferson Davis Highway, Suite 1204, Arlington, VA 22202-4302, and to the Office of Management and Budget, Paperwork Reduction Project (0704-0188) Washington DC 20503.			
1. AGENCY USE ONLY (Leave blank)	2. REPORT DATE September 1996	3. REPORT TYPE AND DATES COVERED Master's Thesis	
4. TITLE AND SUBTITLE <b>A COMPARISON OF DDS AND DRFM TECHNIQUES IN THE GENERATION OF "SMART NOISE" JAMMING WAVEFORMS</b>		5. FUNDING NUMBERS	
6. AUTHOR(S) Watson, Charles J.			
7. PERFORMING ORGANIZATION NAME(S) AND ADDRESS(ES) Naval Postgraduate School Monterey CA 93943-5000		8. PERFORMING ORGANIZATION REPORT NUMBER	
9. SPONSORING/MONITORING AGENCY NAME(S) AND ADDRESS(ES)		10. SPONSORING/MONITORING AGENCY REPORT NUMBER	
11. SUPPLEMENTARY NOTES The views expressed in this thesis are those of the author and do not reflect the official policy or position of the Department of Defense or the U.S. Government.			
12a. DISTRIBUTION/AVAILABILITY STATEMENT Approved for public release; distribution is unlimited.		12b. DISTRIBUTION CODE	
13. ABSTRACT (maximum 200 words) This thesis presents a comparison of the effectiveness of "smart noise" jamming waveforms against advanced threat radars, which are generated using either Direct Digital Synthesis (DDS) or Digital RF Memory (DRFM) based support jamming. The challenge lies in the fact the modern radar employs advanced waveforms, ultra-low sidelobe antennas, coherent sidelobe cancelers, and sidelobe blankers to inhibit signals entering through its sidelobes. This thesis compares the effectiveness of using DDS versus DRFM techniques to meet this challenge. In particular, the effect of mismatched frequency on the DDS jamming waveform is described, as is the effect of quantization and multi-signal storage in the DRFM. A quantitative comparison of these jamming techniques against the AN/TPS-70 surveillance radar is made.			
14. SUBJECT TERMS DDS, DRFM, Digital RF Memory, Direct Digital Synthesis		15. NUMBER OF PAGES 150	
		16. PRICE CODE	
17. SECURITY CLASSIFICATION OF REPORT Unclassified	18. SECURITY CLASSIFICATION OF THIS PAGE Unclassified	19. SECURITY CLASSIFICATION OF ABSTRACT Unclassified	20. LIMITATION OF ABSTRACT UL



**Approved for public release; distribution is unlimited.**

**A COMPARISON OF DDS AND DRFM TECHNIQUES IN THE  
GENERATION OF "SMART NOISE" JAMMING WAVEFORMS**

Charles Joffery Watson  
Captain, United States Army  
B.S., University of Pittsburgh, 1988

Submitted in partial fulfillment  
of the requirements for the degree of

**MASTER OF SCIENCE IN SYSTEMS ENGINEERING**

from the

**NAVAL POSTGRADUATE SCHOOL**

**September 1996**



## ABSTRACT

This thesis presents a comparison of the effectiveness of "smart noise" jamming waveforms against advanced threat radars, which are generated using either Direct Digital Synthesis (DDS) or Digital RF Memory (DRFM) based support jamming. The challenge lies in the fact the modern radar employs advanced waveforms, ultra-low sidelobe antennas, coherent sidelobe cancelers, and sidelobe blankers to inhibit signals entering through its sidelobes. This thesis compares the effectiveness of using DDS versus DRFM techniques to meet this challenge. In particular, the effect of mismatched frequency on the DDS jamming waveform is described, as is the effect of quantization and multi-signal storage in the DRFM. A quantitative comparison of these jamming techniques against the AN/TPS-70 surveillance radar is made.



## TABLE OF CONTENTS

I.	INTRODUCTION .....	1
	A. BACKGROUND .....	1
	B. THESIS PROBLEM .....	2
	C. PRINCIPAL CONTRIBUTIONS .....	3
	D. THESIS OUTLINE .....	4
II.	MODERN RADAR SYSTEMS: TARGETS FOR "SMART NOISE" JAMMING .....	5
	A. INTRODUCTION .....	5
	B. MODERN RADAR SYSTEM TECHNOLOGY .....	5
	1. Design Features .....	5
	2. Stand-Off Jamming Considerations .....	10
	C. AN/TPS-70 SYSTEM DESCRIPTION .....	12
	D. SUMMARY .....	18
III.	THE TECHNIQUE OF DIRECT DIGITAL SYNTHESIS .....	19
	A. INTRODUCTION .....	19
	B. DDS THEORY AND TECHNIQUE .....	20
	1. Theory and Objective .....	20
	2. Technique .....	30

C.	ANALYSIS OF RADAR SIGNAL SYNTHESIS METHODS .....	36
1.	Biphase Coding .....	37
2.	Doppler Effects .....	40
3.	Quadrphase Coding .....	42
4.	Summary .....	50
D.	OBSERVATIONS AND EVALUATIONS .....	50
1.	Biphase Coded Results .....	51
2.	Biphase Code Observations .....	64
3.	Quadrphase Code Results .....	65
4.	Quadrphase Code Observations .....	65
E.	SUMMARY .....	68
IV.	THE DIGITAL RF MEMORY TECHNIQUE .....	69
A.	INTRODUCTION .....	69
B.	THEORY AND OBJECTIVE .....	70
1.	Theory .....	70
2.	The DRFM Technique .....	76
C.	OBSERVATIONS AND EVALUATIONS .....	85
1.	Spurious Responses Due to Quantization Effects .....	86
2.	Spurious Responses Due to Intermodulation Effects .....	88

3.	Test Evaluation .....	92
D.	DRFM SPUR REDUCTION DEVELOPMENTS .....	103
1.	1-Bit DRFM Spur Reduction .....	103
2.	The GaAs-Based DRFM .....	104
3.	The Superconducting DRFM (S-DRFM) .....	106
E.	SUMMARY .....	109
V.	COMPARATIVE ANALYSIS .....	111
A.	INTRODUCTION .....	111
B.	SMARTER RADARS .....	111
C.	SMARTER JAMMERS .....	113
1.	The Digital Advantage .....	113
2.	Spurious Response Performance .....	114
3.	Synthesis Versus Memory .....	116
4.	DEAs Versus Sidelobe EPs .....	119
5.	Systems Engineering Considerations .....	119
D.	SUMMARY .....	121
VI.	CONCLUSION .....	123
	APPENDIX A. PCMISS PROGRAM .....	125
	APPENDIX B. QUADRIPHASE PROGRAM .....	127
	APPENDIX C. DRFMBITS PROGRAM .....	131

LIST OF REFERENCES ..... 135

INITIAL DISTRIBUTION LIST ..... 137

## LIST OF FIGURES

Figure 2.1.	AN/TPS-70 Tactical Radar [Ref. 7] .....	13
Figure 2.2.	Summary of AN/TPS-70 Performance Characteristics .....	17
Figure 3.1.	Digital Open-loop Adaptive Processor [Ref. 9] .....	25
Figure 3.2.	CSLC Radar and Auxiliary Receiving Systems [Ref. 9] .....	26
Figure 3.3.	Simple Sidelobe Blanker [Ref. 15] .....	29
Figure 3.4.	Direct Digital Synthesizer [Ref. 20] .....	31
Figure 3.5.	DDS With Phase and Frequency Modulation [Ref. 20] .....	31
Figure 3.6.	Uncompressed Transmit Pulse Signal Modulation .....	47
Figure 3.7.	Biphase Coded PC, $f_d/BW=0.0$ .....	52
Figure 3.8.	Biphase Coded PC, $f_d/BW=0.01$ .....	53
Figure 3.9.	Biphase Coded PC, $f_d/BW=0.02$ .....	54
Figure 3.10.	Biphase Coded PC, $f_d/BW=0.03$ .....	55
Figure 3.11.	Biphase Coded PC, $f_d/BW=0.04$ .....	56
Figure 3.12.	Biphase Coded PC, $f_d/BW=0.05$ .....	57
Figure 3.13.	Biphase Coded PC, $f_d/BW=0.06$ .....	58
Figure 3.14.	Biphase Coded PC, $f_d/BW=0.07$ .....	59
Figure 3.15.	Biphase Coded PC, $f_d/BW=0.08$ .....	60
Figure 3.16.	Biphase Coded PC, $f_d/BW=0.09$ .....	61

Figure 3.17.	Biphase Coded PC, $f_d/BW=0.10$ .....	62
Figure 3.18.	Biphase Coded Frequency Mismatch .....	63
Figure 3.19.	Compressed Pulse Response (a) .....	66
Figure 3.20.	Compressed Pulse Response (b) .....	67
Figure 4.1.	Digital RF Memory [Ref. 14] .....	77
Figure 4.2.	I/Q Circuit [Ref. 9] .....	79
Figure 4.3.	Table: Required Bits Per Sample .....	88
Figure 4.4.	Delay Flip-Flop [Ref. 23] .....	91
Figure 4.5a.	DRFM Frequency Spectrum .....	93
Figure 4.5b.	DRFM Frequency Spectrum .....	94
Figure 4.6a.	DRFM Frequency Spectrum .....	95
Figure 4.6b.	DRFM Frequency Spectrum .....	96
Figure 4.7a.	DRFM Frequency Spectrum .....	97
Figure 4.7b.	DRFM Frequency Spectrum .....	98
Figure 4.8a.	DRFM Frequency Spectrum .....	99
Figure 4.8b.	DRFM Frequency Spectrum .....	100
Figure 4.9.	DRFM Multiple-Signal Efficiency .....	101
Figure 4.10.	Simplified PDLE [Ref. 18] .....	104

# **I. INTRODUCTION**

## **A. BACKGROUND**

The new world order has affected important changes to the way we perform the Electronic Warfare (EW) mission, or what the U.S. Army terms Intelligence and Electronic Warfare (IEW). However, some things remain unchanged. First and foremost, the primary mission of IEW, regardless of the world situation is to support the Commander's priority requirements; the IEW system supports the commander by accomplishing four major tasks: situation development, target development, EW, and counterintelligence [Ref. 1]. Secondly, even though our threat may seem less threatening, and indeed, even less defined as to who or what he is, technology improvements and investment into "smart" warfare all signal that at the very least, the world is very unstable. Hence, the priority to support the commander, and the demand for doing more with less have contributed to aggressive restructuring of the way we fight the electronic battle. Support jamming is an area that is particularly affected by the impending restructuring; and as such, it merits considerable examination.

The rapid pace of modern radar developments and the export of these techniques throughout the world has raised questions as to the effectiveness of the way that we conduct support jamming operations in this emerging high-technology radar environment. This concern has resulted in a number of support jamming upgrade programs across each of the U.S. military service components, which both increase the effectiveness of the jamming waveform and the complementary electronic support equipment which provides situational awareness and target development for the jamming systems. What is important is that current support jamming systems have proven highly effective in recent conflicts against operational

enemy air defense systems which have employed imported radar technology; in fact, "support jammers promise to be more effective is suppressing air defenses against stealth targets" [Ref. 2].

This thesis presents a comparison of the effectiveness of "smart noise" jamming waveforms against advanced threat radars, which are generated using either Direct Digital Synthesis (DDS) or Digital Radio Frequency Memory (DRFM) based support jamming. The mission of support jammers dictates that jamming be accomplished in the side lobes, both to prevent strobing on the jamming aircraft and also to shield spatially displaced strike aircraft. The increased challenge lies in the fact that modern radars employ advanced waveforms, ultra-low side lobe antennas (ULSA), coherent side lobe cancelers (CLSC), and side lobe blankers (SLB) to inhibit signals entering through the side lobes. This project compares the effectiveness of using DDS versus DRFM techniques to meet this challenge. In particular, the effects of mismatched frequency on the DDS jamming waveform is described, as is the effect of quantization and multi-signal storage in the DRFM. A quantitative comparison of these techniques against the TPS-70 high performance, 3-D search radar system -- which has been exported to at least eight different countries -- is presented. Additionally, we hope that the U.S. Army might consider how these techniques might be employed to meet its particular stand-off jamming requirements for its close air support missions.

## **B. THESIS PROBLEM**

Comparison and analysis of DDS and DRFM techniques requires that we consider a number of issues: first, the tactical mission which might employ these techniques in support of the commander's priority requirements; second, we have to consider the effectiveness of the jamming with respect to the physical challenges of coherency in the radar's transmitted form; third, we must consider and address the

question of multiple simultaneous threats, which will result in a depletion of our effectiveness in the application of jamming energy available to address each threat; and finally, we must give consideration to the trade-offs that we might be willing to settle for, in regards to measurements of effectiveness. Careful consideration of each of these challenges has made the analysis more focused, and, consequently, has made the comparison of techniques more applicable to the stand-off jamming problem.

### **C. PRINCIPAL CONTRIBUTIONS**

A number of important undertakings were involved in an effort to reach satisfactory analysis of the problem presented in this thesis. These contributions which merit highlighting and elucidation, are as follows: problem definition, theoretical and mathematical analysis, computer application, coordination with the U.S. Department of Defense corporation contracted for the test system featured in this thesis, and compilation of necessary supporting technical documentation. Each of these areas is developed with considerable attention to how they collectively enhance the outcome of the research and findings entailed herein.

Firstly, problem definition involved focusing in on the impending support jamming problem; as the "threat" no longer seems to dictate, and shrinking budgets require that we do more with less, it appears that the most effective solution may not necessarily be the solution of choice. Secondly, the "smart jamming" techniques which this thesis compares have been analyzed with a significant theoretical and mathematical appreciation. Thirdly, perhaps the most important part of this thesis has been elicited through computer applications employed for each of our jamming techniques. Fourthly, coordination with the Northrop Grumman corporation afforded an outstanding opportunity to examine the DDS and DRFM techniques in light of a globally important radar system such as the TPS-70; this immensely enhanced the

value of the research and the learning experience of this thesis. Finally, the research documentation included here has been compiled for its relevance and applicability.

#### **D. THESIS OUTLINE**

This thesis project assumes the following course of treatment:

1. Introduction of the Stand-Off Jamming Problem and Presentation of Competing Techniques.
2. Theory of Techniques in Application to Current Radar Systems.
3. Analysis of the DDS Technique.
4. Analysis of the DRFM Technique.
5. Comparative Analysis of Techniques.
6. Conclusions.

## **II. MODERN RADAR SYSTEMS: TARGETS FOR "SMART NOISE" JAMMING**

### **A. INTRODUCTION**

How effective will support jamming be in the growing high- density, high- technology, and also high-expectation radar environment -- particularly in light of the rapid pace of modern radar development and exportation of these technologies throughout the world? To begin to answer this question, we must take into consideration many smaller factors which add up to produce an informed response. In this chapter, we do just that; that is, we examine how targetable or jam-prone modern radar systems are, given improvements in design technology and electronic protection (EP). Furthermore, we take this information into account in considering the tactical stand-off jamming (SOJ) mission, and implications to targeting. Finally, we provide some practical insight by incorporating a detailed system description of a modern tactical radar system into this thesis: the AN/TPS-70.

### **B. MODERN RADAR SYSTEM TECHNOLOGY**

#### **1. Design Features**

The defining factor that makes a modern radar system *modern* is primarily determined by its signal processing capability -- or more precisely, its digital signal processing capability. The purpose of radar signal processing is to extract desired data from radar signals. The data usually concerns the detection of some target, the location of the target in space about the radar, the time rate of change of the target's location in space, and in some cases, the identification of the target as being a particular one of a number of classes of targets. The accuracy of the data available from a radar is limited by thermal noise introduced by the radar receiver, clutter, and externally generated interference. What modern radar designers seek to accomplish

is to achieve the least possible loss in signal-to-noise ratio (SNR), the greatest possible range resolution consistent with the target size, and the ability to discriminate between what is target and what is not target ( i.e., some kind of EA or clutter).

Ironically, the defining factor for EA designers is also the signal processor; specifically, the DDS and DRFM are deceptive EA techniques designed to attack the radar's signal processor. The challenge for the EA engineer, then, is to give the utmost consideration to the digital signal processor, particularly when pulse compression waveforms are used. There are many design features which must be considered, but here we concentrate on three: pulse compression, phase coding, and EPs.

Pulse compression is employed in radar to increase the signal energy transmitted without sacrificing range resolution, nor encountering excessively peak high powers that can cause electrical breakdown. Pulse compression techniques are employed to distinguish the useful signal bandwidth (range resolution) from the transmitted pulse length. The radar signal bandwidth to be transmitted is increased by modulating the signal within the transmitted pulse. This modulation may consist of amplitude, phase, or frequency changes of the signal carrier within the pulse. Target echo signals are then passed through filters matched to the transmitted signal, and hence the energy is compressed into a pulse having time duration  $\tau$ , which is approximately equal to the reciprocal of the transmitted bandwidth  $B_t$ . The ratio of the transmitted to compressed pulse lengths is called the pulse compression ratio. This is an important consideration for the EA designer, not so much for the value of the compression ratio, but because compression produces more than just a single pulse in time; in fact, the pulse formed has both precursors and followers of reduced amplitude called range-time sidelobes, which are distinct from the sidelobes produced by the antenna. Antenna sidelobes are undesirable for the radar designer, and need

to be suppressed as much as possible; however, for the EA designer, the antenna sidelobes represent windows of opportunity, because ultimately they signify just how prone a radar system might potentially be to jamming. Since modern radars are most vulnerable to jamming in the sidelobes produced by their antennas. This is an area which in itself merits a considerable amount of attention; hence, we place special emphasis on this topic in the next chapter.

A second design feature consideration is the type of waveform to transmit. This concerns both the radar and the EA designers. Pulse compression waveform design is predicated upon simultaneously achieving wide pulse width for detection and wide bandwidth for range resolution; hence the spectrum of a waveform is critical [Ref. 3]. Choice of waveform is based upon many factors, some of which are the following: 1) the principal target environment that the radar must successfully contend with in terms of the number of simultaneous targets, their range, range rate, accelerations, and radar cross sections, 2) target parameters to be measured and the degree of accuracy required, 3) the required range resolution, 4) the effects on system performance on ambiguities such as range Doppler coupling, the generation of spurious targets or self-generated clutter, 5) the amount of time that can be allotted per target to achieve the required accuracy, resolution, and ambiguity removal, and 6) the limitations due to practical considerations such as cost, complexity, and bandwidth. In short, we seek an optimum compromise in selecting a waveform which provides adequate performance with reasonable cost and complexity [Ref. 4].

Waveform codes used are numerous; they include, but are not limited to, the following codes: Barker binary phase, pseudorandom binary phase, linear frequency modulation, step-frequency-derived polyphase, and -- of special interest in this thesis -- quadriphase modulation. The phase coded waveforms are digital waveforms, which usually consist of a pulse of a monotonic sinusoid which is divided into

subpulses, with the phase of the sinusoid varied between subpulses. Biphase Barker coding is used in many applications because, for a given sequence, it produces the greatest bandwidth (desirable for range resolution), and produces sidelobes that are less than or equal to  $1/13$  in magnitude of the peak lobe. The AN/TPS-70 tactical 3-D air surveillance radar now in production at Northrop Grumman, employs the quadriphase coded waveform - - where quadriphase codes represent a unique class of radar signals. In addition to the quadriphase coded waveform, this radar system also employs a special filter called a Gaussian filter; we will explore both of these interesting features later in much greater detail. One fundamental disadvantage of phase coded pulse compression which, paradoxically, is also a disadvantage for the jammer, is sensitivity to Doppler shift; phase coded waveforms, in general, are much less tolerant of Doppler shift, with significant loss in peak output and increases in sidelobe levels when the product  $f_d\tau$  reaches about .2 (i.e., when the accumulated phase error  $2\pi f_d\tau$  over the transmitted pulse reaches one radian). As mentioned, the sensitivity can be advantageous in rejecting an out-of-band target echo, converting it from a strong lobe to a series of sidelobes. Hence, waveform type must be considered by the EA designer as an important design feature.

The last design feature -- or category of design feature -- is the radar EP. The EP represents the radar designer's response to EA. This is important because most military applications have built-in EPs, which were designed in response to an EA specification, and accommodates the best estimate of the EA threat as perceived by the radar designer [Ref. 5]. Modern radar designers realize the importance of making the radar impractical to jam, because a given is the fact that in the EA-EP world, any radar can be jammed and any EA can be countered depending upon the amount of resources which either side is willing to commit. And this is of particular importance regarding surveillance radars.

According to Schleher, the TPS-70 3D surveillance radar faces five major EA threats: 1) noise jamming, 2) deceptive jamming, 3) chaff, 4) decoys and expendables, and 5) anti-radiation missiles. To combat these threats, the radar designer has many EP options available to him, some of which are worth mentioning. Noise jamming, the most common type of jamming, forces the radar to maximize the energy received from the target with respect to the energy received from the jammer; EPs to reduce noise jamming include frequency agility (the radar's ability to rapidly change frequencies) and raising the transmitter frequency in order to narrow the antenna's beamwidth -- thus providing strobes which pinpoint the jammer's location. The TPS-70 produces ultra-low sidelobes, which it accomplishes with an array antenna that performs sidelobe blanking and can be used for jamming analysis; and this in itself represents an extremely effective EP. In fact, technology advancement has led to the advent of a class of sidelobe EPs such as the ultra-low sidelobe antenna (ULSA), the coherent sidelobe canceler (CSLC), and sidelobe blankers; we examine these in detail in the next chapter.

One final EP worth mentioning, because it too is employed by the TPS-70, is the constant false alarm rate (CFAR) threshold control; CFAR detection extracts a point target (such as an aircraft) by averaging the range cells about the target cell in order to obtain an estimate of the noise. This is extremely important to EA designers, because the TPS-70 jam strobes are developed from the non-CFAR signals in the processing channels. These strobes indicate the azimuth angle of the jamming source, and the low sidelobe levels of the TPS-70 improve this capability by reducing the possibility of false strobes detected in antenna sidelobes.

In essence, modern radar technology is defined by certain design features. These design features are as important to consider for the EA designer as they are for the radar designer. These features include, but are not limited to, digital signal

processing, pulse compression, choice of waveform, and built-in EPs. Ultimately, the signal processor is the radar component that the DDS or DRFM will target, and it is the heart of the features we have outlined above. We next examine these features with respect to stand-off jamming.

## **2. Stand-Off Jamming Considerations**

We've examined modern radar systems from the radar system's perspective. We emphasized design features which were important to both the radar designer and the EA designer. Now, we briefly consider modern radar systems from the jammer's perspective -- particularly, the stand-off jammer. SOJ considerations include the concept of the stand-off EA mission, advantages, disadvantages, and the implications of smart noise in SOJ.

Stand-off EA missions are those which are conducted outside the lethal zones of hostile weapon control systems to provide EA support for friendly forces subject to hostile fire; the SOJ has the advantage of carrying a large EA payload, which can be advantageously positioned for maximum jamming effectiveness [Ref. 5]. These systems employ high-power noise jamming (1 to 2 KW average jamming power per band) which must penetrate through the antenna receiving sidelobes of enemy systems at long ranges. This represents the primary disadvantage of SOJ, which is the amount of effective radiated power (ERP) that is required to jam into the sidelobe pattern of the threat antenna. The typical SOJ consists of the following components: an ESM system with direction finding capability for location of possible jamming targets, a computer programmed to assess the degree of threat of the target emitters and to allocate jamming resources, and multiple jamming transmitters coupled through directive antennas in order to provide high ERP throughout the radar bands of interest.

Conducting the SOJ mission will have several notable advantages and disadvantages associated with it. We first address some of the advantages. First, a dedicated jammer can reasonably afford to employ higher jamming power, and, by design, can simultaneously protect several attack vehicles. Second, a dedicated aircraft (such as the EA-6B) may be able to operate at optimum altitude to maximize the jammer-to-radar propagation factor. Third, the use of stand-off jammers precludes the use of home-on-jam missiles against attack vehicles or high-value targets. Fourth, multiple jammers can be employed for maximum protection. And finally, the precise direction to the attack is not revealed before burn-through -- which is the minimum target range at which a target is observed by jamming [Ref. 6].

There are basically two disadvantages associated with SOJ that are worth mentioning. First, radar-to-jamming range is relatively large, and as a result, high jamming power is required. The other disadvantage is that it may be difficult for the stand-off jammer to provide maximum protection by remaining behind the strike aircraft. These disadvantages are amplified significantly when considering features of modern radars which we previously discussed such as quadriphase code waveforms, and various forms of EPs.

One SOJ consideration, which has the potential of greatly improving EA effectiveness, is the employment of "smart noise". The smart noise concept represents a compromise between deception and noise jamming; essentially, an intercepted waveform is used to create a custom-designed waveform which bursts about the radar's center frequency, and is timed to coincide with and cover the true target return. An advantage of using smart noise for this mission is that we attain better power management; basically, our available jammer energy is optimized by tailoring our waveform to match the threat emitter's center frequency and by precisely estimating the bandwidth of the emitter's receiver. Consequently, our smart noise

waveform has a reasonable chance of being unaffected by either sidelobe blankers or cancelers. The primary disadvantage lies in the fact that our waveform may not be "smart enough"; specifically, smart noise jamming requires a great deal of knowledge of the threat radar system to be effective.

In summary, this section treated modern radar system technology from two basic perspectives. From the perspective of the modern radar system, we examined design features which are of importance to both the radar system designer and the EA system designer. We then proceeded to consider the jammer perspective; here, we assessed the SOJ mission with respect to some of the advantages, disadvantages, and the implications of employing smart noise in stand-off jamming. These concepts will be instrumental in our analysis of actual DEA techniques. To complete the laying down of a foundation for analysis, this thesis includes a description of the TPS-70, whose capabilities will be the prime focus of our comparative analysis.

### **C. AN/TPS-70 SYSTEM DESCRIPTION**

The AN/TPS-70 is a tactical 3D air surveillance radar now in production at Northrop Grumman. It is a mobile E/F (and also S-band) precision radar that is designed to detect and track hostile aircraft in a variety of environments at ranges out to 240 nmi (see Figure 2.1). It incorporates clutter rejection and EP features, and an ultra low sidelobe antenna making it very difficult for enemy countermeasures to jam the system. Also incorporated are advanced signal analysis and processing, as well as a digital coherent Moving Target Indicator (MTI) system. In this section, we highlight some of the most important features of the TPS-70 -- features which will be revisited in subsequent chapters of this thesis. Since we are examining the TPS-70 as if it were a threat emitter, we will consider the following three features: the radar signal processor, the antenna subsystem, and EP capabilities [Ref. 7].

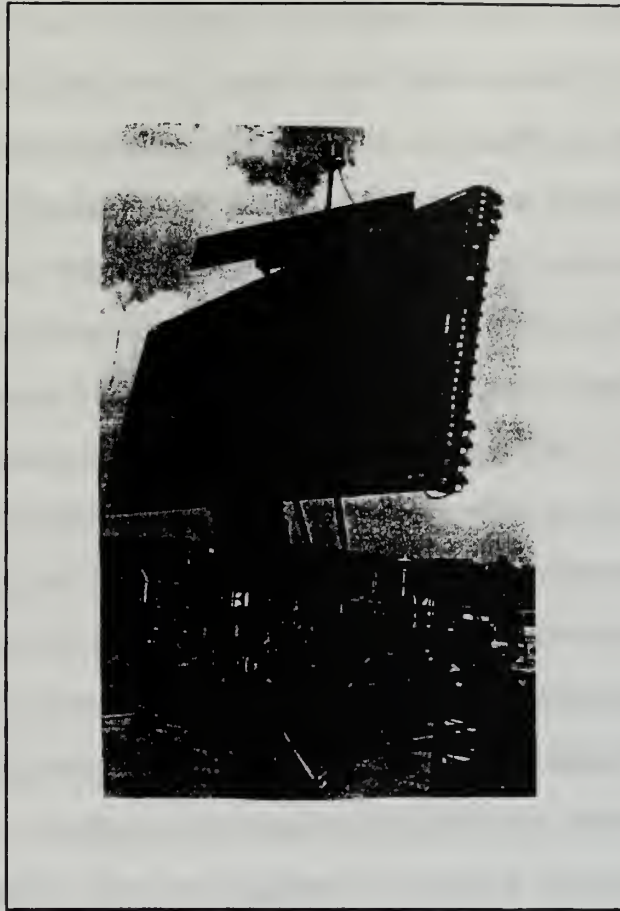


**Figure 2.1. AN/TPS-70 Tactical Radar [Ref. 7]**

The digital signal processing system is the most important component of the TPS-70. Ironically, it's also the most important component for the jammer, because, as mentioned above, the component of a radar that is targeted by DEA techniques, is the signal processor. Functions of the signal processor include target detection, height evaluation, detection processing for (MTI) search, non-MTI search, monopulse processing, data processing, and radar control.

Signal processing takes place in each of the radar's six receiving channels, and each of the identical channels provides MTI search, non-MTI search (or Normal

search), and monopulse height processing; as a result, the entire elevation angle is covered on each radar transmission. Furthermore, both in-phase (I) and quadrature (Q) information are processed in each channel; this processing can maintain maximum target detection sensitivity and prevents blind phases that would otherwise reduce detection at some aircraft velocities. Digital pulse compression (to 0.5 microseconds) occurs in each channel using a 3-bit compressed pulse anti-clutter system (CPACS) decoder, which improves system sensitivity over the conventional hard-limiting CPACS. MTI signal processing is also performed separately in each channel; each MTI processor is a linear 4-pulse I and Q canceler which attenuates ground clutter by more than 50 dB with the antenna scanning. In general, normal and MTI signals are decoded and compressed in linear decoders, where the log function of the target amplitude is used for digital height finding. Since amplitude monopulse is used for height finding, the sensitivity time control (STC) attenuation that is applied to each channel is compensated for prior to height computation.

Of particular interest for the EA designer, is the fact that the TPS-70 radar signal processor also detects and processes jamming signals. These are coded to identify them as "jam strobes", with the bearing of the jammer. The azimuth of the jammer can be identified with minimum ambiguity because of the ultra-low sidelobe antenna. This is not possible with antennas of conventional design, since they tend to show many apparent directions for the same jammer at each of the principle sidelobes. This information is obtained via the signal processor's interference processor; the processor's inverse Jamming Amplitude Versus Azimuth (JAVA) displays -- as a function of azimuth -- the loss in detection range in the presence of jamming, as well as the relative strength of the jammer.

The radar antenna group is arguably the next most important subsystem of the TPS-70. The antenna per se is a planar array (flat plate) antenna which provides the

precision 3-D coverage pattern required for continuous surveillance of the total air space at a 10-second data rate. The coverage extends to 240 nmi from the horizon to high altitudes. In general, the array antenna has been designed to meet four major requirements: 1) very low azimuth sidelobes to combat EA and prevent both ring-around and strong clutter, 2) precise elevation beams for height accuracy, 3) operation in extremes of high weather and high winds, and 4) deployability (rapid set-up and take down). The design is such that the antenna easily meets military environmental requirements for tactical equipment; the antenna can operate in winds up to 78 knots.

The key antenna feature for the EA designer is the very low azimuth sidelobes; in fact, according to specifications, the sidelobe levels are greater than -45 dB down, which qualifies the TPS-70 antenna as an ultra-low sidelobe antenna (greater than -40 dB) [Ref. 5]. The ultra-low sidelobe level is achieved through the use of precisely slotted waveguide assemblies. The design and manufacturing process is completely computer controlled using technology evolved from the AWACS antenna system [Ref. 7]. The resulting ultra-low sidelobes throughout the 200 MHz frequency range of the radar effectively combats jamming and greatly reduces the effects of clutter, including ring-around due to strong returns -- where ring-around is self-oscillation due to recirculation of amplified noise energy, caused when conventional antennas detect excessively large targets in their sidelobes and backlobes. Also, the bearing of an active antenna can be determined precisely by the data processor and is automatically included in the target messages sent out to the command center.

The last feature of the TPS-70 that we want to highlight is the EP capability. In actuality, this is a multi-faceted capability, with a number of measures combining to accomplish the EP mission. EPs employed by the TPS-70 include frequency agility, CFAR, and complex phase coding. We have already mentioned these in the general context, but for clarity's sake, we re-emphasize them here.

Frequency agility is used to minimize or avoid the signal received from the jammer; in the TPS-70, frequency agility forces the jammer's power to be distributed over a much wider bandwidth (200 MHz, containing 64 frequencies), within the narrow radar bandwidth. Frequency agility is accomplished either pulse-to-pulse or changed after a group of pulses. The actual frequency control can be at random, or controlled by what's called the jamming analysis transmission selection (JATS) system; JATS samples jamming power during the period between each radar transmission, and ultimately forces the jammer to operate in a wideband mode -- thus avoiding peaks in the jamming power.

CFAR is actually an indirect EP feature, since jam strobes are developed primarily from the non-CFAR signals in the processing channels. What qualifies it as an EP, however, is that CFAR detection in the Normal and MTI signal paths is extremely effective in rejecting signals and clutter which could cause false targets and false tracks.

Finally, perhaps the least obvious and most unusual EP incorporated by the TPS-70 is the transmitted waveform: the quadriphase coded pulse with pulse compression. The radar generates this complex phase code within each 6.5 microsecond pulse, which, according to Northrop Grumman, is extremely difficult to duplicate. The signal processing is designed to reject extraneous signals (such as interference or jamming) which do not accurately duplicate the transmitted phase code. This is critical for EA designers to consider, which our subsequent analysis will demonstrate in great detail.

The TPS-70 radar and its technology are currently available on the world market (exported to eight different countries), and therefore, represent a realistic potential threat. This threat factor increases exponentially when we consider how advanced the system is in terms of its signal processor, its state-of-the-art antenna system, and the EPs it employs. Figure 2.2 is a summary of the radar's performance characteristics.

Radar Frequency -----	2.9 - 3.1 GHz
Data Rate -----	9.4 secs, nominal
Instrumented Coverage Range -----	240 nmi, 44 km, 360°
Azimuth -----	0° - 360°
- Elevation Angle -----	0° to 20°
- Altitude -----	100 K ft; 0 - 32.6 km
Detection Range -----	>190 nmi
T-38 target aircraft (Tgt Size = 1.7m <sup>2</sup> ; P <sub>D</sub> = 0.75, PFA = 1 x 10 <sup>-6</sup> )	
MTI Improvement Factor - All elevations, full range -- 50 dB	
Accuracies	
- Range -----	260 feet (80 m)
- Azimuth -----	0.25° RMS
- Height -----	±2K ft (610 m) to 333 KM & 75%)
Reliability	
- MTBF -----	600 hours
- MTTR -----	0.5 hour
False Alarm Control Capabilities	
- Low antenna sidelobes	
- Elevation discrimination (multiple beams	
- Frequency agility	
- Excellent CFAR detection and digital integration - all channels	
- Quadriphase pulse compression (Normal & MTI) - all channels	
- Complex (quadriphase) coded pulse	
- Staggered PRF and digital integration	
- Weather Monitor Video	

**Figure 2.2. Summary of Performance Characteristics**

## **D. SUMMARY**

In this chapter, we addressed the question of how important stand-off jamming will be in the current high-density, high-technology, and high-expectation radar environment. We submit that the answer depends upon how well we respond to a number of critical considerations. These considerations include design features of modern radar systems such as digital signal processing, pulse compression, and waveform selection -- from the radar system's perspective. From the jammer's perspective, these considerations include the EA mission per se -- particularly the type of jamming (i.e., noise or deceptive) we intend to employ -- and what the trade-offs are in employment. We gave this examination some practical dimension by describing some of the most important features that the EA designer must consider for use against modern radar systems such as the TPS-70 3D surveillance radar. In the next two chapters, we analyze how two different forms of smart noise jamming techniques might be effective against such systems.

### III. THE TECHNIQUE OF DIRECT DIGITAL SYNTHESIS

#### A. INTRODUCTION

The primary impact for DDS technology on future radar design will be in the areas of operational flexibility and error correction for system and component effects. The flexibility in waveform control provided by the synthesizer allows the generation of waveforms with a wide range of carrier frequencies, pulse widths, and pulse repetition frequencies; in particular, the DDS technique has great potential for use of synthesized waveforms as a deceptive jamming technique. These waveforms as discussed here are termed "smart noise" waveforms because they are matched (as closely as possible) to a target radar's transmitted waveform. The beauty of this technique lies in the fact that we attain a very effective use of jamming power by crafting a "match", which essentially removes the processing gain advantage of modern radars against noise-like jamming interference. In general, the process as applied to the stand-off jamming problem, involves the DDS-configured jammer completely synthesizing the victim radar's waveform. To effectively accomplish this for use as a deceptive EA (DEA) measure, involves storage of the radar's intercepted signature in the jamming system for reconstitution and modification. The overall effectiveness of the DDS technique, then, is determined almost completely upon the degree of accuracy that we can obtain regarding the radar's parameters in the jammer.

In this chapter, we analyze the technique in both theory and application. We begin examination of the technique from the conceptual stage as an application for radar development, as well as a DEA option; the focus here is on the viability of DDS as a jamming technique. After analysis of the conceptual and theoretical foundations, we shift our focus to the application of the DDS technique; here, we consider the mathematical development of our intended application, with concentration on the

recent transition of current state-of-the-art radar systems from the use of binary phase coded signals to the use of quadriphase coded signals. We then experiment with the MATLAB programs designed so that we can analyze the generation of both biphasic and quadriphase generated signals, and ultimately, to provide us with data which will provide us with measurement-of-effectiveness criteria (namely, loss) for subsequent comparison with the DRFM technique.

## **B. DDS THEORY AND TECHNIQUE**

### **1. Theory and Objective**

The primary objective of electronic attack (EA) measures is to "introduce signals into an enemy's electronic system which degrade the performance of that system so that it is unable to perform its intended mission" [Ref. 5]. The stand-off support jammer is characterized as a jamming vehicle which stands-off at a distance beyond the effective range of target defenses (an advantage), but operates with the distinct disadvantage that in order for it to be effective, large amounts of effective radiated power is required due to the potentially long jamming range and the need to jam into the sidelobe pattern of the victim antenna. This mission-related requirement is an important consideration regarding the design of EA systems. A fundamental question that arises is what kind of jamming is the most effective under a given circumstance -- noise or some kind of "smart" form. The approach that we examine here is the DDS deceptive jamming technique, which would be employed against the surveillance or search radar.

The objective of a DEA system is to mask the real signal by injecting suitably modified replicas of the real signal into the victim system. Of note, is that DEA attempts to jam a radar in range as well as angle; the jammer requires significantly less ERP to jam a radar, in contrast to an equivalent noise jammer - - whose objective is to obscure the radar target by saturating the radar in noise, which has an advantage

in that very little need be known about the victim radar's parameters. This is particularly important considering that DEA affords the possibility of jamming a number of radars simultaneously, given a dense threat environment. This jammer is most effective against search radars, which is evident if we view the search radar as a rotating antenna beam whose main lobe sequentially scans the search volume, while its sidelobes provide some response in all directions. It is this multi-path sidelobe response that represents the vulnerability of the radar system to jamming.

Conceptually, what we expect to accomplish by using the DDS technique against the sidelobe vulnerability of the radar system is straightforward. First, we observe that (with respect to the antenna beam's main lobe) the magnitude of the sidelobe response will be dictated by the type of antenna that our radar system employs; some examples are the ordinary, low, and ultra-low sidelobe antennas, and those with or without some form of sidelobe cancellation. Secondly, given the antenna type and sidelobe response, we observe the type of waveform that the radar transmits, which after reflection from the target, is detected in a receiver noise background by a matched-filter receiver; this is extremely important because the purpose of using a matched filter is to maximize the received signal SNR. This SNR of the radar depends on the energy received from the target and, of course, the receiver noise spectral density -- where noise consideration (as well as clutter effects) are of paramount importance regarding any system of this type.

Having made the observations outlined above, we must inject jamming into the search radar; the DDS synthesizes the signal for accomplishing this. Essentially, the synthesized signal (with modification) is injected into either the radar's main lobe or side lobe response to confuse or deceive the radar with respect to the location of the real target. What is transmitted is "smart noise", so named because it represents a signal that has been matched to the radar's transmitted waveform. This is done by

storing the threat radar parameters based upon signals intelligence (SIGINT) information which has been stored in the jammer's threat library. This interception and subsequent storage are paramount to the success of this process; the degree of accuracy we attain in determining the threat parameters allows us to keep our databases current with respect to specific emitters. These parameters include -- but are not limited to -- frequency, pulse width, and pulse compression factors. The primary challenge incurred with the DDS is that DDS jamming waveforms are not generally coherent with the radar pulse [Ref. 2]. They are, however, coherent over the intra-pulse processing period of the radar, which affords DDS-jamming with the potential to alleviate the radar's intra pulse processing gain.

At this point, a key observation is the realization that we must avoid introducing our signal into the main lobe, in order to prevent jam strobing, and revealing our tactical intentions. This presents us with a considerable challenge; that is, the sidelobe challenge. In particular, the advent of ultra-low sidelobe antennas and high performance sidelobe cancelers potentially provide the target radar with a distinct advantage. Electronic protection (EP) technology, particularly, coherent sidelobe cancelers and sidelobe blanking measures, merit a great deal of attention.

The antenna is the most important area of the radar for consideration when incorporating EP, because it represents the transducer between the radar and the environment in which the radar must work. Explicitly, the antenna is the first line of defense against undesirable spurious signals, including jamming. From a systems engineering perspective, it is of note that EP features such as those we are about to examine, are very valuable and worthwhile, in spite of the complexity, cost, and possible weight they might add to the antenna.

We begin our evaluation of EP techniques, as incorporated into the target radar, by analyzing the mathematics involved in predicting a radar's performance in

a jamming environment. We start by reviewing the Jam-to-Signal (J/S) ratio, as outlined by Hoisington [Ref. 6]:

$$J/S = \left( \frac{4\pi P_j B}{P_r \sigma L_p} \right) \left( \frac{G_{jr} G_{rj}}{G_r^2} \right) \left( \frac{R_t^4}{R_j^2} \right) \left( \frac{g_j^2}{g_t^2} \right) \quad (1)$$

where

where  $P_j$  = jammer power per unit bandwidth

$B$  = radar receiver noise bandwidth

$G_{jr}$  = gain of the jammer antenna toward the radar

$G_{rj}$  = gain of the radar toward the jammer

$R_t$  = radar-to-target range

$g_j$  = propagation factor on the jammer-to-radar path

$P_r$  = radar power output

$G_r$  = gain of radar antenna toward target

$\sigma$  = target radar cross section

$R_j$  = radar-jammer-range

$g_t$  = the radar-to-target propagation factor

This expression is commonly used as a measure of jamming effectiveness because it relates one radar's theoretical performance to another's. Now, the technical purpose for either the CSLC or the SLB, as EP technique, is to generate a high degree of radar space discrimination. The radar inherently does this when it provides directivity to the transmitted and received electro-magnetic energy. This is enhanced by the use of

CLSCs and SLBs, as is evidenced by taking (1) and examining the second term, which incorporates the antenna space discrimination EP (below,  $D_A$ ):

$$D_A = \left( \frac{G_{jr} G_{rj}}{G_r^2} \right) \quad (2)$$

Basically,  $G_{rj}$  represents antenna sidelobe gain and  $G_r$  represents antenna main lobe gain, since formal radar operation in SOJ usually results in the antenna's main lobe illuminating the target and the jamming signals entering the radar through the antenna sidelobes. This leads to our aforementioned primary observation regarding sidelobe vulnerability; specifically, if by good antenna design, or addition of appropriate circuitry elements, the antenna sidelobes can be reduced to such a level that jamming energy is effective only when introduced into the radar's main lobe, then the SOJ will be effective only in preventing detection in the small sector -- encompassing the width of the radar's azimuth -- centered on the jammer. Ultimately, this leads us to the bottom line, which is that low inherent antenna sidelobes or general sidelobe control is extremely important and effectively restricts jamming and detection to the main lobe. Antenna engineers have been very successful in designing radars with just such a capability, which in itself is quite an outstanding achievement, in light of the fact that the level of sidelobes required to suppress jamming through the sidelobes is very difficult to produce in any practical antenna design; antennas, such as that used by the TPS-70, are currently achieving sidelobes which are 50 dB or more below the peak main lobe gain -- which is considered exceptional as applied against SOJ.

The two techniques that we prescribed above, which have been effectively employed to keep sidelobe levels low are the CLSC and the SLB. According to Widrow [Ref. 8], CLSCs were invented by Paul Howell to cancel high-duty-cycle interference entering the sidelobes of a radar antenna. Current digital systems far

outperform previous analog systems, though the principle remains the same. A diagram of a digital overloop adaptive process is shown in Figure 3.1.

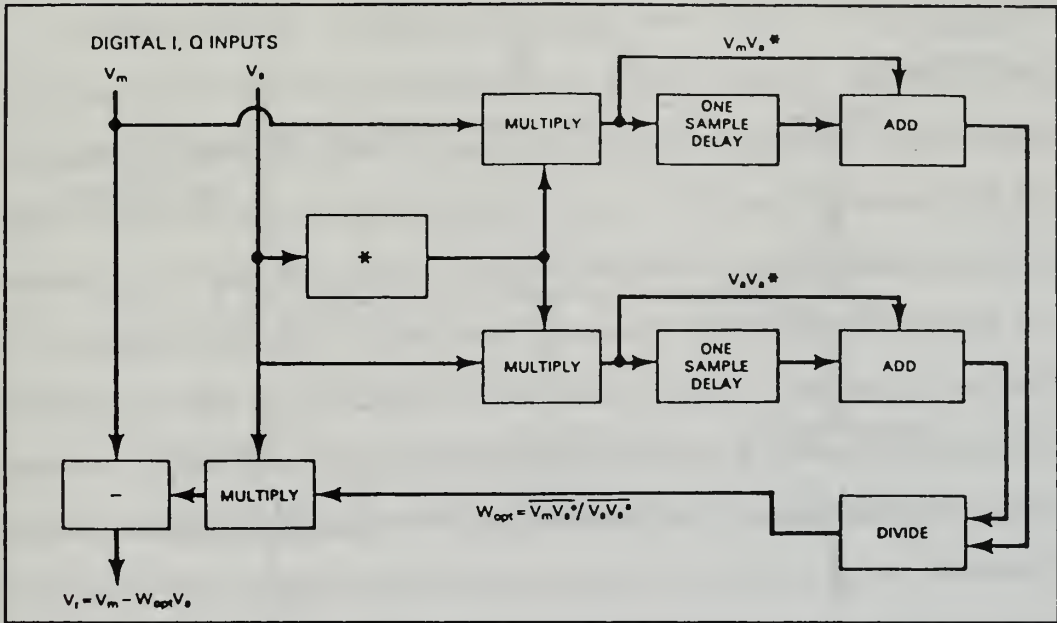


**Figure 3.1. Digital Open-Loop Adaptive Processor**

The process starts with an auxiliary antenna(s), which has a gain that is less than the main lobe gain of a radar antenna but greater than the highest sidelobe gain of the radar antenna used to obtain samples of any high-duty-cycle interference that may be present. This antenna is placed sufficiently close to the phase center of the radar antenna to ensure that the samples of the interference which it obtains will be correlated with the interference received in the radar antenna sidelobes. This requires that the separation between the radar antenna's phase center and the auxiliary antenna's phase center divided by the speed of light,  $c$ , be much less than the reciprocal of the smaller of the radar bandwidth  $B_r$  or the interference bandwidth. See Figure 3.2. for a physical description.

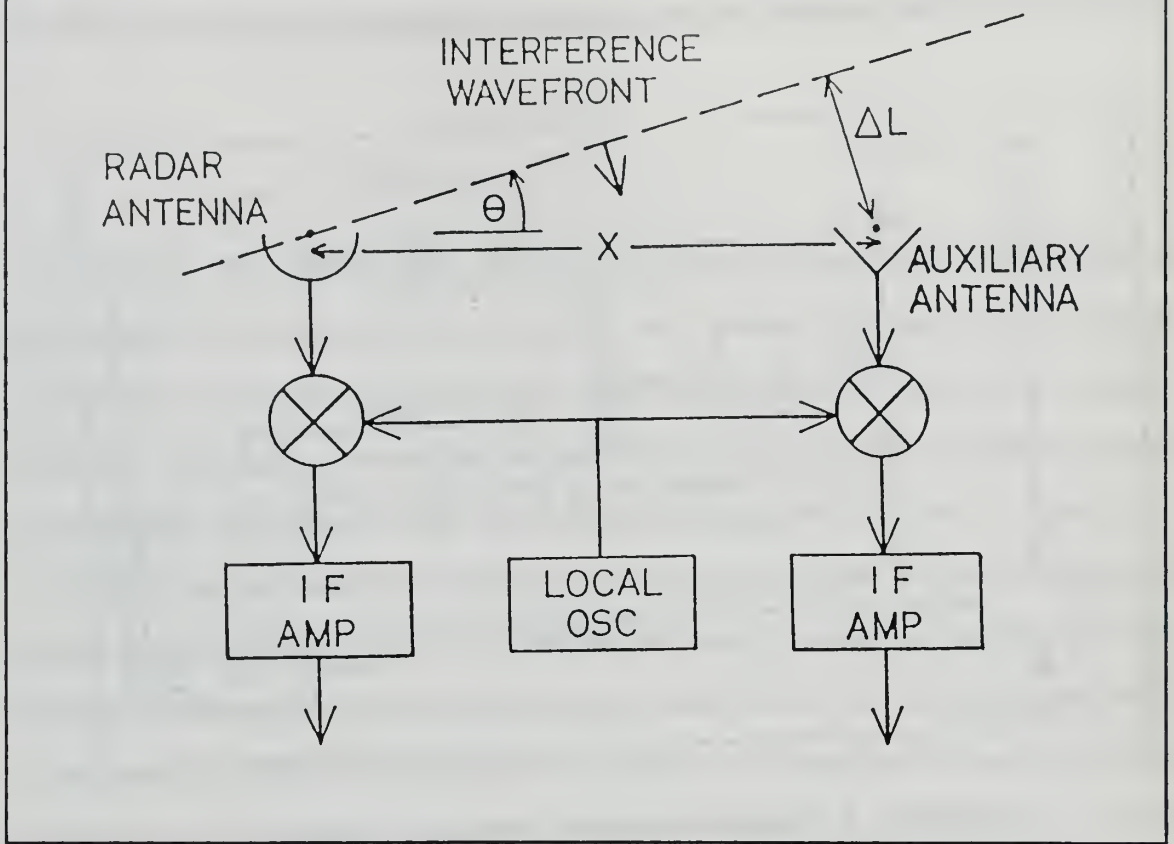


**Figure 3.2. CS LC Radar and Auxiliary Receiving Systems**

It is apparent that the maximum amplitude of difference between the time of arrival of the interference at the radar and at an auxiliary antenna, separated by some distance  $X$ , is  $X/c$ , and this is reached at arrival angles of  $\theta = +90$  or  $-90$  degrees. Thus, the time of arrival difference for any value of  $\theta$  is given by the equation

$$T_a = \frac{\Delta L}{c} = (X \sin \theta / c) \quad (3)$$

We ensure that the sidelobe canceler works by limiting  $T_a$  so that its amplitude is much less than  $1/B_r$ , which maintains the correlation between the radar and auxiliary interference signals.

Mathematically, we define two input interference voltages, where  $V_s = A(t)\cos(\omega_1 t)$  (our normal input signal), and  $V_a = A(t) \cos(\omega_2 t + \phi)$ , (our signal input to the auxiliary antenna). Both  $V_s$  and  $V_a$  are functions of time  $A(t)$  modulating an I.F. carrier that has a much higher frequency ( $\omega_1 = 2\pi f$ ) than the bandwidth  $B$  of the modulating function  $A(t)$ . Also,  $V_a$  only differs from  $V_s$  by a constant amplitude and by a constant phase shift of the carrier frequency. The difference results from the difference in gain and location of the phase centers of the radar and auxiliary antennas. Essentially, by adaptively controlling the phase and amplitude of the auxiliary channel signal and combining this signal with the main channel signal, a null in the composite antenna pattern response can be produced in the direction of the jammer; this being done continuously will ultimately permit the null to track the jammer. Systematically, the radar receiver's output I.F. is translated to  $\omega_1 - \omega_2$  and the resulting signal  $V_s$  passes through an open loop adaptive processor (see Figure 3.1), producing a complex residue signal  $V_r$  (having I & Q components), where

$$V_r = V_s - W V_a \quad (4)$$

and where  $W = G v_r V_a^*$ , and represents the weighting used by the open loop [Ref. 9]. Digitally, (4) for the  $j$ th sample is as follows:

$$V_r(j) = V_s(j) - W_{opt}(j) V_a(j) \quad (5)$$

where  $W_{opt} = W$ , and is the optimum weighting, which provides optimum cancellation and a cancellation ratio that is independent of the auxiliary signal power level. This weighting is derived by computing sliding-window averages, and is accomplished as follows:

$$W_{opt} = \frac{\sum_{k=j-n+1}^j V_s(k) V_a^*(k)}{\sum_{k=j-n+1}^j |V_a(k)|^2} \quad (6)$$

Ultimately,  $W_{opt}$  becomes  $V_s/V_a$ , which, when plugged into equation (5), results in perfect cancellation. It follows that where jamming is injected, the adaptive digital canceler can reduce jamming levels down to the thermal noise level except in regions where there are targets. This is because of the effective infinite gain associated with the canceler, which enables it to completely cancel correlated signals between the radar and auxiliary channels; furthermore, because the thermal noise is uncorrelated between channels, the thermal noise level represents the floor of the residue.

The Sidelobe Blanker (SLB) is much less complicated than the CSLC. It employs an omni-directional auxiliary antenna, achieving gains that are greater than the highest sidelobe gain of the radar antenna, but less than that of the antenna's main lobe; this gain is typically 3 to 4 dB larger than that of the sidelobes of the main antenna. Basically, the auxiliary antenna feeds a receiver which is identical to that used by the radar, and the detected output of this receiver is compared to that of the radar receiver. If the detected output of the auxiliary receiver is larger than that of the radar receiver, the signal in the main channel is assumed to have been received through the sidelobes, and hence, the latter is blanked in all range cells where this occurs. Signals entering the radar main lobe are not blanked because they produce

larger radar outputs than the auxiliary system. See Figure 3.3 for a simplified description of the sidelobe blanker.

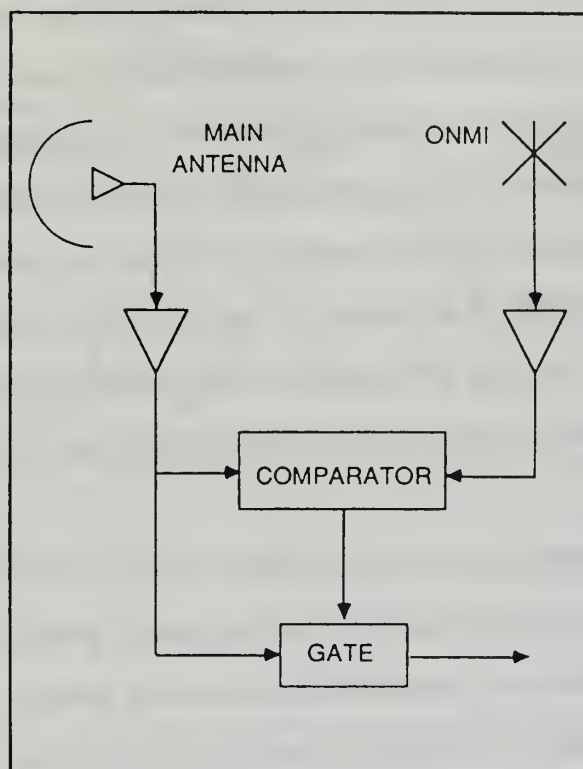


**Figure 3.3. Simple Sidelobe Blanker [Ref. 15]**

Of notable importance regarding the SLB, is that an effective sidelobe blanker confines deception returns to the same azimuth direction as the jammer-carrying target [Ref. 5]. Also, the SLB is only effective for low duty cycle pulse or swept frequency jamming high duty cycle, and noise jamming effectively blanks the main channel most of the time -- rendering the radar ineffective.

In general, both techniques described above are very effective as EP measures for the given radar system. This makes systems which use the CSLC, very difficult

to jam. And the bottom line is that very low antenna sidelobes are probably the single most effective means of reducing the effectiveness of Stand-Off Jamming.

In summary, we have thus far examined the concept of DDS as a viable jamming technique, by defining the primary objective and the method involved; that is to say, the concept of DDS is to inject jamming into the radar's sidelobe response in order to deceive the radar with respect to the location of the real target. The signal that we inject is synthesized from signature data, and is not necessarily coherent with the radar pulse. This implies that we must be as accurate as possible in determining the threat radar parameters in the jammer. Finally, we've emphasized the fact that modern radar systems employ EP techniques such as CSLCs and SLBs designed to protect the radar against jamming, and have summarily been very effective in doing so.

## **2. Technique**

DDS is a coherent technique by which a signal is generated in the form of a series of digital numbers and converted into an analog form by a digital-to-analog converter (DAC). Here, we examine the technique involved in the process of generating the appropriate waveform with respect to the DDS architecture. Waveform generation circuitry such as modulators and local oscillators must adhere to strict tolerances in order to allow the desired signals to be produced and though the architecture for accomplishing this is quite simple and straight-forward, the actual process per se is very sophisticated. Note that we do not specifically weigh-in the advantages and disadvantages in this section -- this is done in depth in Chapter V of this thesis.

We begin with the components of a DDS system. The following is a listing of common digital components: an adder/accumulator, a Read Only Memory (ROM), a DAC, and a lowpass filter. This configuration is ideally suited to provide the phase

coded (i.e., with Barker coded waveforms) pulse compression signals, such as those used in the TPS-70 radar (See Figures 3.4 & 3.5).

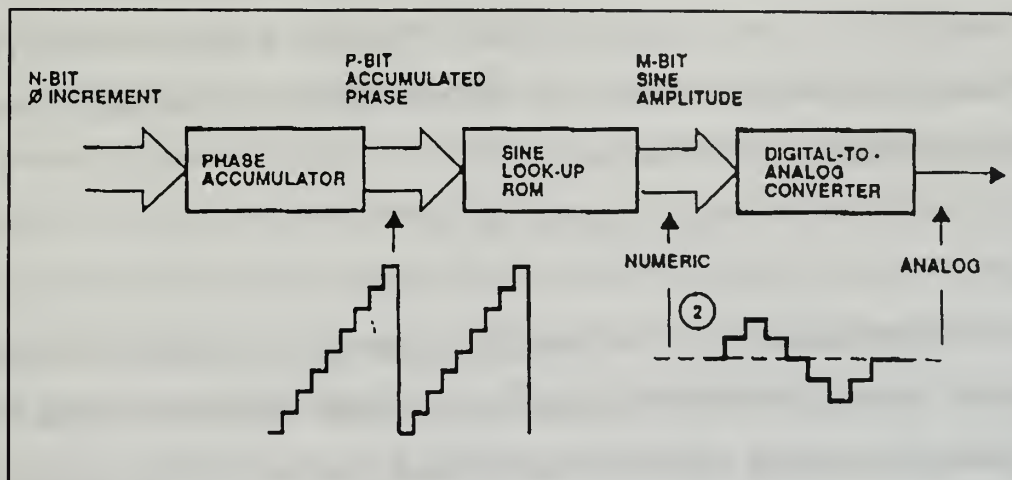


**Figure 3.4. Direct Digital Synthesizer [Ref. 20]**

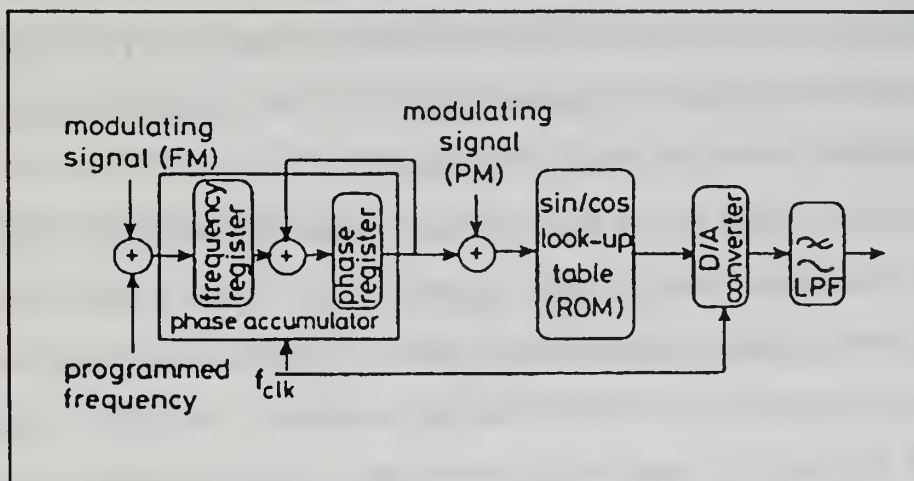


**Figure 3.5. DDS With Phase and Frequency Modulation [Ref. 20]**

The adder/accumulator is a linear modulo counter which increments with each clock cycle at a rate dependent upon the frequency control word; it produces a time series of binary integer values. It is comprised of a binary adder and a latch -- the latch being built in to reduce spurious effects. The adder adds some binary phase input value,  $N$ , to a previous output value. Mathematically, the input-output relation of the accumulator may be written as

$$Y(nT) = Y(nT - T) + N \quad (7)$$

where  $n$  = the time index and  $T$  = the sampling period. Hence, the name accumulator is justified. The value of  $Y(nT)$  is bounded by the number of bits of the input  $N$  and of the accumulator output. The restriction imposed upon the phase accumulator by the bit number results in an overflow (inherent in the binary adder), which implies a phase zero crossing upon overflow. We numerically control the frequency by varying  $N$ , the increment parameter. Also, it's important to note that as a digital process involving sampling, clocking for the adder and accumulator latches adhere to the Nyquist Sampling Theorem, which means that the clock operates at twice the highest desired synthesized frequency. In general, the accumulator generates an address for the next element of the DDS, which is the ROM.

In a ROM, binary data is physically and permanently stored by defining the state of the constituent memory cells. A set of input signals is identified as an address; the input signals comprising this address are decoded (binary information is converted from one form to another). Once the conversion is complete, a readout is provided in the form of a word, which is stored there. This is termed a "memory."

In particular, the ROM of the DDS acts as a phase-to-amplitude converter, where the accumulator output is converted to a sinusoidal amplitude. The ROM, which contains the stored values of desired output waveforms, is addressed by the

digitized phase mapping from the accumulator. Subsequently, the phase-to-amplitude conversion process maps the sequence of instantaneous binary phase values provided by the phase accumulator through corresponding phase values into the quantized amplitude time samples of the generated waveform.

The ROM table typically has its address bus (common path link) connected to the parallel output of the phase accumulator and its output routed to the next element of the DDS, which is the DAC input. The bus size is determined by the spurious level that is required of the DDS system, and to preserve symmetry, the phase input and data output buses are of the same size. The size, speed, accuracy and configuration of the phase-to-amplitude converter all influence the overall performance of the DDS, particularly with respect to the bandwidth and distortion by spurs. Ultimately, the output of the ROM is a digital word, which is next input into the DAC.

The function of the DAC, paired with the lowpass filter, is to reconstruct the discrete waveform. The fundamental principle of digital-to-analog conversion is the Nyquist Sampling Theorem, which as applied here, implies that a band-limited analog signal which has been sampled (at least) at twice the maximum desired frequency, can be reconstructed from its samples without distortion. The DAC actually interpolates between the samples; the ideal reconstruction formula, or more precisely, the ideal interpolation formula is [Ref. 10]:

$$x(t) = \sum_{n=-\infty}^{\infty} \frac{x(nT) \sin\left(\frac{\pi}{T}(t-nT)\right)}{\left(\frac{\pi}{T}\right)(t-nT)} \quad (8)$$

where the sampling interval  $T = 1/F_s = 1/2B$ ,  $F_s$  is the sampling frequency and  $B$  is the bandwidth of the analog signal. What this represents is the reconstruction of the

signal  $x(t)$  from its samples as an interpolation problem and this generally describes the common

$$g(t) = \frac{\sin(2\pi t/T)}{\pi t/T} \quad (9)$$

which is the ideal interpolation function here. The actual interpolation function used, given by (8), is basically a linear superposition of time-shifted versions of  $g(t)$ , with each  $g(t - nT)$  weighted by the corresponding signal sample  $x(nT)$ .

As mentioned above, the DAC which the DDS employs, is paired with a lowpass smoothing filter. The DAC accepts at its input electrical signals that correspond to a binary word and produces an output voltage or current that is proportional to the value of the binary word. Generally speaking, suboptimum interpolation techniques can result in passing frequencies above the folding frequency, and such frequency components are undesirable; this is why we pass the output of the interpolator through a proper analog filter. So, the output is passed through the lowpass filter which highly attenuates any undesirable frequency components, smoothing the signal and removing any sharp discontinuities.

As it pertains to the DDS, the DAC is a major contributor to the performance characteristics of the DDS. Ironically, it's also the least ideal element of the system due to problems such as static and differential non-linearity -- which produces quantization errors and spurious responses. Integral non-linearity causes problems of harmonic distortion, largely due to the deviation of the line that represents the full range of DAC output from the reference straight line. Jitter and clock feed-through are both responsible for the production of high frequency spurious signals and phase noise. And in addition to the general dynamic problems, settling time and glitches are

also responsible for spurious responses. Settling time is the time required for the output of the DAC to reach and remain within a given fraction (usually, + or -  $\frac{1}{2}$  the least significant bit, LSB) of the final value, after application of the input code word.

Glitch performance is a critical parameter in high speed DAC applications. Glitches are the switch transitions that occur whenever a change in input occurs, which is significant when several bits change state such as one-half of full scale (when all bits change). These transitions can be propagated to the analog output where they may contribute to the total noise and are usually seen as the ringing or the spikes observed in the DAC output. Glitch performance depends largely on the internal mechanisms of the DAC, e.g., whether the DAC has been designed to minimize glitch effects by employing appropriate drive circuitry and specified to be used only with suitable loads. In short, glitch energy places jitter onto the synthesized waveform and, thus, may increase the phase noise floor. Switching removes this effect to a large extent, and is expressly the reason for incorporating a built-in latch with the DAC.

One final note regarding the DAC is that it approximates the ideal amplitude value for a given clock frequency. This is important because it means that while the DAC does not determine the frequency of the output waveform, it does determine the amplitude accuracy of the waveform. It follows, then, that the most significant bit (MSB) of the phase accumulator is a pulse waveform whose individual pulses are sub-harmonics of the clock pulse. It also follows that the most prevalent component of the MSB output waveform is, in fact, the desired output frequency.

In summary, we have examined the technique of DDS, with emphasis placed upon the architecture of the synthesizer. DDS architectures, as commercially implemented, generally use a phase accumulator, a look-up table ROM, a DAC to generate signals, and a lowpass smoothing filter; additionally, for some applications

a frequency accumulator is placed in front of the phase accumulator to provide fast frequency changes, and a phase adder is placed at the output of the phase accumulator to generate phase modulation. The direct digital synthesizer can produce a very close to carrier phase noise profile comparable to the very best oscillators available, and is thus, suitable for applications which require very low noise floor properties. One important observation that we have made regarding the DDS technique is the criticality of the DAC; this is essentially because the phase noise floor of the synthesizer (as pertains to spurious responses and glitches) all depend largely on the specific properties of the DAC used. In the next section, we analyze DDS from the perspective of the target radar, as it is this radar signal which our DDS jammer will be required to replicate and modify for use as a DEA technique.

### **C. ANALYSIS OF RADAR SIGNAL SYNTHESIS METHODS**

The effectiveness of the DDS generated waveform depends upon the synthesizer's ability to match its synthesized waveform with the actual radar signal. This ability depends upon a number of factors; it depends upon how complete and up-to-date the jammer's analysis receiver is with respect to specific emitters, it depends upon Doppler shifting effects, and, as our research here has discovered, it can depend in large part upon the type of phase coding that is employed. It is this latter discovery that will serve as the focus of this portion of this thesis. In particular, the most popular search radar systems around the world today, have been designed to operate with binary phase coded Barker pulse compression waveforms, based on Barker codes. According to Mr. Thomas Keast of Northrop Grumman Corporation, biphasic is still used by many TPS-43 users, and the Chinese use it a lot too. But technological advancement has led to the design of a unique class of radar signals that use a quadriphase coded signal. We examine both methods, with emphasis placed upon the quadriphase code -- which is the type used by the TPS-70.

## 1. Biphase Coding

We begin with biphase pulse coded waveforms, since this type of signal was used in earlier (then state-of-the-art) radar systems, such as the previously mentioned TPS-43. Biphase coding was initially selected for radars which use digital processing (for Doppler filtering), pulse compression, and CFAR operation due primarily to its peak-to-sidelobe ratio (PSR); the PSR is the ratio of the main lobe magnitude to the magnitude of the peak sidelobe of the autocorrelation function. Another reason for choosing a biphase code is that for a given sequence, it produces the greatest bandwidth, which is desirable for range resolution. The Barker codes (so-called perfect codes because the highest normalized time sidelobe at zero Doppler frequency is only one code element high), are optimum in this sense because an  $N$ -element code produces an autocorrelation function whose peak value is  $N$  and whose peak sidelobes are unity. For these codes, the  $PSR = N$  which is the largest value that can be obtained for a biphase code with  $N$  elements. There are no known Barker codes for lengths greater than 13; though research continues for obtaining such codes, the question remains as to whether they are of any value in practice.

The process of producing and implementing biphase coded signals starts with a transmitted radar pulse of duration  $T$ . The waveform usually consists of a pulse of a monotonic sinusoid which is divided into  $N$  subpulses, each of duration  $\tau = T/N$ ; these subpulses are coded in terms of the phase of the carrier. The phase variations of 0 degrees and 180 degrees are represented in this thesis by  $+1$  or  $-1$ , respectively. Such phase shifting is applied with a digital phase shifter, where  $f_d = 1/2\pi (d\phi/dt)$ .

Essentially, the radar using this biphase code transmits a signal which is a vector of 13 subpulses; this vector contains a phasing element of the form  $e^{-j2\pi Ft}$  which is a complex exponential. This kind of signal can be transmitted intact because of tapped delay lines (matched filters). In contrast to frequency modulated codes, the

biphase coding-decoding operation involves simply the summation of  $N$  data samples, with no complex multiplications being required if the sample spacing is equal to the spacing of the subpulses of the transmitted code. This occurs because the phase values of the transversal matched-filter tap weights are multiples of 90 degrees.

On transmission, the desired biphase code is normally read out of a ROM, and is used to modulate the carrier to be transmitted. On reception, the echo signals are in-phase (I) and quadrature (Q) detected in order to eliminate the blind phases and to maximize the signal-to-noise ratio (SNR). In general, we code a transmit pulse and then use this modulation to effect compression through a digital tapped delay line, which acts as a matched-filter. Physically, this process is implemented with ADCs which are placed after the I and Q detectors (charge coupled devices), cascaded shift registers, and digital adders.

The biggest challenge that the biphase coding presents to the DDS-coded jamming signal lies in its autocorrelation processing. The autocorrelation output represents a compressed output in response to some point target; the autocorrelation is found by passing the received waveform through its matched filter, whereby the waveform is correlated with itself (hence, the term autocorrelation). The process of correlation per se merits some elucidation.

Correlation is a mathematical operation that closely resembles convolution. The objective in computing the correlation between two signals is to measure the degree to which the two signals are similar and, thus, to extract some information that depends to a large extent on the application. Specifically, we examine two signal sequences  $x(n)$  and  $y(n)$ , where  $x(n)$  represents the sampled version of the radar's transmitted signal and  $y(n)$  represents the sampled version of the received signal at the output of the ADC. If a target is present in the space being searched by the radar, the received signal  $y(n)$  consists of a delayed version of the transmitted signal,

reflected from the target, and corrupted by additive noise. The problem is to compare  $y(n)$  and  $x(n)$  in order to actually determine if a target is present, and if so, to determine the time delay (which is assumed to be an integer multiple of the sampling interval) from which we can calculate the distance to the target.

Mathematically, the correlation of our transmitted signal  $x(n)$  with itself (that is, where  $y(n) = x(n)$ ) is performed by the following operation: shift one of the sequences, multiply the two sequences, and then sum over all values of the product sequence. The autocorrelation of  $x(n)$  is defined [Ref. 10] as:

$$r_{xx}(l) = \sum_{n=-\infty}^{\infty} x(n)x(n-l) \quad (10)$$

or, equivalently

$$r_{xx}(l) = \sum_{n=-\infty}^{\infty} x(n+l)x(n) \quad (11)$$

where  $l = 0, +/- 1, +/- 2, \dots$

The index  $l$  is the time shift (or lag) parameter, and the subscript  $xx$  on the autocorrelation sequence  $r_{xx}(l)$  indicates the sequences being correlated. Of course, in dealing with finite duration sequences, we must express the autocorrelation in terms of the finite limits on the summation. In particular, if  $x(n)$  is a causal sequence of length  $N$  [i.e.,  $x(n) = 0$  for  $n < 0$  and  $n > N$  or  $n = N$ ], the autocorrelation may be expressed as

$$r_{xx}(l) = \sum_{n=i}^{N-|k|-1} x(n)x(n-l) \quad (12)$$

where  $l = 1, k = 0$ , for  $l > 0$ , and  $l = 0, k = 1$ , for  $l < 0$ .

We note that the autocorrelation sequence of a signal obtains its maximum value at zero lag; this is consistent with the notation that a signal matches perfectly with itself at zero shift. Another important property of the autocorrelation function is the following:

$$r_{xx}(l) = r_{xx}(-l) \quad (13)$$

which means that the autocorrelation function is an even function (real process only).

Upon completion of the autocorrelation process, we get an output which is a compressed signal (compressed 3dB pulse length). Also, the effective amplitude of the peak response is 13 times that of the amplitude of the inserted coded pulse. Generation of the appropriate waveform is not what makes DDS so challenging, however. The challenge is Doppler; Doppler is the time-varying phase of an echo pulse which is produced by a target moving either toward or away from the radar during the time of interest. It must be accounted for in a predicted response of a pulse compressor by computing the compressor output for all expected Doppler. Doppler effect strongly favors the target radar in the use of the DDS technique, and as a result, merits further analysis.

The reason Doppler favors the target radar in the case of DDS jamming is that biphasic codes have very little tolerance for Doppler; performance is significantly degraded by moving targets. As my research has revealed, quadriphase coded radars have even less tolerance -- much less, in fact.

## **2. Doppler Effects**

As aforementioned, both biphasic and quadriphase coded pulses have very little Doppler tolerance, and, as a result, their performance is significantly degraded by

moving targets. In general, target motion results in Doppler frequency shifting, which the radar may attempt to measure; and platform motion may make it difficult to actually measure (or account for) the target Doppler frequency without knowledge of or compensation for the platform motion.

Mathematically, for a target moving relative to the radar, the returned signal experiences a Doppler shift given by [Ref. 4] the following:

$$\nu = 2 \frac{v}{c} f_{RF} \quad (14)$$

where  $v$  is the relative radial velocity between the target and the radar,  $c$  is the velocity of light, and  $f_{RF}$  is the radio frequency carrier of the transmitted signal. Actually, each frequency in the transmitted spectrum will be shifted an amount proportional to that frequency; in practice, the spectrum width is usually such a very small percentage of the RF carrier that it is assumed the entire spectrum is translated an amount  $\nu$ . According to Barton, negligible error results from this assumption.

The radar return signal, shifted an amount  $\nu$ , is modulated down to the I.F. range of the collapsing and weighting networks. The I.F. signal resulting from a moving target has a different center frequency than the signal of a stationary target. It is the effect of the collapsing and weighting network on the Doppler-shifted signals that must be calculated. Specifically, the DDS jammer must provide some means of interpolating the intermediate Doppler shifts.

The most important effect that the Doppler shift will have on the synthesis of a jamming signal is the incursion of mismatches. Mismatching effects show up in the peak-to-sidelobe response after the returned signal has been compressed. In particular, at very large frequency shifts (meaning a significant fraction of the radar bandwidth), the signal bandwidth becomes limited by the radar receiver's passband,

only passing a fraction of the original signal spectrum; this is apparent in the ensuing section of this thesis, "Observations and Evaluation." This bandwidth and signal energy loss causes the compressed pulse to widen in time as well as drop in amplitude. The increased pulse length induces another effect, which is that of reducing the radar's range resolution. Ultimately, the reduced peak amplitude reduces the PSR in the compressed pulse [Ref.9].

In summary, Doppler is arguably the most important consideration in the synthesis of jamming waveforms, particularly because part of our goal in jamming is to introduce false Doppler frequency shifts onto the repeated signal. According to Schleher and Pace, we can basically expect that a frequency mismatch on the order of .07 bandwidths (i.e., 140 kHz in the case of the TPS-70) would negate the effect of the coherent jamming in this application. In the DDS's favor, however, is one advantage: biphasic coding (of the carrier) is inherently a very well-developed phase coding technique, due to the fact that a radar system using binary phase code compression produces a waveform with both rectangular pulse and a rectangular amplitude spectrum; this is relatively simple to synthesize, and, most importantly, the high pulse compression ratio achieved will meet the range resolution requirements for deceiving the target radar system.

### **3.      Quadriphase Coding**

The quadriphase coded signal was introduced to radar by J.W Taylor, Jr. and has been successfully used in radar systems for the past 10 years. It is Taylor's model that has been used in this thesis to provide a major source of analysis regarding Direct Digital Synthesis [Ref. 11]. In general, the quadriphase coded radar signal is used in state-of-the-art radar systems, such as the TPS-70. This coded signal is extremely attractive for radars which use digital processing for Doppler filtering, pulse compression, and CFAR operation. We use Taylor's mathematical model to examine

the assertion that quadriphase coded signals out-perform the biphas coded signals -- at least from the target radar's perspective. In this section, we analyze the following aspects of the quadriphase technique: 1) synthesis of the quadriphase code from the biphas code, 2) quadriphase code characteristics -- specifically, the autocorrelation function, 3) the Doppler effect, and 4) the digital decoding process. These aspects combined represent precisely the span of consideration that will have to be given to synthesizing an effective jamming signal.

The quadriphase code has a very important relationship with the biphas code; in fact, the generation of the quadriphase is built squarely upon the biphas in that quadriphase is actually derived from the biphas code. A quadriphase code is one whose subpulses are phased in four states (in contrast to the two states of the biphas): 0, 90, 180, or 270 degrees; these states are actually coded as +1, +j, -1, or -j, respectively. The method used to convert the biphas to quadriphase is called the biphas-to-quadrphase (BTQ) transformation; this transformation has the property that the autocorrelation function and energy density spectrum from the code can be expressed in terms of the prototype biphas-code autocorrelation function, which we examine in detail later. To achieve the BTQ transformation, our DDS algorithm will start with the same 13 - chip Barker coded input (vector) that we used to generate our biphas coded signal

$$xx = [1 \ 1 \ 1 \ 1 \ 1 \ -1 \ -1 \ 1 \ 1 \ -1 \ 1 \ -1 \ 1] \quad (15)$$

where we have  $N = 13$  subpulses of width  $T$  at intervals of  $T$ . We indicate their phases by  $W_k$  (this is  $xx$ , with the phase terms factored in).

The key to the transformation is the application of some complex-valued function. Mathematically, we accomplish this by taking  $W_k$  and doing the following:

$$V_k = j^{s(k-1)} W_k \quad (16)$$

where  $V_k$  is now a quadriphase code containing  $N$  subpulses at intervals of  $T$ , and  $s$  is fixed at  $+1$ . It follows that each subpulse is of the desired phase values, 0, 90, 180, or 270 degrees. Essentially, what we have done is take each rectangular subpulse, and run it through a tapped delay line that has the appropriate phases built into the taps. Furthermore, we have a code which we can define as  $f(t)$  that can be resolved in terms of its in-phase and quadrature components -- a relationship that will ultimately result in a piecewise linear phase modulation over the entire pulse. Hence, we have  $f(t)$  such that

$$f(t) = i(t) + jq(t) = a(t)e^{j\psi(t)} \quad (17)$$

where  $a(t)$  is the amplitude modulation, and  $\psi(t)$  is the phase modulation. It follows that the amplitude and phase modulation functions can be expressed in terms of  $I(t)$  and  $q(t)$  as

$$a(t) = \sqrt{i^2(t) + q^2(t)} \quad (18)$$

and

$$\psi(t) = \tan^{-1}[q(t)/i(t)] \quad (19)$$

At this point, we take (16) and we represent each value as an impulse function at  $t = kT$  as

$$V_k(t) = j^{s(k-1)} W_k \delta(t - kT) \quad (20)$$

We can then represent the sequence of  $N$  impulse functions as  $d(t)$ , where

$$d(t) = \sum_{k=1}^N V_k(t) = \sum_{k=1}^N j^{s(k-1)} W_k \delta(t - kT) \quad (21)$$

This will be convolved with our modulator to form our transmit pulse.

We next discuss our modulator, since it represents perhaps the most pronounced contrast of the quadriphase code with the biphasic code; that is to say, the pulse shape. Recall, the biphasic code employs a rectangular subpulse. In contrast, the quadriphase features a subpulse with a half-cosine shape. Mathematically, this subpulse  $p(t)$ , our modulator, is actually the half-cycle cosine wave of length  $2T$ , whose 3 dB width is the spacing  $T$ . Hence,

$$p(t) = \cos(\pi t/2T) \quad (22)$$

for  $-T \leq t \leq T$ . This shape eliminates the spectral splatter that results from the phase steps associated with the rectangular subpulse.

The final step in the formation of our quadriphase coded transmit pulse  $f(t)$  is applying our half-cosine subpulse  $p(t)$  to modulate the impulse function outputs  $d(t)$ . This is accomplished by convolving the functions, giving

$$f(t) = p(t) * \sum_{k=1}^N j^{s(k-1)} W_k \delta(t-kT) \quad (23)$$

which finally becomes

$$f(t) = \sum_{k=1}^N j^{s(k-1)} W_k p(t-kT) \quad (24)$$

Now  $f(t)$  is expressed as a sequence of subpulses whose phase is  $W_k j^{s(k-1)}$ , where odd values of  $k$  yield the in-phase component and the even values yield the quadrature portion of  $f(t)$ . The code that we generate looks as follows:

$$V_k = [+1 \ +j \ -1 \ -j \ +1 \ -j \ +1 \ -j \ +1 \ -j \ -1 \ +j \ +1] \quad (25)$$

We observe that this equation reads the same backwards as forwards, which shows the symmetry that gets obscured in the binary representation. Figure 3.6, "Transmit Pulse (Uncompressed)," combines the effects of (21) through (24) in graphic format, showing the signal envelope, the real part of the signal (the  $I(t)$  component), and the imaginary part of the signal (the  $q(t)$  component).

Next we examine the autocorrelation function. Recall, the most important operation of the biphase coding was the autocorrelation process. Autocorrelation is an important feature in quadriphase coding, too. It is important because it's proportional to the matched-filter response in the noise free condition and thus represents the compressed pulse in an ideal pulse compression system. Autocorrelation with the quadriphase coding is much more complicated, however, because the signal autocorrelation is actually a series of a combination of autocorrelation functions: the autocorrelation function of our biphase tapped delay line elements ( $W_k$ ), the autocorrelation function of the quadriphase tapped delay line elements ( $V_k$ ), and the autocorrelation function of the subpulse  $p(t)$ . The expression for the quadriphase signal autocorrelation function, then, is given by

$$\phi_q(t) = \sum_{m=-(N-1)}^{N-1} j^{sm} \phi_b(m) p_T(t-mT) \quad (26)$$

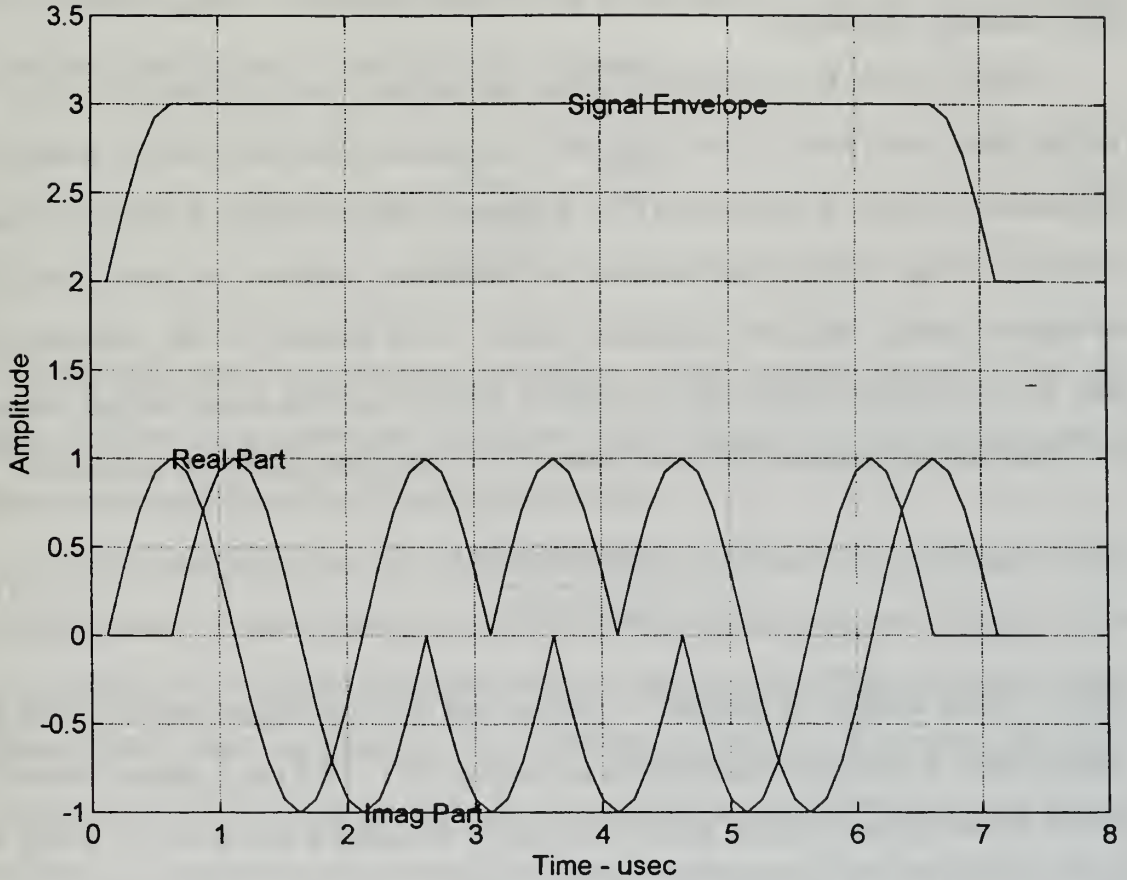


**Figure 3.6. Uncompressed Transmit Pulse Signal Modulation**

where  $\phi_b(m)$  is the autocorrelation function associated with  $W_k$ ,  $j^{sm}\phi_b(m)$  is the autocorrelation function associated with  $V_k$ , and  $P_T(t)$  is the autocorrelation function associated with subpulse  $p(t)$ . In general, the autocorrelation function of the quadriphase code signal is a linear combination of shifted versions of our half-cosine subpulse  $P_T(t)$ , each scaled by the product of  $j^{sm}$  and the biphasic autocorrelation function value at the value of the shift.

A quadriphase coded DDS signal will pass through two follow-on states before being passed to the radar's pulse compressor: the first state will incorporate Doppler effects, and the second state will incorporate a special kind of matched-filtering based upon Gaussian excitation.

Recall, when the transmitted signal encounters a moving target it incurs a Doppler shift. As a result of this shift, the compressed-pulse peak value is reduced, the sidelobe structure is altered, the PSR is reduced, and ultimately, a mismatch loss is accrued. In fact, the Doppler behavior of quadriphase codes is the same as that of the biphasic codes, which we described earlier. If we assume that the compressed pulse for the Doppler shifted case is sampled at the peak value and at integer values of  $T$ , then the magnitude of the peak value of the compressed pulse  $u_p$  is given by

$$u_p = \frac{\sin(N\pi f_d T)}{\sin(\pi f_d T)} \quad (27)$$

where  $N$  is the number of samples. It follows that the degradation resulting from a Doppler shift is considered acceptable as long as  $Nf_d T < 0.3$  (as a general rule-of-thumb), which means that the phase shift across the pulse is less than  $(0.3)(360) = 108^\circ$ . For  $Nf_d T = 0.3$ , the peak value in (25) relative to the zero Doppler peak value of  $N$  is 0.86, a 1.3 dB decrease in peak value. We experiment with Doppler effects in the follow-on section "Observations and Evaluations."

The next state that our quadriphase coded pulse will go through is matched filtering. Here we employ what is called a Gaussian filter. For the half-cosine impulse response, the matched filter must have a half-cosine impulse response, which is why we design a filter with approximately a Gaussian response. We begin with the transfer function for a Gaussian filter with gain of one:

$$H(j\omega) = e^{-2k(\omega/\Delta\omega_0)^2} \quad (28)$$

where  $k = 2(\ln 2) = 1.386$ . This lowpass response is attenuated 6 dB at  $\omega = +\Delta\omega_6/2$ , which is the 6 dB bandwidth of  $\Delta\omega_6$ . We note that because including the usual linear phase only causes a constant delay in the filter response, we set the filter phase function equal to zero. Now, the filter response is

$$h(t) = \frac{\Delta\omega_6}{2\sqrt{2\pi k}} e^{-\frac{(\Delta\omega_6 t)^2}{8k}} \quad (29)$$

And this response is also a Gaussian function, which is symmetric about  $t = 0$ . We then convolve our transmit pulse with this Gaussian filter prior to pulse compression. We will observe the actual physical effects later.

The final stage that our DDS-coded signal will have to go through is pulse compression. A transmitted pulse with the appropriate Doppler shifting will be passed through some kind of decoder, which is the case of the TPS -70 radar is a non-linear coded pulse anticlutter system (CPACS) decoder. The CPACS provides a control of the CFAR under a wide variety of conditions. The CPACS decoder is most effective in radars with pulse lengths less than 13 microseconds, because false alarms for i.e., rain clutter are controlled only when the transmitted pulse length is shorter than the diameter of the storm cell.

The CPACS decoder uses a phase detector giving the following outputs:

$$I'_n = K \cos(\phi_n) \quad (30)$$

$$Q'_n = K \sin(\phi_n) \quad (31)$$

where  $\phi_n$  is the phase angle of the  $n$ th range sample, and  $K$  is some constant. The phase detector ignores any amplitude variations, giving an output waveform with a pulse shape that is similar to the original biphas code. Also, since the CPACS which is used by the TPS-70 is digital, it produces samples of these waveforms which are at intervals equal to the subpulse spacing; additionally, digital CPACS decoders introduce some statistical deviation due to the fact that phase is quantized to a finite number of bits. The final output of the decoder is a pulse that is compressed, having a much lower mismatch loss than that incurred by the biphas code process.

#### **4. Summary**

We have examined the two most prevalent forms of coding for radar use that our DDS will encounter as a jammer: the biphas coded radar signal, which was adopted for earlier radar systems such as the TPS-43, and the quadriphase coded radar signal, which has been adopted for newer radar systems such as the TPS-70. We have analyzed the actual synthesis process from a mathematical perspective -- in the quadriphase case, based upon the mathematical model as described by J.W. Taylor, Jr. In the ensuing section we apply the techniques outlined so far, and analyze the data we produce.

### **D. OBSERVATIONS AND EVALUATIONS**

The Direct Digital Synthesis technique must incorporate many different effects in order to be a viable choice for Stand-Off Jamming. Up to now, we've presented analysis of current radar technology, different methods of synthesizing signals, and we've briefly discussed the challenges inherent in performing DDS. In this chapter we present results of actually trying to apply the techniques, with focus on the advantages and disadvantages that have become apparent through experimentation and research. This has been accomplished with computer application and cross analysis. We present both biphas and quadriphase coding results and observations.

## 1. Biphase Coded Results

To simulate what the DDS will have to do, we obtained results via a MATLAB computer program entitled PCMISS.M (see Appendix A). This program allows for investigation of pulse compression frequency mismatches which might be incurred during synthesis of a biphase coded signal. Essentially, we apply a 13 - chip Barker code (vector) which has all the properties we mentioned earlier. In general, we expect that an  $N$  - element autocorrelated code will produce a compressed waveform peak value of  $N$ , with peak sidelobes all equal to 1.

As aforementioned, one of the primary challenges of pulse coded waveform generation is accounting for the Doppler effect; in this case, this simply involved including our MATLAB code a phase shifting term " $f_d/BW$ ," which is designed to discretely place a phase element upon each subpulse output. The actual test procedure involved changing the frequency inputs in sequence, and then examining the change in magnitude of the peak response. Figures 3.7 through 3.17 show the effects of frequency mismatching against a 13 - chip Barker coded pulse compression waveform.

We start with a zero frequency input (stationary target); the result is a perfectly symmetrical  $\sin x/x$  waveform, with a peak lobe of magnitude of 13, and a peak sidelobe at 1 (Figure 3.7) -- and this is exactly what is expected. However, the change is relatively dramatic when we include some frequency change (Figure 3.8,  $f_d/BW=.01$ ); we incur a mismatch response, as evidenced by the reduction in main lobe response from 13 to 12.64, and sidelobe increase to 1.854.

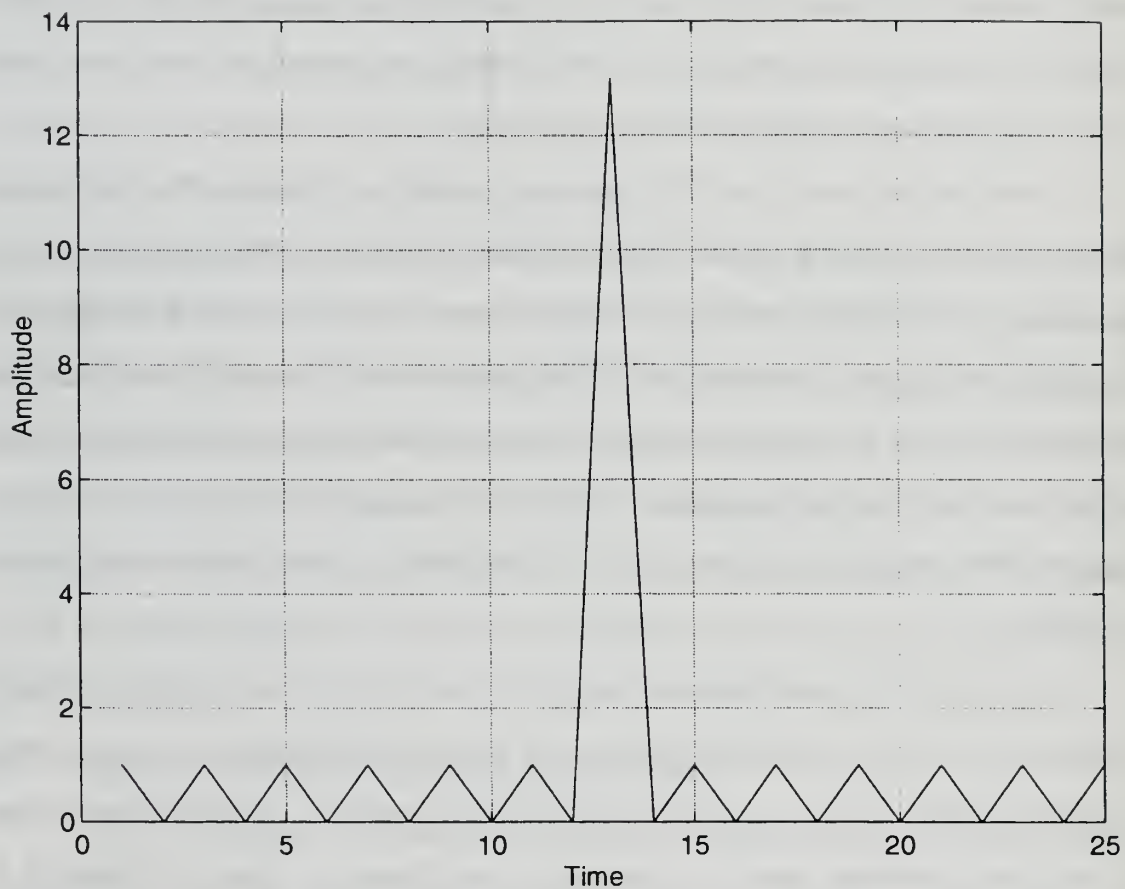


**Figure 3.7. Biphase Coded PC,  $f_d/BW=0.0$**

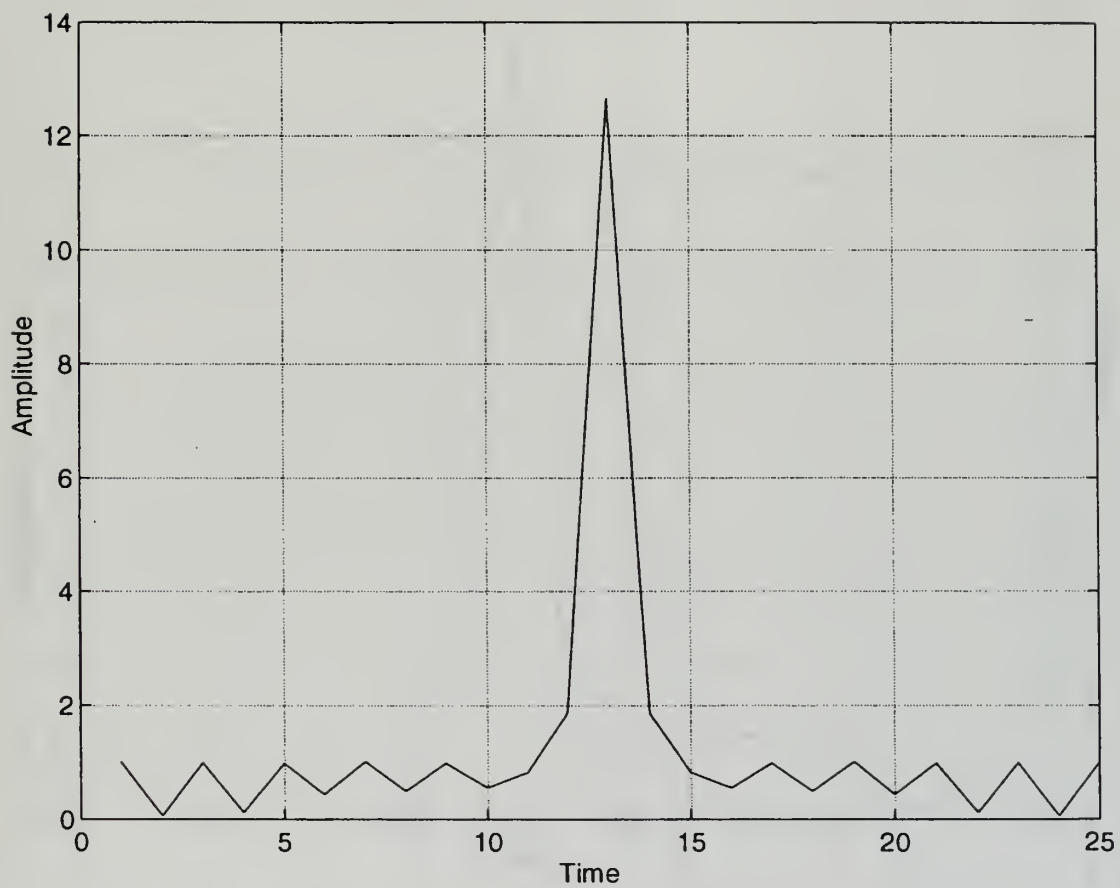


**Figure 3.8. Biphase Coded PC,  $f_d/BW=0.01$**

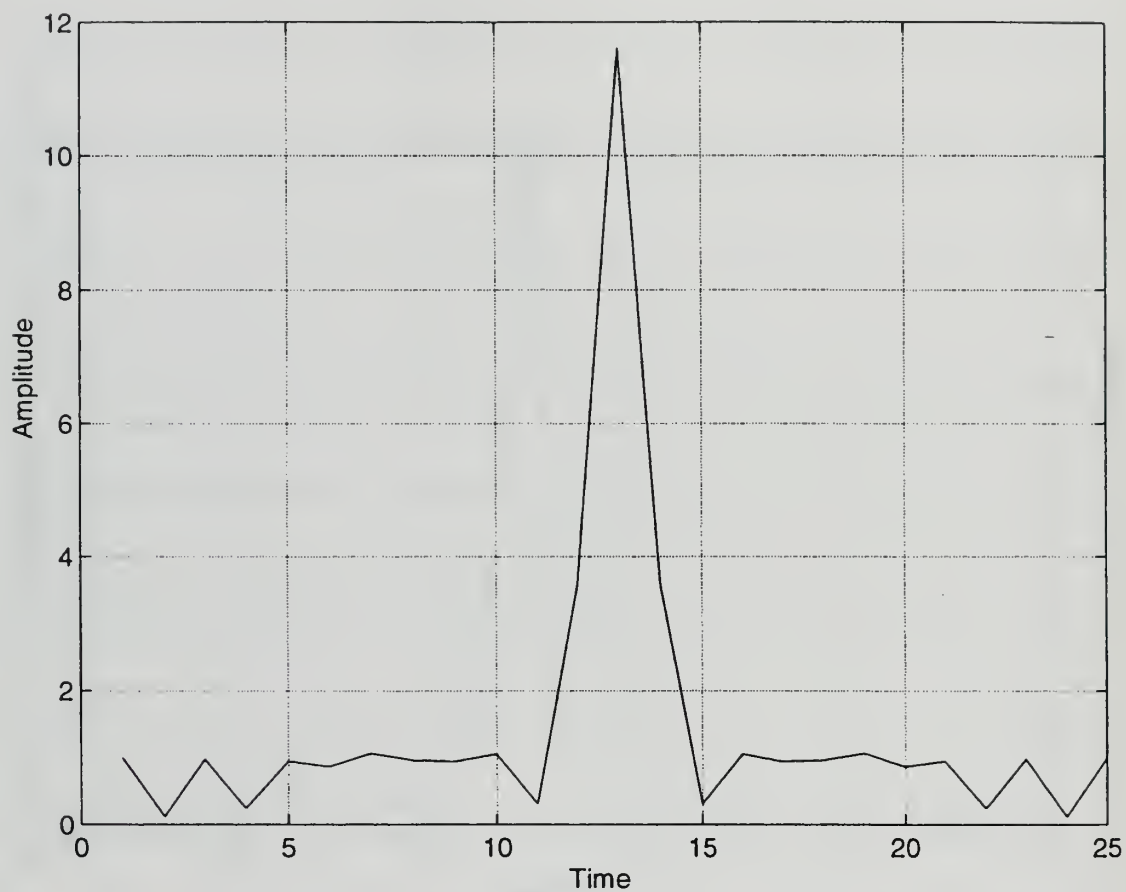


**Figure 3.9. Biphase Coded PC,  $f_d/BW=0.02$**

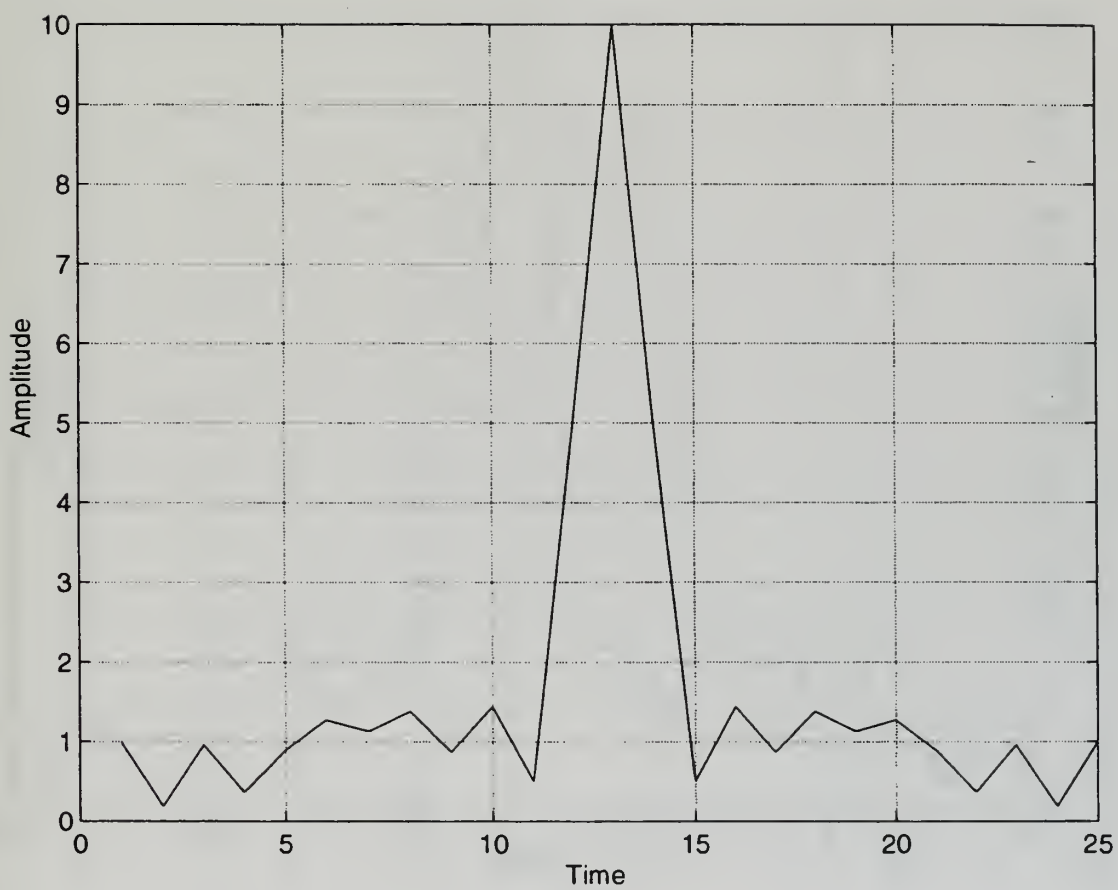


**Figure 3.10. Biphase Coded PC,  $f_d/BW=0.03$**

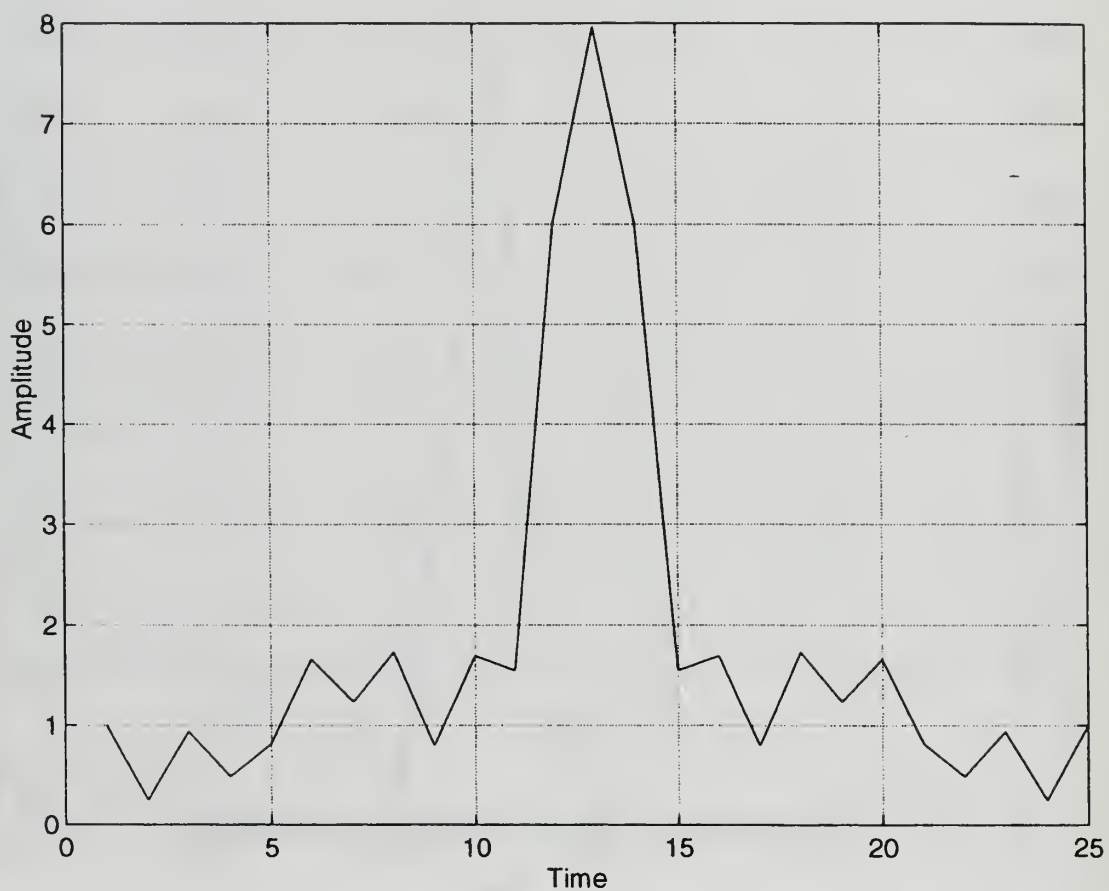


**Figure 3.11. Biphase Coded PC,  $f_d/BW=0.04$**

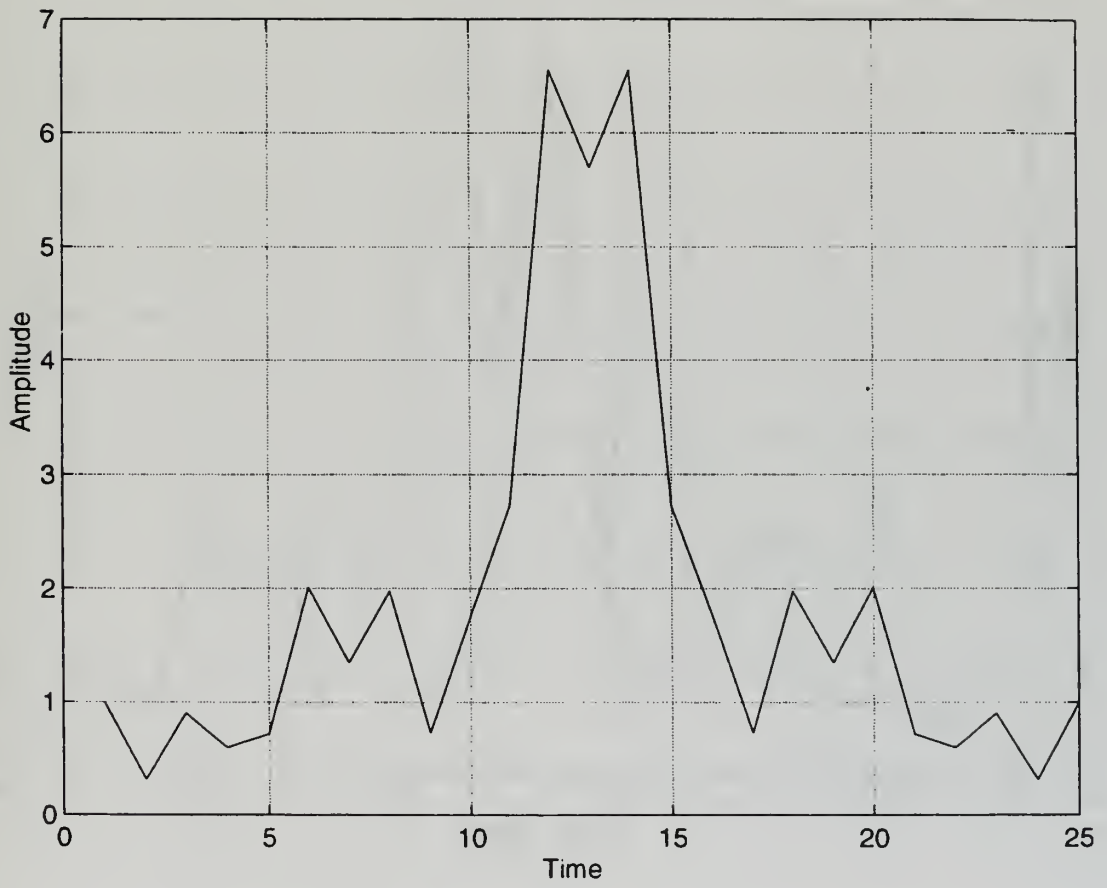


**Figure 3.12. Biphase Coded PC,  $f_d/BW=0.05$**

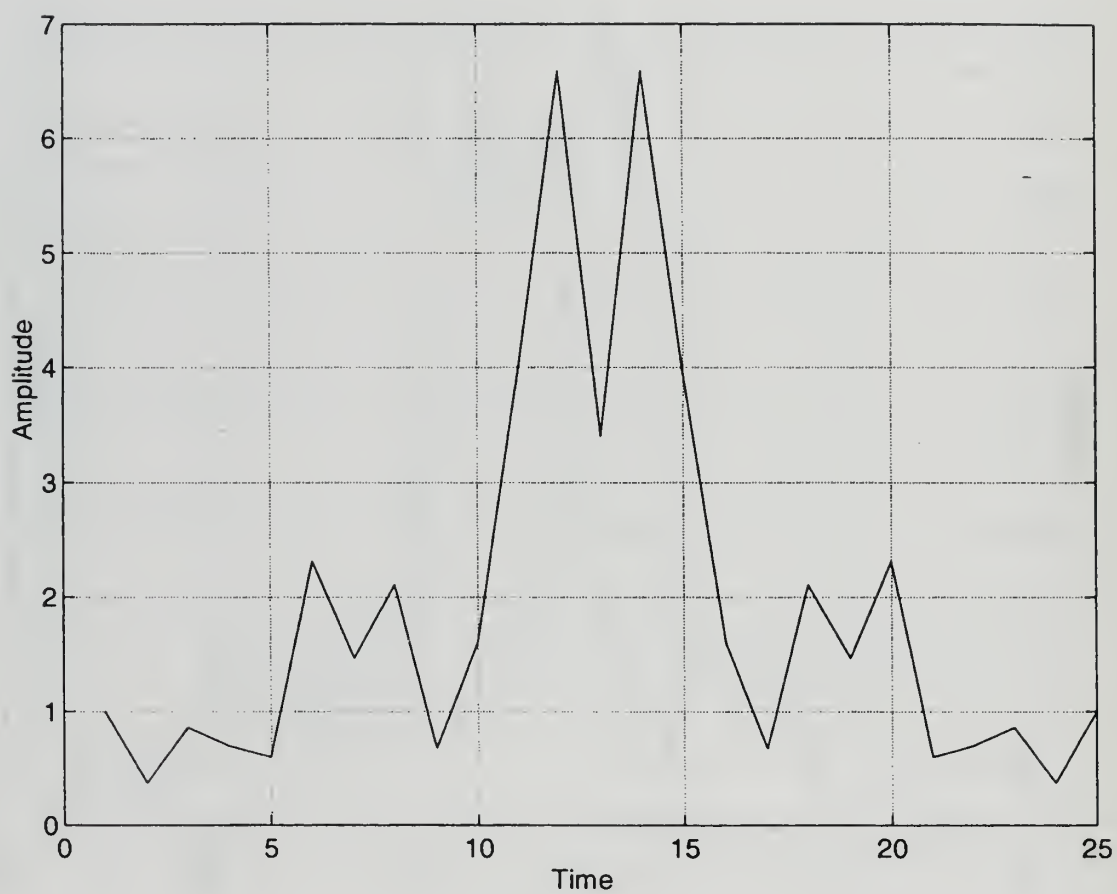


**Figure 3.13. Biphase Coded PC,  $f_d/BW=0.06$**

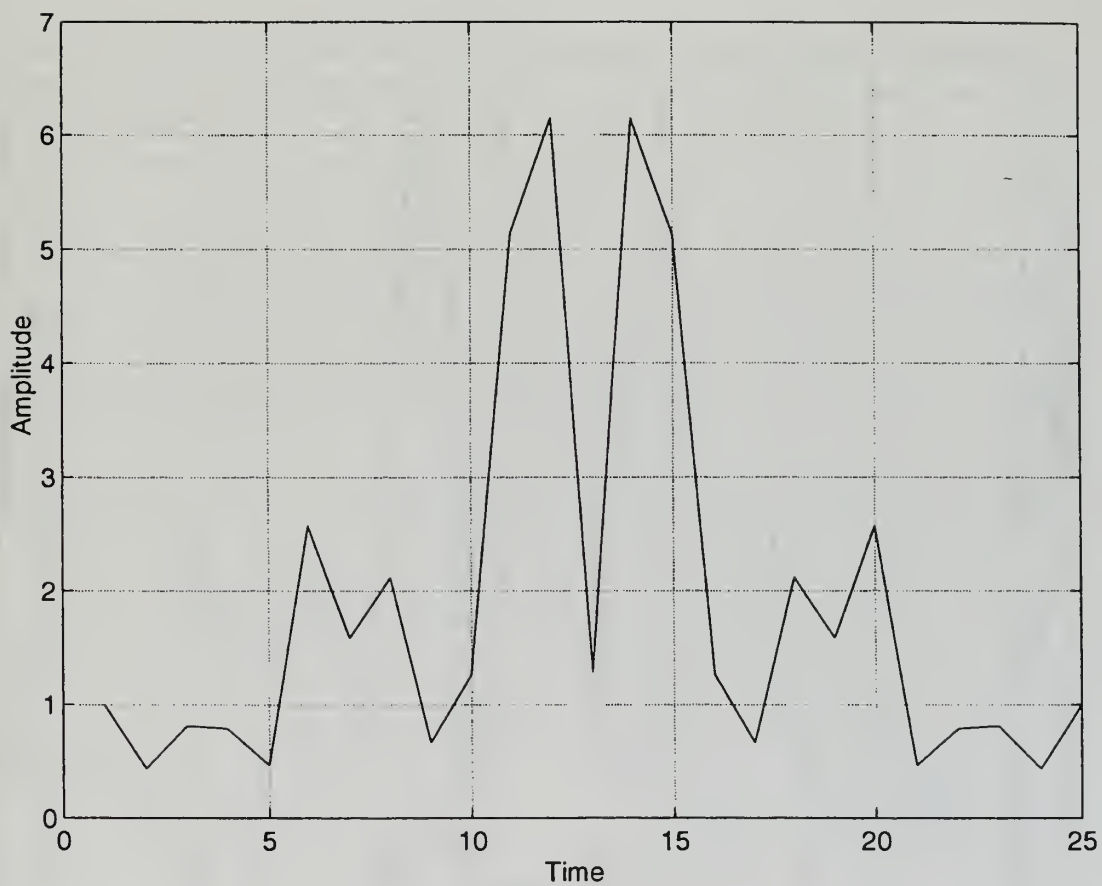


**Figure 3.14. Biphase Coded PC,  $f_d/BW=0.07$**

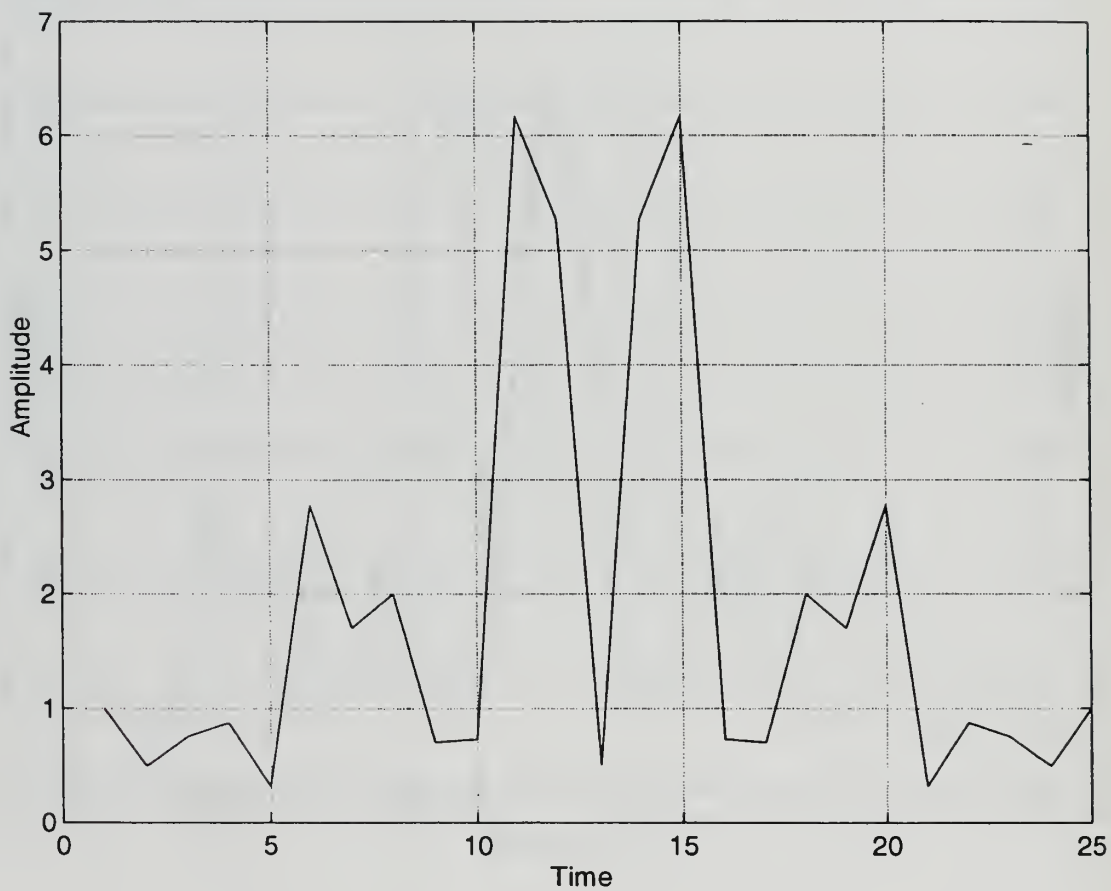


**Figure 3.15. Biphase Coded PC,  $f_d/BW=0.08$**

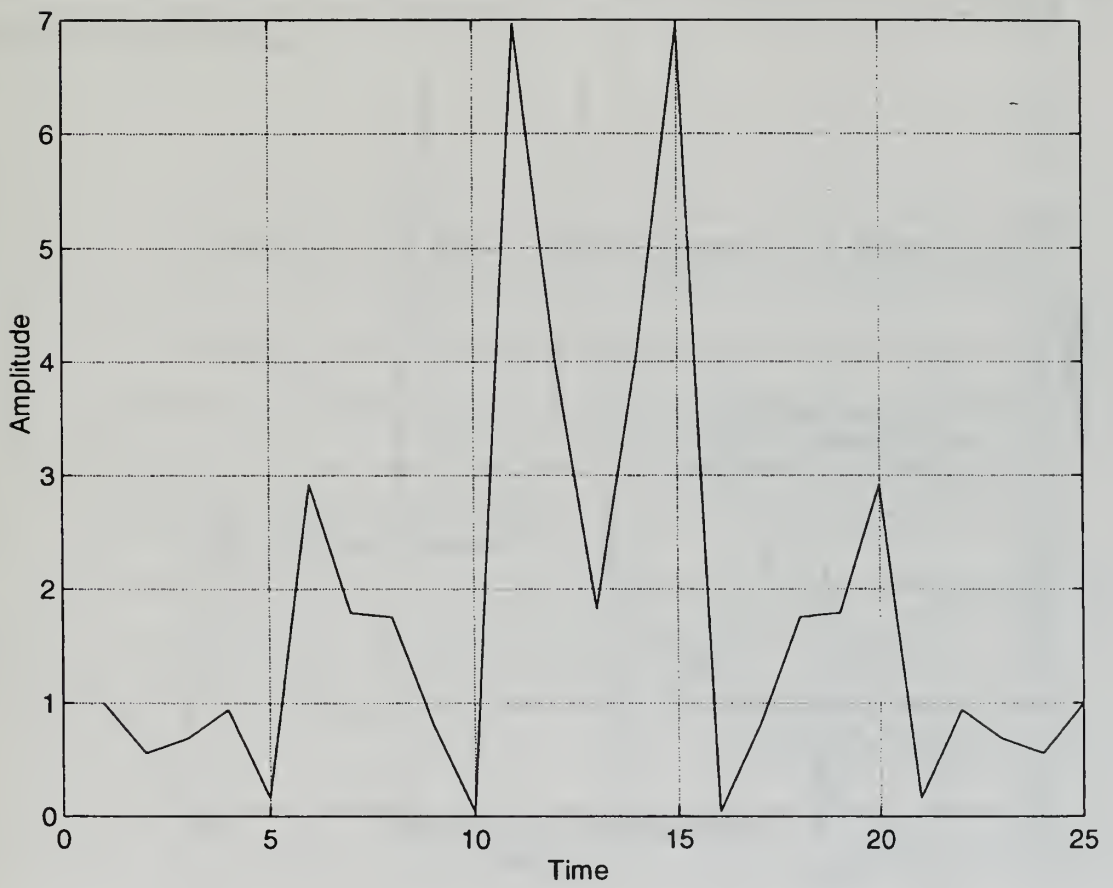


**Figure 3.16. Biphase Coded PC,  $f_d/BW=0.09$**

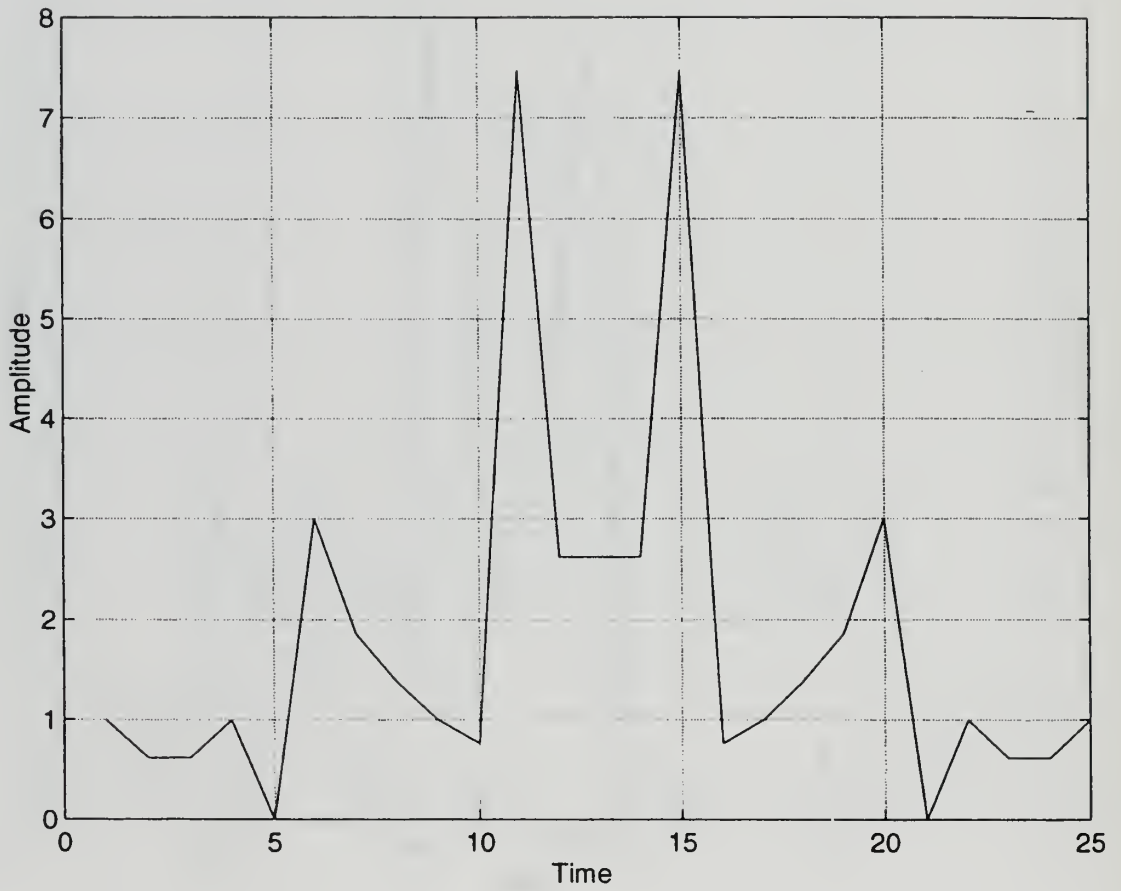


**Figure 3.17. Biphase Coded PC,  $f_d/BW=0.1$**

This changing of output increases geometrically as we increase the frequency offset. This is consistent with everything that we have discussed about the challenge of DDS as a DEA technique. Figure 3.18 really sums up this challenge in terms of frequency mismatches; in particular, what these results tell us is that a frequency mismatch on the order of .07 bandwidths as we pointed out earlier, which would negate the effect of coherent jamming in this particular application. This is significant because it confirms the assertion we made that systems employing biphas coded waveforms have a very low tolerance for Doppler shifting (or more precisely, for frequency mismatching).

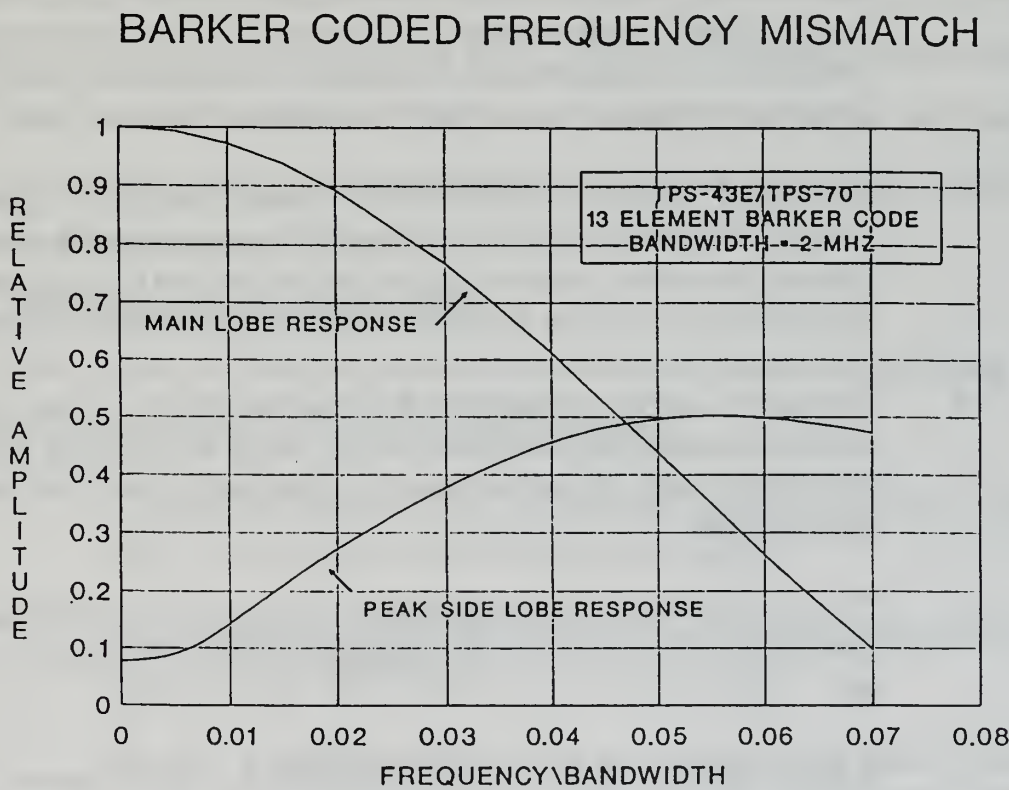


**Figure 3.18. Biphas Coded Frequency Mismatch**

## **2. Biphase Code Observations**

What follows is a listing of observations made in the course of researching and gathering empirical data for the biphase procedure.

1. The primary disadvantage of the biphase coded pulse is that it may be becoming obsolete as a coding technique with the advancement of technology.
2. The use of pulse compression techniques and matched filtering favor the DDS jammer and the target radar equally. These biphase waveforms produce rectangular pulses which are relatively easy to synthesize, as is the application of a frequency shift for the output.
3. Biphase DDS jamming is a procedure that is readily adaptable to time multi-plexing; with this operation the DDS can be used to jam several threat radars simultaneously. Alternatively, the employment of multiple accumulators makes it possible to simultaneously synthesize jamming waveforms for several threat radars at the same time.
4. The energy density spectrum of the biphase generated signal was determined to fall off at 6 dB per octave. This is important because this is used to determine emission bandwidth (which must meet government specifications in order to minimize interferences with other equipment).
5. The use of a Barker code affords the radar two things: 1) the sidelobe structures contain the minimum energy that is theoretically possible, and 2) this energy, as we have shown, is uniformly distributed among the sidelobes.
6. The 13 - bit Barker coded pulse that we used produced a peak sidelobe level (PSL) of -22.3 dB and an integrated sidelobe level (ISL) of -11.5 dB.
7. Range-sampling loss has proven to be about 2.3 dB for biphase coded signals; range sampling loss is the increase in SNR required to achieve a specified probability of detection under random sampling conditions, as compared to the optimum sampling at the pulse peak. We note that

double-sampling of a biphasic code can reduce its range-sampling loss to 0.8 dB.

### **3. Quadriphase Code Results**

A computer program was written to obtain the quadriphase response; it is based upon the Taylor's mathematical model described above. The program performs the BTQ transformation, which derives the quadriphase signal from the biphasic signal; mathematically, this is a simple process. Once the appropriate output was obtained, the transmitted pulse was generated, passed through the Gaussian filter, and finally compressed in a decoder. Figures 3.19 and 3.20 display the outcomes in two different forms: a) Relative Amplitude, and 2) Relative Gain (dB). What is evident is that we get a response similar to that of the biphasic, but with a vastly improved sidelobe level; where we obtained a PSL of -22.3 dB for the biphasic, we obtain better than -45 dB for the quadriphase. This is quite dramatic! Regarding the Doppler effect, according to Taylor, both quadriphase and biphasic waveforms are equally tolerant to frequency mismatches.

### **4. Quadriphase Code Observations**

What follows is a listing of observations made in the course of researching and gathering empirical data for the quadriphase procedure.

1. The half-cosine shape of the quadriphase coded subpulse will highly favor the radar system in a jamming environment.
2. The quadriphase code affords the TPS-70 system with achievement of range sidelobe levels which are -45 dB and lower.
3. The BTQ transformation allows the quadriphase coded pulse to benefit from all of the biphasic features, in addition to its own inherent features; this includes the PSR = 13, and PSL = 1.

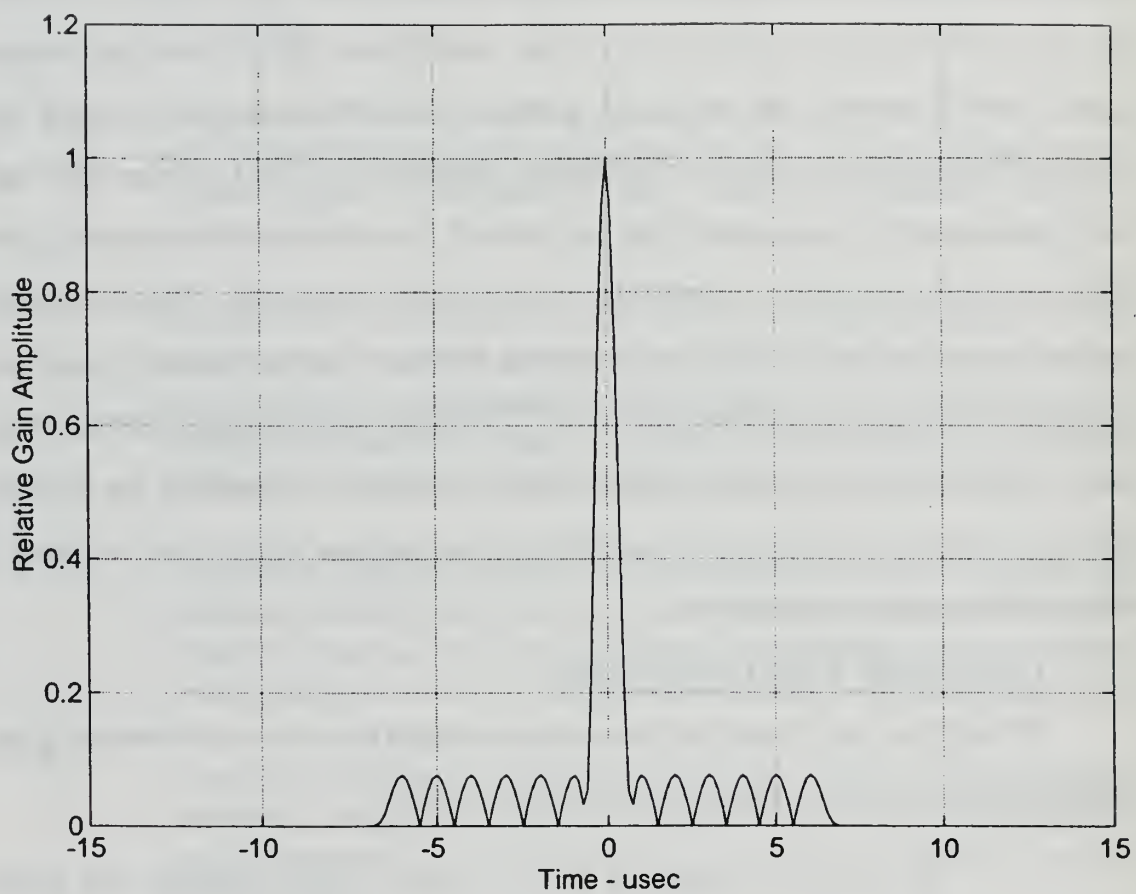


**Figure 3.19. Compressed Pulse Response (a)**

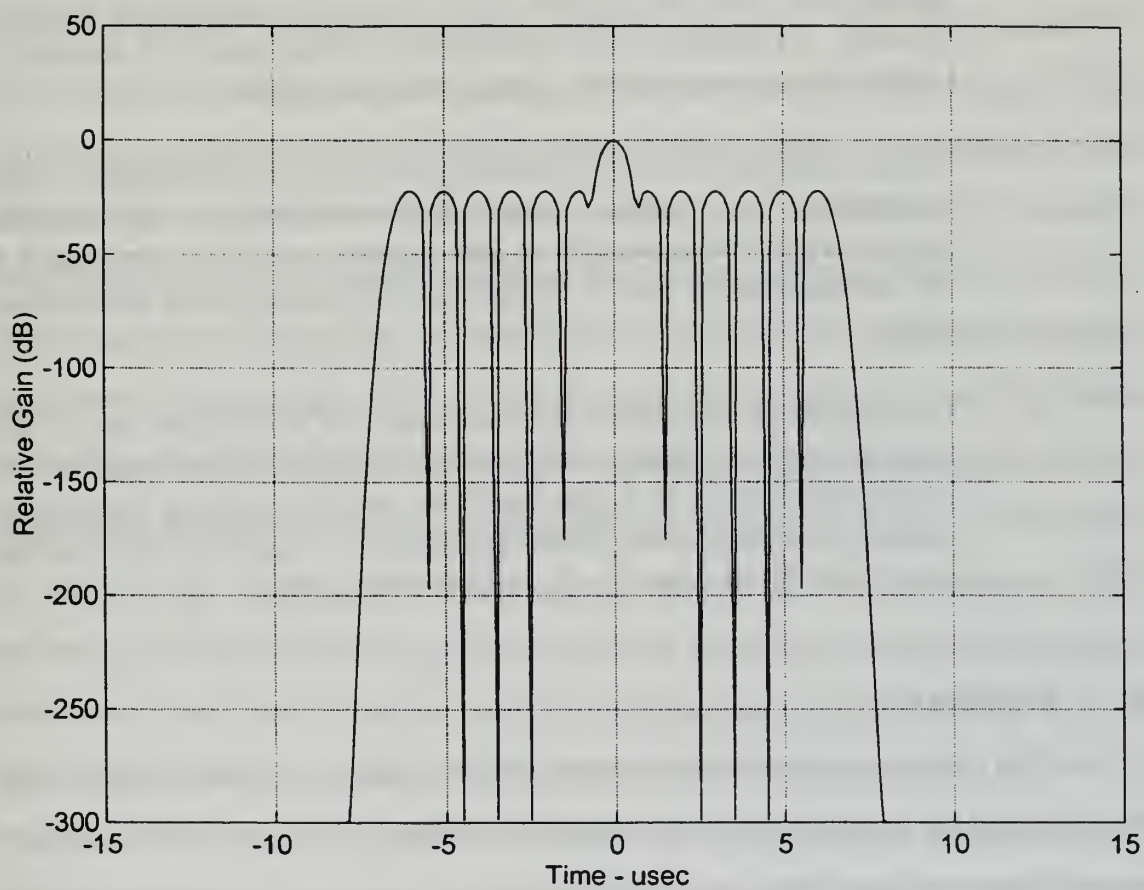


**Figure 3.20. Compressed Pulse Response (b)**

4. The radiated spectrum fall-off of the quadriphase code is a distinct improvement over the biphas-coded spectrum fall-off; specifically, the quadriphase code fall-off is about 12 dB per octave, in contrast with the 6 dB fall-off of the biphas. This is a by-product of the use of the half-cosine shape subpulse. Also, the Gaussian filter at the receiver improves the rejection capability of off-frequency interference. Regarding the mismatch losses, 0.1 is considered nominal for the quadriphase, and this is about .4 dB less than that associated with the biphas. Collectively, this represents an outstanding EP capability which will prevent the radar system from deception.
5. Range sampling loss is yet another area where the quadriphase code outperforms the biphas code; when averaged over all possible locations of an echo, relative to data samples, the loss is less than 0.8 dB, as compared to the 2.3 dB loss that we observed with the biphas code.
6. In comparison with linear and non-linear FM waveforms, one of the biggest benefits of using quadriphase coded signals is the simplicity of pulse compression in digital hardware and the resulting increase in speed; the biphas code shares this benefit. In general, this benefits equally the DDS as well as the target radar system.

## **E. SUMMARY**

This chapter examined the technique of DDS. This involved analysis of the theory behind the technique, the mathematical foundation, and a quantitative comparison of biphas and quadriphase radar signal synthesis methods. We emphasized the most critical challenges facing the DDS as a DEA technique, namely the ability to match the actual radar waveform. These factors all weigh in when we consider which jamming techniques will be the most effective for the current SOJ requirements. Above all, the DDS technique can be considered a very viable option for the SOJ mission. Whether or not it's a better option than other methods, such as the DRFM is the subject of the next chapter.

## IV. THE DIGITAL RF MEMORY TECHNIQUE

### A. INTRODUCTION

Modern radar systems have become "smarter" with the vast improvement in EA technology. These systems are designed with matched receivers and can produce coherent spread spectrum emissions which provide a very high degree of discrimination against unwanted signals, interference, and noise jamming. This is important because early radars were designed using produce non-coherent pulse trains, and as a result, were vulnerable to noise jamming. The primary EP available was the directivity of the antenna, because the receiver itself responded to any energy present within its bandwidth, which allowed the signal to be squelched if the noise power was high enough. So, as a means of updating the effectiveness of the radar system, particularly the EP aspect of discrimination between incoming signals, the engineers were able to develop systems designed with matched filters -- systems such as the TPS-70. herein lies the challenge for electronic counter measures; DDS technology proposes generating a smart waveform based upon parameter information intercepted and stored in the jammer. The problem here is that the jam form is not necessarily coherent. It stands to reason then that EA techniques (i.e., against RF missile systems) might be enhanced when the EA equipment has the capability of preserving the radar waveform for subsequent deceptive retransmission to the target radar system. This is precisely the reasoning behind development and implementation of the digital RF memory (DRFM); that is, it is a tool which allows the EA technique to employ deceptive modulation on a replica of the radar waveform at precisely the optimum time for maximum deception.

In this chapter we analyze the DRFM technique. As with the previous chapter covering DDS, we begin with an examination of the technique at the conceptual stage

as an application for radar development as well as a DEA option; specifically, we examine the theory followed by a look at the actual technique of how the DRFM generates a smart noise jamming waveform. In the course of examining this technique, we re-focus our attention on the primary challenges involved with employing the DRFM jamming technique; in particular, we analyze the ability for the DRFM to store multiple signals. This ability (or the lack thereof) represents a very distinct measure-of-effectiveness for this technique. In the section "Observation and Evaluations," we apply a MATLAB program which allows us to empirically examine the effects of multiple signal storage, and subsequently, we evaluate how much trade-off is involved with different DRFM techniques. These results will serve as a fundamental basis for comparison and contrast with the DDS technique, which we do in the following chapter.

## **B. THEORY AND OBJECTIVE**

### **1. Theory**

A digital radio frequency memory (DRFM) is a high speed, analog-to-digital converter and storage system which provides the capability to sample, process, and play back RF signals with minimum loss of fidelity. The first DRFMs employed from 1973 - 1975 were designed to replace the recirculating microwave memory for repeater function in EA systems. During the 1970s, companies such as Westinghouse, Raytheon, the Whittaker Corporation, and Design Electronics Laboratories began building DRFMs. Needless to say, because of the relatively recent development of the DRFM, as compared to analog radar technology development, there are many unanswered questions regarding its viability as a deceptive EA technique.

The conception of the DRFM as a DEA technique has revealed a great deal of potential and possibility; it has presented the possibility for much greater manipulation of an intercepted signal, as well as create a new dimension for EA, in

general. Recall, the purpose of DEA is to do two things: first, we introduce signals into the enemy's system, with the intent of degrading the performance of that system; second, the signal that we inject must be able to accurately mask the actual transmit signal with suitably modified replicas of the actual signal. This is in significant contrast with noise jamming. Now, both the DDS and the DRFM smart noise jammer's attempt to replicate the target radar's signals, which leads to a much more efficient application of energy to jam the radar, particularly important in a dense threat environment. But the jamming waveform understandably requires an appreciable amount of knowledge of the target radar. Early radar deception methods involved the reception of interrogating waveforms, followed by a relatively short time delay and reradiation to mislead the enemy trackers [Ref. 12]. But advancements in technology have made this technique obsolete. Coherent radars, particularly those that are employed by 3-D search radar systems such as the TPS-70 and in RF missile guidance systems, have considerably changed the dynamics for effective EA operations. Coherence is the proverbial fork-in-the-road that forces us to make a decision between whether to apply a DDS or a DRFM, because -- as we have examined -- the DDS technique does not assume coherence in the synthesized waveform; rather, we must account for it during the synthesis process. In contrast, an inherent feature of the DRFM-generated jam waveform is that we assume coherence. This concept of coherence merits attention, from both the radar and the jammer perspective.

Coherent transmitted pulses have a phase continuity from pulse to pulse as if they were gated portions of a continuous RF signal. In fact, coherent pulses are most often generated as a low-level continuous RF signal and then are processed by one or more stages of pulsed amplification. This is in contrast to pulse trains generated by

pulsed oscillators (e.g., magnetrons), which have random starting phase compared to some continuous wave reference oscillator -- this is non-coherence.

An important benefit of transmitting coherent pulses is that a sequence of return pulses can be subjected to Doppler analysis. The Doppler analysis bandwidths are actually very small compared to I.F. bandwidth; hence, the process provides a signal-to-noise improvement. The most important benefit, however, is the ability to differentiate among relatively small differences in velocity. This is the primary purpose of Doppler filtering; that is, to sort incoming signals on the basis of their Doppler frequencies, thereby allowing rejection of unwanted signals.

Coherent signal processing requires that both the amplitude and phase of signals be used in the process. Therefore, in coherent systems which use digital signal processing, each signal sample must specify both amplitude and phase or their equivalents. We accomplish this by using complex numbers to represent each signal, and lowpass filters, which perform averaging and then pass only the frequencies contained in the signal modulation amplitude  $A(t)$  and phase  $\phi(t)$ . The actual circuit (detector) used removes the signal from the carrier, but it preserves the signal phase information; as a result, the coherence is preserved. Coherence also allows the radar to provide large processing gains against interfering noise-like signals such as non-coherent jamming waveforms; the result of increased processing gain is a dilution of the effective jamming power with respect to the available target power. We will examine the mathematics a little more closely in the next section entitled "The DRFM Technique."

Regarding coherent jamming, we point out that it is best performed using two phase synchronized sources, which are designed to tolerate large angular errors. This kind of jamming imposes severe requirements both on the amplitude match between the sources and maintaining a phase differential of 180 degrees. The key to

effectiveness is maintaining the phase relationship, as is determined by the echo Doppler. A coherent system generally "knows" the phase of each illumination pulse prior to transmission and can compare the phase of any echo to it. In the context of the DRFM, it must be able to intercept the illumination signals, and store the signal intact -- "remembering" it. The built-in playback capability preserves the phase information and allows coherent processing in the receiver of the radar. The advantage of coherent processing is that the signal energy of a simple pulse can be added directly to previous pulses. For a train of  $N$  pulses, coherent processing can theoretically give a maximum  $N^{1/2}$  improvement over non-coherent processing [Ref. 9]. Subsequently, this coherency by the DRFM affords the capability to detect and process lower power signals as well as implement countermeasures which affect the signal phase. Hence, maintaining the coherence relationships is what distinctively differentiates the DRFM from the DDS as a smart jamming tool, as well as distinguishing it from all other jamming methods.

Having given due consideration to the coherence aspect, we note that technological advances in the areas of analog-to-digital converters and memories have made it possible to sample and store signals that were previously processed with analog techniques. The capability of the DRFM to digitally record, store, and reconstruct the received signal offers significant enhancements over analog low-speed techniques. This is what gives the DRFM viability as a jamming technique. An array of apparent targets can be simulated which impart range, angle, or velocity information to the victim radar; these targets can be false, misleading, or nonexistent. And since the DRFM preserves the coherence relationship, particularly the phase of the incoming signal, retro directive jamming signals can be generated with no need to measure or control the phase of the output signal. Additionally, we obtain a much

more effective use of jammer power, and this essentially removes the processing gain advantage of modern radars against noise-like jamming interference.

The process is straightforward. The target radar waveform is intercepted and subsequently converted down to baseband; this produces in-phase and quadrature components of the signal waveform. Then, an analog-to-digital converter (ADC) samples and digitizes the signal. The resultant I and Q waveforms are then digitally stored in the DRFM memory. Next, the I and Q waveforms are reconstituted in the DAC, but with appropriate modifications to accomplish deceptive jamming. Finally, the original down conversion oscillator is applied to provide a single side band up-conversion modulation of the I and Q samples, which produces the RF jamming waveform. Since we stored the threat radar's phase and frequency in memory, the RF jammer waveform can coherently jam Doppler radars as well as frequency hopping and pulse compression radars [Ref. 2].

As a DEA technique, we attempt to transmit the intercepted signal back towards the radar, transmitted with some modification and a suitable delay built into it with the aim of that signal being received as a target, and the real target being effectively masked. Furthermore, the false target then appears to be much farther away from the radar than the DRFM by a distance which is governed by the delay that we imposed during processing on our DRFM. It follows that the target will appear to be at some angular orientation which the radar antenna main lobe determines. Additionally, the DRFM can be used to create continuous radio signals by repeatedly playing back all or part of a stored signal. This, of course, will require some adjustment be made to the play-back signal as a correction measure for any discontinuities incurred to the phase of the signal; such a technique can be used to create continuous jamming signals.

This DRFM deceptive jamming technique has considerable appeal in addition to its coherence preservation feature. S.J. Roome highlights four of these factors [Ref. 13]. Firstly, once a radar signal has been intercepted and digitized, it can be stored indefinitely without degradation -- in contrast to analog storage methods; this holds an advantage over the DDS technique as well since the threat library doesn't have to be updated as often. Secondly, with a suitable high-speed memory design, several signals (conceivably) may be simultaneously recreated with different delays; we say "conceivably" because herein lies one of the primary challenges to this technique, which we will later examine in some detail. Thirdly, the amount of delay introduced by a DRFM may be adjusted in steps as small as one sample period. And, fourthly, a DRFM is inherently compatible with computer control so that systems with the short reaction times necessary for modern electronic warfare can be implemented.

The DRFM has some significant disadvantages associated with its technique which need to be addressed. The primary disadvantage lies in the fact that the technique employs digital signal processing which means that digitization errors are automatically incurred. Also, errors of implementation are incurred, and they result from a number of factors such as ADC and DAC non-linearities, dc offsets at ADC inputs, relative gain errors between I and Q channels, local oscillator coupling to RF inputs, clock jitter, and phase errors in quadrature phase shifters. The ultimate by-product is undesired spurs which advanced radar systems can detect and thereby recognize the signal as a DEA output. Consequently, when such signals are identified, they can be jam strobed and prevented from disturbing a radar's search or track loop. The spurs are produced in the digitization process, particularly when the RF signal is quantized into discrete levels. Other spurious effects (i.e., intermodulations), which we mentioned above, are due to non-linearity responses by mixers and

bandlimiting. We examine spurious effects and ways of mitigating them later in this thesis.

In general, the DRFM is a technique in which high-speed sampling and digital memory is used for the storage of radio frequency and microwave signals. The ability to coherently store and recall radio and microwave signals makes this technique a very viable deceptive jamming method in its capacity to store and recreate intercepted radar signals. In the next section, we examine the actual technique involved in the operation of a DRFM.

## **2. The DRFM Technique**

Thus far, we have examined the viability of using the DRFM for a DEA technique and the concept behind it; the DRFM is particularly attractive for the purposes because it can accurately store the threat radar's transmitted waveform for later transmission at a time of the EA designer's choosing. In contrast, repeater jammers and conventional transponder jammers were an attractive option in themselves, but repeater jammers can only amplify the radar signal and transmit it back to the radar, and transponder jammers can transmit complex waveforms back to the radar, but can not replicate the radar waveform with enough precision or fidelity. With the DRFM, precise replicas of the threat radar signal can be generated which contain the identical phase, frequency, and timing characteristics of the original transmitted signal. Here, we examine the technique involved in the process of generating the smart noise waveform with respect to the DRFM architecture. The architecture is somewhat more involved and sophisticated than that of the DDS, and this will have to be taken into account when we perform the final analysis in the next chapter of this thesis.

We begin with the components of the typical DRFM. At a minimum, the DRFM consists of the following components: a synchronous detector (consisting of

a down-converter and a local oscillator), and analog-to-digital converter, a dual-port high-speed digital random access memory (RAM), and a digital-to-analog converter. Figure 4.1 shows a typical DRFM [Ref. 14]. This configuration is ideally suited for employment against modern radar systems such as the TPS-70, which use coded waveforms with signal bandwidths up to several hundred megahertz, and which require sampling rates of comparable magnitude for the DRFM. It is very important to recognize that the accuracy of sampling degrades as the sample rate increases, and the coarseness of quantization also grows as the time available for each A/D conversion decreases [Ref. 12]. We now examine the DRFM process of generating the smart noise jamming waveform.

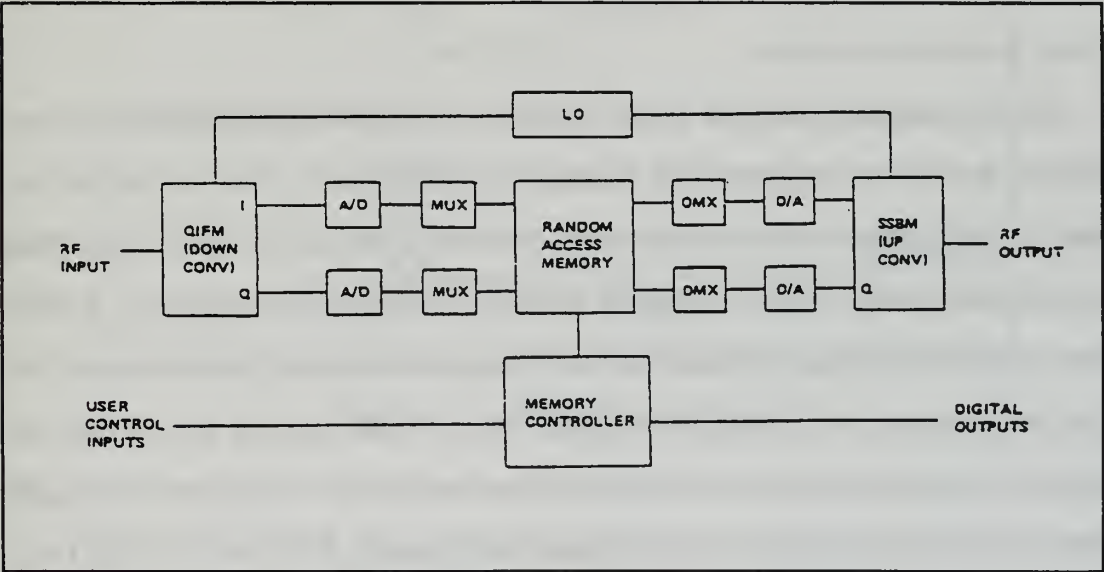


**Figure 4.1. Digital RF Memory [Ref. 14]**

We suppose that our SOJ platform approaches an area under surveillance by a TPS-70 search radar that has been purchased by a hostile nation. We intercept its signal waveform, and we begin tuning the local oscillator (LO) of our synchronous

detector to the approximate frequency of the intercepted signal. The LO works in conjunction with mixers to convert a received echo to an intermediate frequency (IF), which is convenient for filtering and processing operations. We note that our DRFM must be able to handle IFs of modern radar system receivers which have been implemented sufficiently high enough to provide the necessary bandwidth for the received echoes. Our LO can coherently process a series of echoes, acting essentially as a timing standard by which the echo delay is measured to extract the range information that is stable to within a very small fraction of the radar wavelength. We note that in addition to the pulse trains of search radars, a variety of emissions can be integrated and processed, including the lock-on signal of an active missile, or an Identification Friend or Foe (IFF) interrogation. After interception and tuning, the next step is down conversion.

The intercepted signal, still in our synchronous detector, next undergoes down conversion; both phase and amplitude information are retained. This was part of our original goal to maintain the coherence of the intercepted signal, and the fundamentals are worth elaborating upon at this point from a mathematical standpoint. Recall, coherent signal processing requires that both the amplitude and phase of signals be used in the process, and, hence, each signal sample must specify both phase and amplitude. We accomplish this with complex expressions which represent each signal sample; these expressions have two orthogonal components which we write as  $I+jQ$ . We examine this expression in more detail; it represents the result of down conversion.

In general, we let our intercepted signal  $s(t)$  be as follows:

$$s(t)=A(t)\cos[\omega_0t+\phi(t)] \tag{32}$$

where  $\omega_0$  represents the I.F. carrier frequency,  $A(t)$  is the amplitude modulation, and  $\phi(t)$  is the phase modulation. The value  $\phi(t)$  includes any phase modulations of the transmitted signal, Doppler shift effects, and constant phase shift. The I and Q components of  $s(t)$  are obtained by mixing (or beating) the signal with the LO signal,  $\cos\omega_0 t$ , and with the LO phase shifted 90 degrees in the other channel [Ref. 15]; Figure 4.2 shows this. The I and Q components can be regarded as vector projections on two orthogonal axes at any given instant of time. It is the availability and use of the transmitter carrier frequency at the receiver which makes the process coherent.

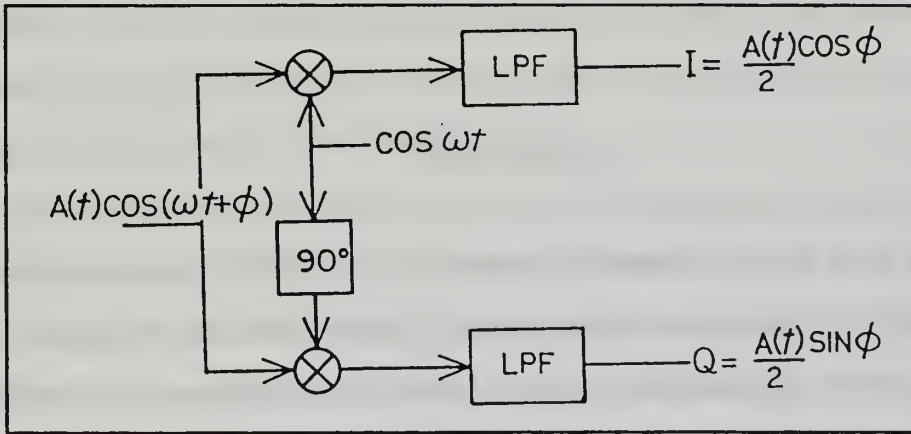


**Figure 4.2. I/Q Circuit [Ref. 9]**

Now, the values of I and Q in Figure 4.2 result from the following trigonometric identities:

$$2\cos A \cos B = [\cos(A+B) + \cos(A-B)] \quad (33)$$

$$2\sin A \cos B = [\sin(A+B) + \sin(A-B)] \quad (34)$$

$$\cos(A-90^\circ) = \sin A \quad (35)$$

where  $A=\omega_0 t$ ,  $B=\omega_0 t + \phi(t)$ , and the averaging performed by the low-pass filter removes the higher frequencies represented by the  $(A + B)$  terms, and passes only the frequencies contained in the signal modulation  $A(t)$  and  $\phi(t)$ . The output  $I+jQ$  can be appropriately expressed as:

$$A e^{jx} = A(\cos x + j \sin x) \quad (36)$$

where  $A$  is the amplitude of the number, and  $e^{jx}$  defines its angle with respect to the positive  $I$  axis. Now we have the following relationships:

$$I = A(t)/2 \cos \phi \quad (37)$$

and

$$Q = A(t)/2 \sin \phi \quad (38)$$

Resolution into these components represents a complete down-conversion to baseband. We note that because the circuit of Figure 4.2 removes the signal from the carrier, it is called the detector; however, because it also preserves the signal phase information (keeping the coherence intact), the more precise definition of this component is *synchronous detector*.

Once our incoming RF band signal has been translated into in-phase and quadrature baseband signals, the resulting baseband signals are sampled and digitized in the analog-to-digital converters. A/D conversion is a three step process; generally, we sample the continuous-time (analog) signal at discrete-time instants, we quantize the signal into a discrete-time, discrete-valued (digital) signal, and then we code the signals as some  $b$ -bit binary sequence. Sampling by a standard ADC is done by a sample-and-hold (S/H) circuit; the S/H is a digitally controlled analog circuit that tracks the analog input signal during the sample mode and holds it fixed during the

hold mode to the instantaneous value of the signal at the time the system is switched from the sample mode to the hold mode. The purpose of the S/H is to sample the input signal instantaneously and then to hold the value constant as long as it takes for the ADC to obtain its digital representation. Also, the use of an S/H allows the ADC to operate more slowly compared to the time actually used to acquire the sample. The S/H introduces minimal distortion into the conversion process, resulting in high-resolution digital conversion of signals which have large bandwidths. We also note that jitter, non-linear variations in the duration of the sampling aperture, changes in the voltage held during conversion need to be considered as effects incurred during the process. The A/D converter begins the conversion after it receives the current command; the time that is required to complete the conversion should be less than the duration of the hold mode of the S/H [Ref. 10].

Quantization is a non-linear and non-invertible process that maps some given amplitude  $x(n) = x_a(nT)$  at time  $t = nT$ , into an amplitude  $x_k$  taken from a finite set of values. Basically, the value of each signal sample is represented by some discrete value taken from some finite set of possible values. This is an approximation process; hence, we incur some quantization error, which is the difference between the unquantized sample  $x(n)$  and the quantized output  $x_q(n)$ . What is significant is that with uniform quantization levels, about 6 dB of improvement can be achieved in the signal-to-quantization-noise ratio for each additional bit used [Ref. 13]. We will examine the effects of quantization in more detail later.

The final step, coding, involves assigning a unique binary number to each quantized output  $x_q(n)$ . If we have  $L$  levels of quantization, then we need at least  $L$  different binary numbers. With a word length of  $b+1$  bits, we can represent  $2^{b+1}$  distinct binary numbers. It follows that we have  $2^{b+1} \geq L$  or, equivalently,  $b+1 \geq \log_2 L$ . And the resolution of the ADC is given by the following relationship:

$$\Delta = \frac{R}{2^{b+1}} \quad (39)$$

where  $R$  is the range of the quantizer. Having accomplished sampling, quantization, and coding in the ADC's, the next step is storage of the signal outputs. Just prior to and immediately after storage in memory, the multiplexer (mux) and demultiplexer (demux) components -- which are usually shift registers -- reduce the data rates into and out of the memory, thus increasing the time available for the memory READ/WRITE cycle; with sufficient demultiplexing, the sample rate of the architecture becomes limited by the speed of the mux and demux components rather than the memory.

The digital I and Q waveforms are stored in a high-speed random access digital memory (RAM). The RAM contains an array of memory cells, each consisting of a binary storage element and the associated control logic. It's called *random access* because the words in the memory can be accessed in any order. In general, the computer can store (write) data at any selected location (address) and, at any subsequent time, retrieve (read) the data; for this reason, RAM also stands for Read-And-Write memory. This is in contrast to the ROM used by the DDS, in which data is initially and permanently stored (by the manufacturer or the user), and the computer can read the data at any address, but it cannot alter the stored bits. This high-speed RAM has to be dual ported so that radio signals can be recorded and replayed simultaneously; the dual port memory usually employs a serial-to-parallel/parallel-to-serial circuitry in order to achieve the necessary data rate conversion to match the dual-port memory's I/O bandwidth [Ref. 16]. To reiterate, the challenge with the DRFM lies in its ability to handle multiple signal storage and still be effective.

The next step in the DRFM process is reconstruction of the I and Q video; we accomplish this by running our baseband signals through a DAC at playback time. The digital-to-analog conversion is as we previously described it in the chapter on DDS. For clarity's sake, we briefly re-emphasize a few points. Recall, the function of the DAC is to reconstruct the discrete waveform; it approximates the ideal amplitude value for some given clock cycle, and thus determines the amplitude accuracy and not the frequency of the waveform. And the more the DAC bits added, the increasingly cleaner the output becomes. We also noted a few problems, namely problems with settling time, jitter, and glitch responses -- all of which we've examined earlier. The reconstituted waveforms are suitably modified and are now ready for up conversion.

The final step before re-transmission is the reconstruction of an RF version of the original signal, occurring at an appropriate time as determined by a device not shown in our Figure -- called the control subassembly. The up conversion process starts with the same carrier provided by the original LO that we used for down conversion. The RF output is generated via single sideband modulation with the I and Q video signals producing the modulation waveforms. As a point of interest, we point out that there are many alternative DRFM architectures which are designed to accomplish the same task, which is to convert the signal input RF signal to a frequency which is low enough to be sampled by a high-speed ADC, and then to convert the output of the DAC back to the original RF signal. The following are some examples: single sideband, double sideband, phase sampling, direct digital down conversion, and direct frequency division. We elaborate upon the simplest architecture which is the single sideband option.

The single sideband (SSB) modulated DRFM is perhaps the simplest architecture for up conversion to the radio frequency. The most important advantage

of SSB systems is very effective utilization of the available frequency spectrum, particularly when considering Nyquist sampling. Our basic DRFM in Figure 4.1 doesn't show it, but it would include bandpass and low-pass filters prior to the ADC, and then the same filters in reverse sequence following the DAC. In general, our input signals are bandpass filtered, and then mixed with the LO output; the resulting output is then passed through the low-pass filters to remove any components which exceed the determined Nyquist frequency, along with any mixer by-products. The resulting signal is then sampled and stored in the RAM. The playback of the stored signal(s) involves essentially the same process, but in reverse, and all of the phase information is preserved coherently.

The SSB basically extends the low frequency limit of an amplitude-based DRFM by the use of an image reject mixer, which is by definition, single sideband modulation. The instantaneous bandwidth of the SSB system is determined primarily by the sample clock rate -- where the maximum reproducible frequency is half that of the clock. In practice, the bandpass filter necessary to reject the unwanted sideband reduces this. Typical clock rates range from 100 to 1000 MHZ [Ref. 16]; the low frequency limit of the instantaneous bandwidth is determined by the filters. The up-converted signal can now be used to deceptively jam out threat TPS-70 radar from which we intercepted the original signal waveform.

In summary, we have examined the DRFM technique, with emphasis placed upon the architecture of a generic DRFM, in addition to looking at a specific type of DRFM (SSB modulated). Digital radio frequency memory is a technique for the storage and reconstruction of RF microwave signals based upon the high-speed sampling and digital memory. We examined its objective, then focused on its viability as a DEA in stand-off jamming; specifically, we observed that its great viability as an EW jammer is due to its ability to generate coherent replicas of RF

pulse trains; using replica deception techniques, the jammer duty cycle and emission bandwidth are essentially the same as the threat radar's. Hence, it is feasible for one jammer transmitter to deal with several radars simultaneously transmitting at different frequencies, which requires the storage of multiple signals, in addition to precise replicas which contain the identical phase and frequency information of threat radar. We then analyzed the actual process involved in the DRFM technique. We observed that this process typically involves the following: 1) down converting the intercepted waveform to baseband, producing in-phase and quadrature components of the signal waveform, 2) sampling and digitizing using an ADC, 3) digitally storing the I and Q waveforms in RAM, 4) reconstructing the I and Q waveforms (suitably modified for jamming) to analog form by DAC, and 5) reconstructing the RF jamming waveform using single sideband up conversion modulation of the I and Q samples using the original down conversion LO. We conclude that the DRFM system's performance is primarily determined by the system architecture, the sampling frequency, and the number of quantization bits. According to Roome, the most important performance criteria are the instantaneous bandwidth, the quantization noise level, the level of spurious signals, and the amount of signal distortion incurred [Ref 13]. In the following section of this thesis we explore the impact of quantization error and intermodulation effects.

## **C. OBSERVATIONS AND EVALUATIONS**

The most important observation that we make and consider in analysis of the effectiveness of the DRFM is the biggest problem incurred with its employment -- namely, the production of spurious responses (spurs). These spurs have a beaconing effect when detected by radars such as the TPS-70, which have been designed with EPs that can easily detect and recognize these signals, and, thus, render the DRFM jammer ineffective. In this section we focus on two types of spurious responses: 1)

those produced in the quantization process, and 2) those due to intermodulation effects. We note that there are other causes, which we will mention only briefly. We then evaluate spurious responses with respect to quantization and increased bit number, as tested with a MATLAB computer program specifically created for such analysis.

### 1. Spurious Responses Due to Quantization Effects

Spurs are produced in the digitization process undergone in the DRFM. Recall, quantization is the process of converting a continuous-valued signal into a discrete-valued signal, and this is actually an approximation process. As such, error is inevitably introduced in the process. Physically, this error manifests itself in the form of quantization noise, which is caused by the difference between the received signal and its quantized representation; it's dependent upon the nature of the received signal. In theory, quantization of an analog signal results in the loss of information, due to the uncertainty that is incurred during quantization. This is an irreversible process, and the uncertainty makes the exact quantitative analysis of quantization extremely difficult. In practice, we can reduce the quantization error to an insignificant amount by choosing a suitable number of quantization levels. Mathematically, the error that is introduced can be represented as follows:

$$e_q(n) = x_q(n) - x(n) \quad (40)$$

where  $e_q(n)$  is a quantization sequence defined by the difference between  $x_q(n)$ , the sequence of quantized samples at the output of the quantizer, and  $x(n)$ , the actual sample value [Ref. 10]. Hence, the error is introduced by either truncation or by rounding; furthermore, we point out that the instantaneous quantization error  $e_q(n)$

cannot exceed half of the quantization step and, hence, is always in the range  $-\Delta/2$  to  $\Delta/2$ :

$$-\Delta/2 < e_q \leq \Delta/2 \quad (41)$$

where  $\Delta$  is the quantizer step size. Other properties are valid if we assume that the quantization error is random, the quantization step is small, and the signal sequence  $x(n)$  crosses several quantization levels between two successive samples; three of these properties are as follows: 1) the error  $e_q(n)$  is uniformly distributed over the range of  $-\Delta/2 < e_q(n) < \Delta/2$ , 2) the error sequence  $\{e_q(n)\}$  is uncorrelated with the signal sequence  $x(n)$ . Given these properties, the effect of additive quantization noise power is basically independent of the input signal level, but in practice, is related to the power of a peak level sine wave signal. And for a single  $n$ -bit ADC, this gives a signal-to-quantization level noise ratio of :

$$SNR = 6.02n + 1.76 \text{ dB} \quad (42)$$

It follows that each additional bit in the quantizer increases the signal-to-quantization ratio by 6 dB; this is shown in Figure 4.3. This will actually be enhanced by filtering, as well as degraded by ADC non-linearities; in general, at low bit levels, where quantization levels are low and widely spaced, practical implementation of ADCs and DACs can be very close to their theoretical ideals, and at higher numbers of bits, non-linearities and asymmetries may be modeled (approximately) by considering a reduction in the effective number of bits. We re-emphasize that the accuracy of sampling degrades as the sampling rate goes up, and the coarseness of quantization grows as the time available for each A/D conversion decreases.

## 2. Spurious Responses Due to Intermodulation Effects

The most important challenge for the DRFM as a DEA is its ability to handle the storage of multiple signals; in the digital signal processing of multiple signals, it is necessary to analyze the performance of the heart of the system which is the ADC. The analog-to-digital conversion process not only produces quantization effects, but also generates intermodulation products. The probability distribution of the resulting spurious signals is difficult to predict and will probably need to be estimated for each DRFM application by some type of computer simulation. Total spur power is of great interest, particularly regarding the TPS-70, since it can create a recognizable signature, or afford a sensitive missile an opportunity to execute a home-on-jam

NUMBER OF BITS PER SAMPLE	MAXIMUM QUANTIZATION ERROR (%)	SIGNAL POWER TO QUANTIZATION NOISE POWER RATIO (dB)
3	6.25	19.82
4	3.13	25.84
5	1.56	31.86
6	0.79	37.88
7	0.39	43.90
8	0.20	49.92
9	0.10	55.94
10	0.05	61.96
11	0.02	67.98
12	0.01	74.00

**Figure 4.3. Required Bits Per Sample**

attack. Before actually evaluating the effects of spurious responses -- which we do in the next section -- it is important to examine what causes spurs due to intermodulation products.

The digital signal processing of sinusoidal signals results in the production of harmonics of the DRFM output signal's fundamental frequency. This is because quantization is a non-linear process, and as a result, ideal quantization as well as non-ideal quantization (with bit-threshold errors) produces output intermodulations (intermods) and various other harmonic products. Intermods are spurious signal components which show up at new (unwanted) frequencies. In general, the multiplication of the LO with the received signal (a non-linear process) and a second spurious or interfering signal produces intermods which occur at [Ref. 3]:

$$f_{out} = abs[mf_1 \pm nf_2] \quad (43)$$

where  $f_{out}$  is an output (receiver tuned) frequency,  $f_1$  is one of the interfering input frequencies,  $f_2$  is the other interfering input frequency, and  $m, n$  are positive integer coefficients greater than or equal to one. Additionally, when narrow bandpass filters are involved, as is the case with the DRFM, only third-order and higher order intermods can fall within the bandpass and appear as interfering signals, where

$$IMOrder = |M| + |N| \quad (44)$$

a large number of higher order intermodulation products may fall within the receiver's bandpass; since the amplitude of intermod products falls off rapidly with increased order, their effects are generally negligible. Hence, the third-order IM products tend to be the most critical.

As with the DDS, Doppler effects need to be considered with the DRFM, particularly in terms of spurious responses. The DRFM is a technique which can induce a frequency offset in the transmitted signal. Mixers in the DRFM introduce

a Doppler offset which gives the appearance that the target is moving faster (or slower) than it actually is. By carefully controlling the frequency and rate of returning signals, the DRFM can emulate a range gate stealer to cause a tracking radar to break lock on its target. While mixers play an key role in the production of Doppler frequency offsets, these mixers per se are a source of intermodulation effects and noise within the signal bandwidth when the DRFM local oscillator is very close to the signal center frequency.

Multiple storage has the effect of exponentially increasing intermodulation effects. The amplitudes of the spurs are actually predictable and, indeed, DRFM engineers measure these spurs experimentally, and then incorporate the results into the design specifications. According to Kerins [Ref. 17], a DRFM that has "m" bits has  $2^{m-1}$  amplitude levels in the positive half-cycles. Assuming positive and negative half-cycle symmetry, for which there can only be odd harmonics, the spurious response levels can be found by evaluation of the following expression:

$$b_n = (2/\pi [\int_0^{\theta_2} a \sin nx dx + \int_{\theta_2}^{\theta_3} 2a \sin nx dx + \dots \int_{\theta_2^{m-1}}^{\pi - \theta_2^{m-1}} (2^{m-1})a \sin nx dx + \int_{\pi - \theta_2}^{\pi} a \sin nx dx]) \quad (45)$$

where  $\theta$ s are the transition angles.

The most conclusive studies have been made for 1, 2, and 3 bit DRFMs. Beginning with the 1-bit DRFM, W.J. Schneider [Ref.14] notes that early DRFMs used a very simple, yet effective A/D technique: hard limiting in a baseband comparator followed by a D flip-flop. The flip-flop is a device used in all types of digital data processing systems that inexpensively and reliably ensures that the binary storage device of the system can accommodate rapid state changes by remaining in one state (0 or 1) until instructed to change to another; in a D flip-flop, the transfer of data from input to output is delayed (see Figure 4.4). When the baseband signal exceeded zero during the positive half-cycle of the signal, the flip-flop would register a "1"; when the signal went negative, the flip-flop would register a "0". This is

referred to as 1-bit A/D. The effect of limiting is to produce a square wave representation of the baseband signal. The effect of sampling is to form Intermodulation products between each harmonic of the square wave and multiples of the DRFM sampling clock. Ultimately, every harmonic of the square wave is present in the baseband spectrum, either as the original harmonic or as a folded version. Spurious outputs of the 1-bit DRFM, based upon (45) occur at  $b_n = (4a/n\pi)$ . The symmetry

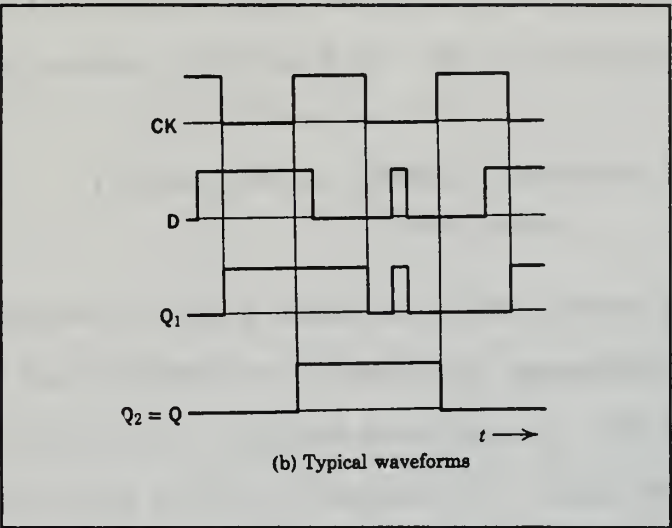


**Figure 4.4. Delay Flip-Flop [Ref.23]**

between the positive and negative half-cycles of the square wave produces only odd harmonics; actually, even harmonics are also produced because it is impossible to achieve perfect positive/negative symmetry in real systems. In the case of the 1-bit DRFM, the third harmonic produces the worst spur at a level of -9.5 dB.

Other DRFMs under test and development are the 2 and 3-bit DRFMs. In contrast with the 1-bit DRFM, which divides the half-cycle sine wave into two discrete levels (0 and 1), the 2-bit DRFM divides the sine wave amplitude space (peak-to-peak) into four discrete levels; this multiple division approach provides a

much better approximation to the wave than the simple square wave of the 1-bit DRFM. The 3-bit provides the best approximation of the three, since it divides the peak-to-peak amplitude space into eight discrete levels. With respect to the spurious responses, the 2-bit DRFM produces spurs (according to 45) as:

$$b_n = (4a/n\pi)(1 + \cos n\theta_2) \quad (46)$$

The third harmonic does not produce the worst harmonic in this case, the ninth harmonic does at the level -18.1 dB. The 3-bit DRFM produces spurs as:

$$b_n = (4a/n\pi)(1 + \cos n\theta_2 + \cos n\theta_3 + \cos n\theta_4) \quad (47)$$

The worst spurious response in this case occurs at the 19th harmonic, which is 25.5 dB down from the fundamental. In general, it is evident that though the signal storage capacity directly effects the replication accuracy of the DRFM, one solution to obtaining better performance is to configure our DRFM with multiple bits -- which is easier said than done! Such systems are currently under development, which we'll examine later.

### 3. Test Evaluation

As mentioned, many of the available DRFMs use only 1 bit of quantization; this creates intermod spurs when multiple signals are present. When broadband DRFMs are employed, however, current technology permits on the order of 3 to 4 bits in tactical sized units [Ref. 2]. In this section, we evaluate spurious effects incurred as a result of varying the number of bits and the number of signals; specifically, we test the responses to 1 through 4 bits of quantization, and we test the responses of these with 1 signal and 5 signals. Also, the number of samples we take in each case is the same (1024), as well as the sample input signal frequency (100 Hz). The results

were the most important here were the amount of loss and the change in signal-to-noise ratio. The program used to generate this data is a MATLAB coded program called DRFMBITS.M.

a. Figure 4.5a illustrates the frequency spectrum for 1 signal and 1 bit of quantization:

(1) loss = .912493 dB

(2) SNR = 4.276926

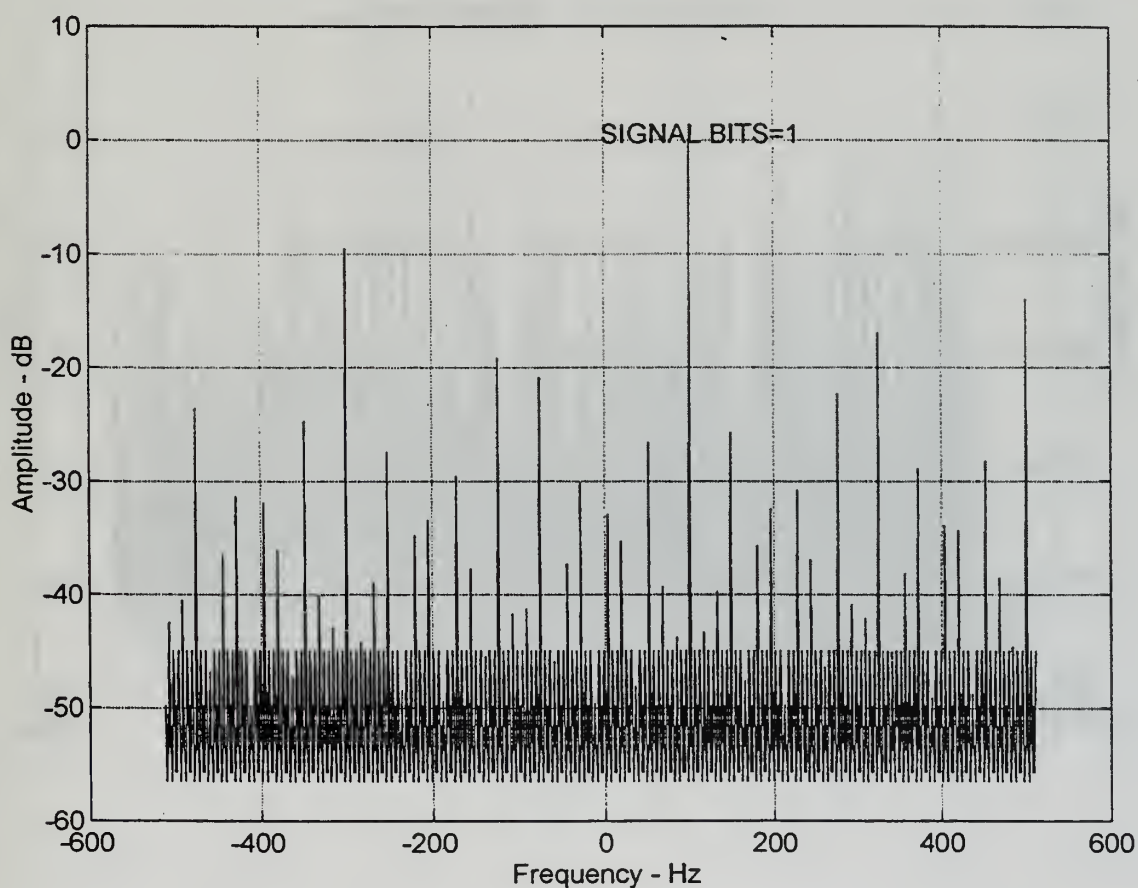


**Figure 4.5a. DRFM Frequency Spectrum**

b. Figure 4.5b illustrates the 1-bit frequency spectrum for 5 signals:

(1) loss = 2.157529 dB

(2) SNR = 1.554155

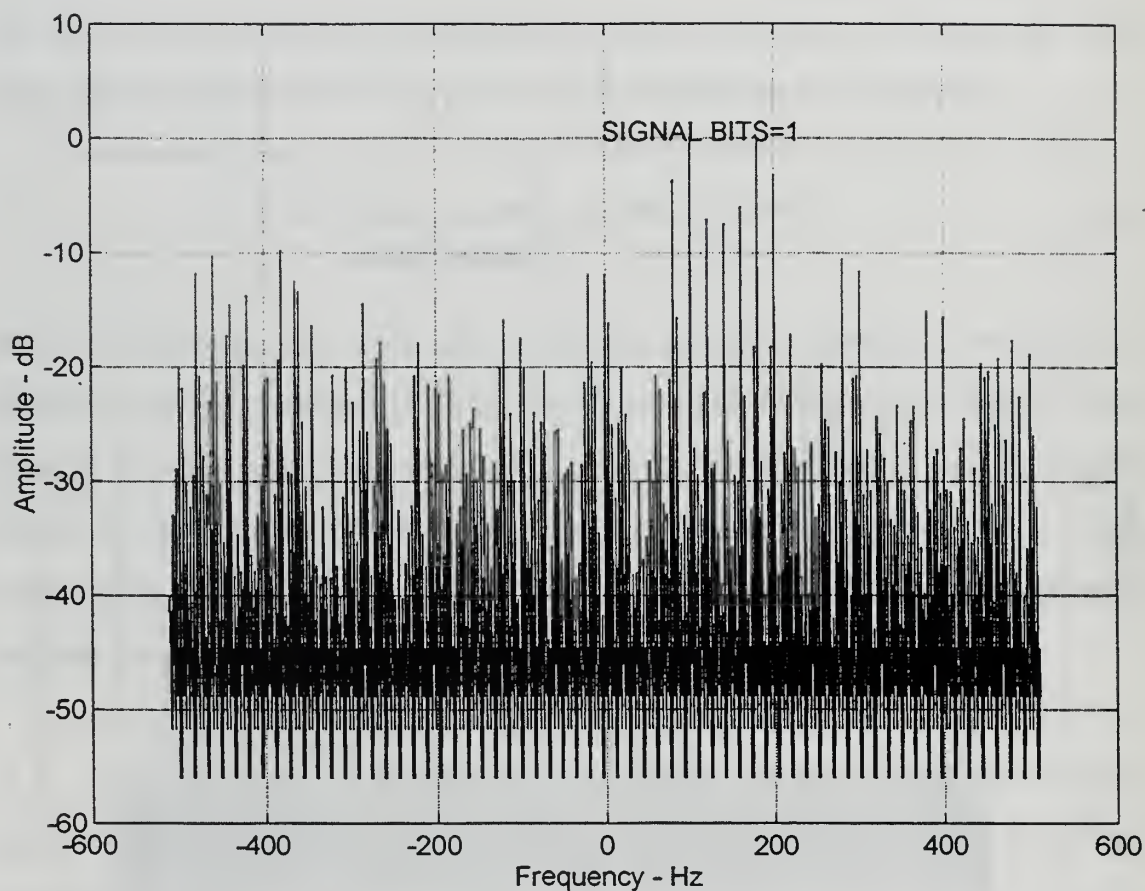


**Figure 4.5b. DRFM Frequency Spectrum**

c. Figure 4.6a illustrates the frequency spectrum for 1 signal and 2 bits of quantization:

(1) loss = .263315 dB

(2) SNR = 15.998392

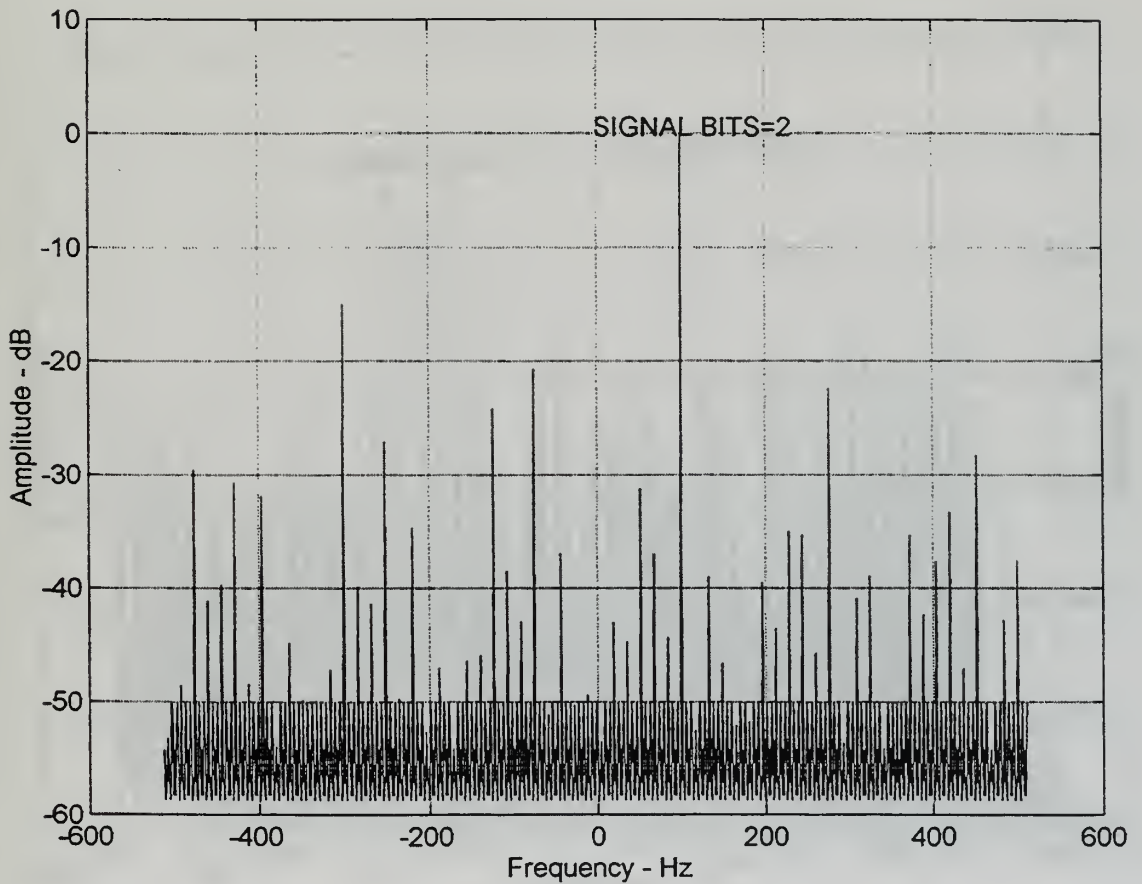


**Figure 4.6a. DRFM Frequency Spectrum**

d. Figure 4.6b illustrates the 2-bit frequency spectrum for 5 signals:

(1) loss = 1.498775 dB

(2) SNR = 2.436365

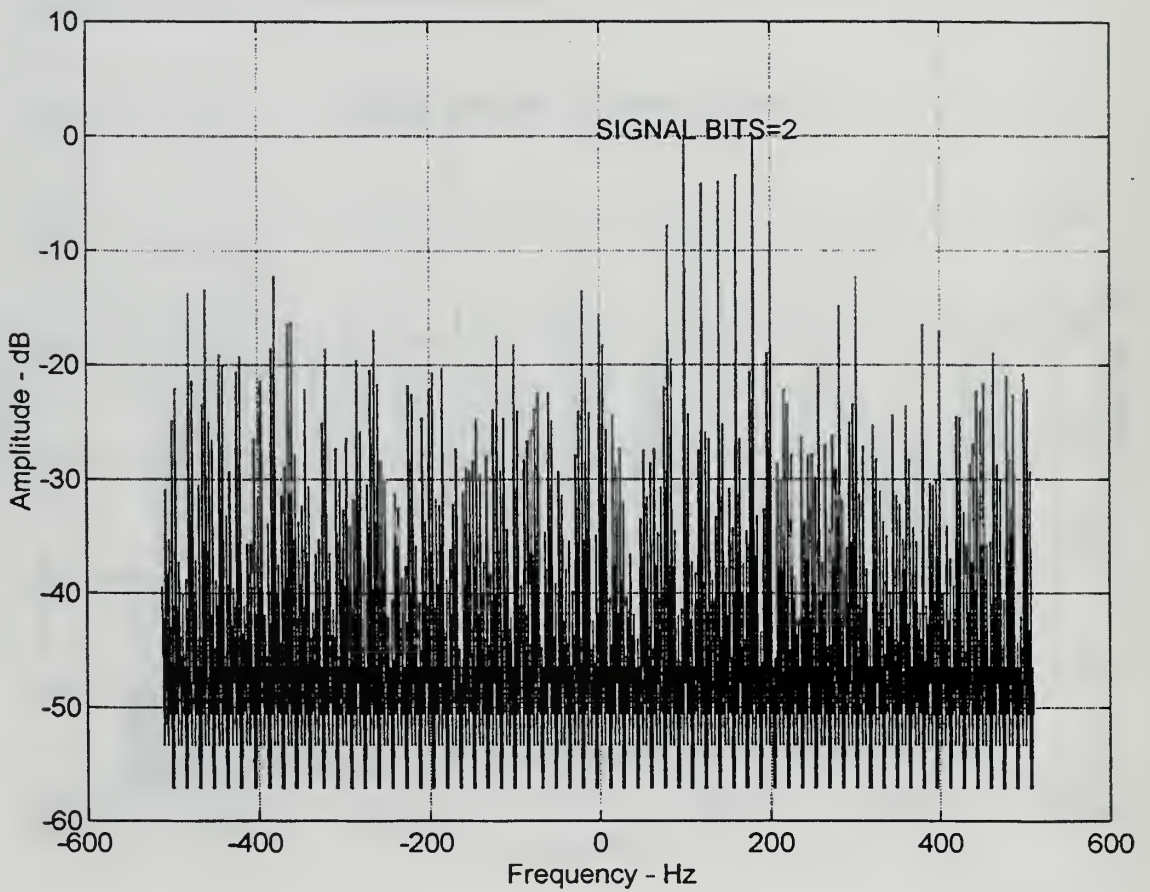


**Figure 4.6b. DRFM Frequency Spectrum**

e. Figure 4.7a illustrates the frequency spectrum for 1 signal and 3 bits of quantization:

(1) loss = .070870 dB

(2) SNR = 60.782094

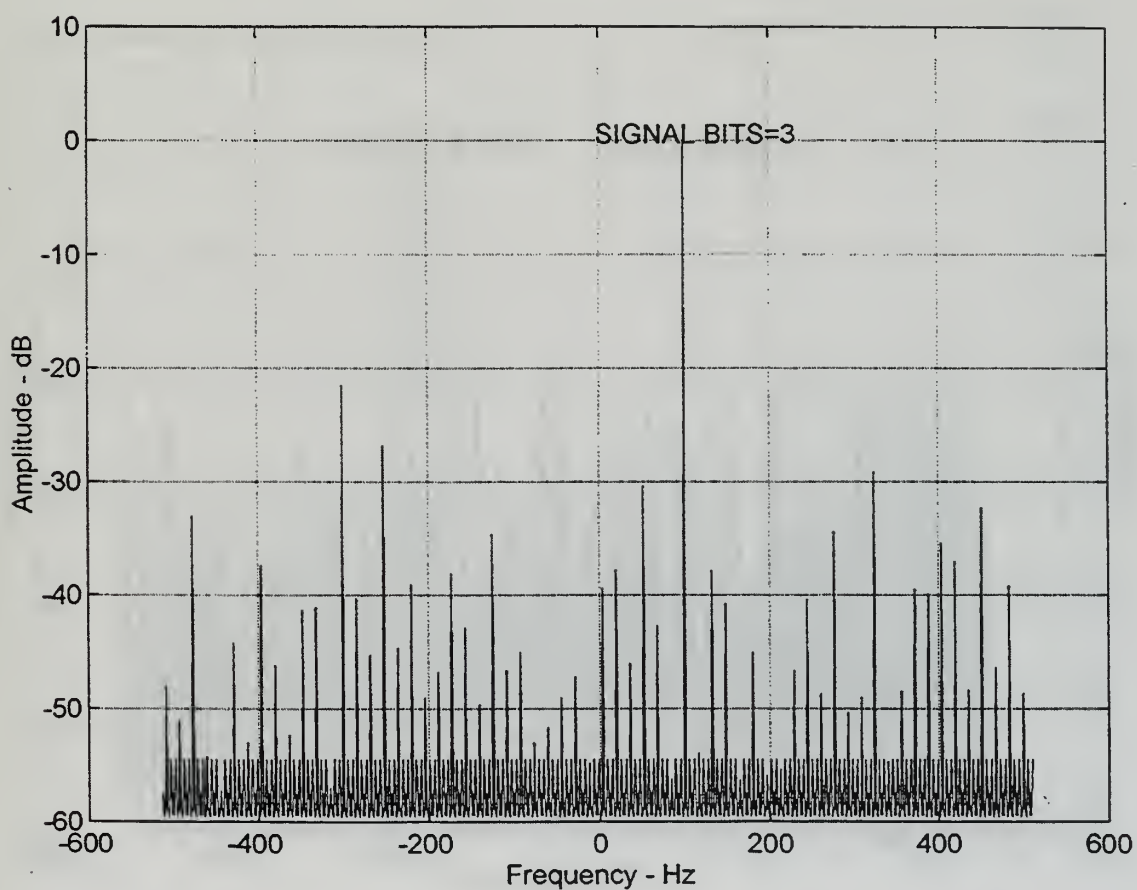


**Figure 4.7a. DRFM Frequency Spectrum**

f. Figure 4.7b illustrates the 3-bit frequency spectrum for 5 signals:

(1) loss = .542907 dB

(2) SNR = 7.509837

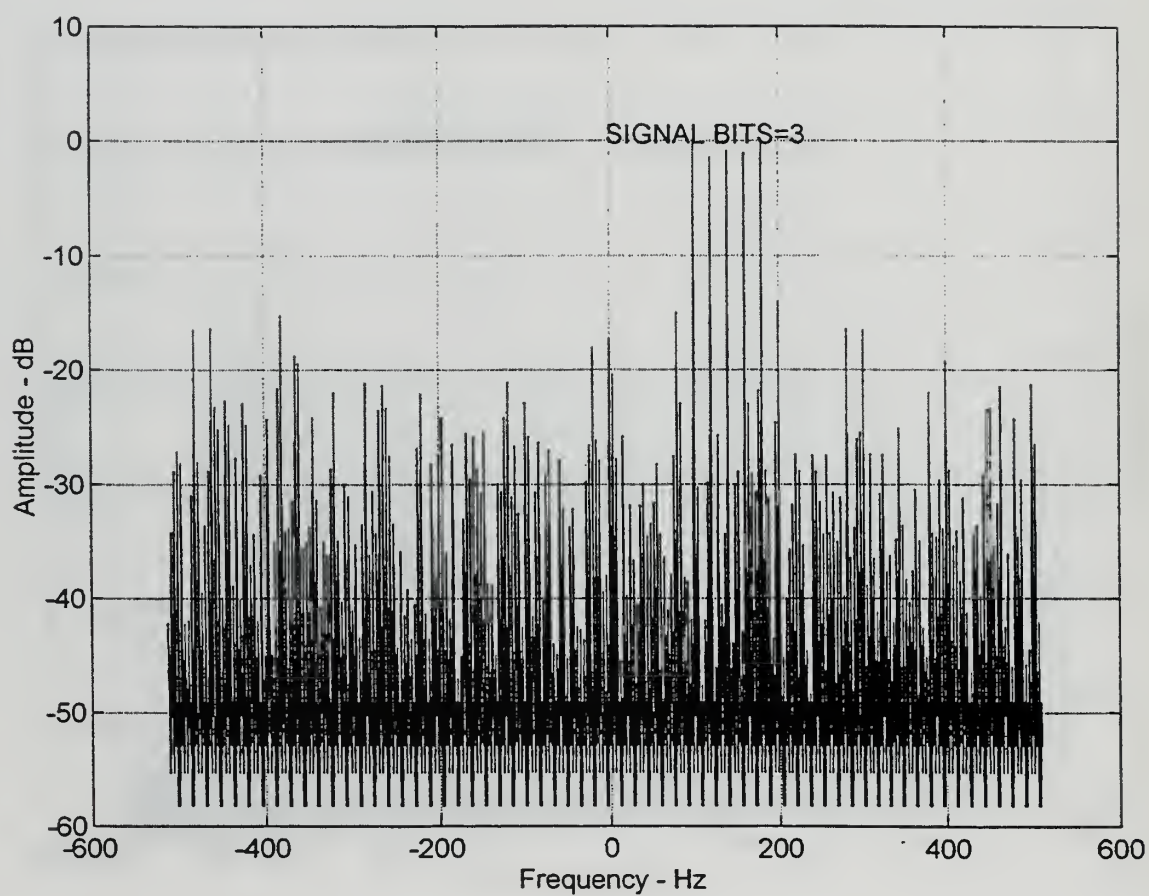


**Figure 4.7b. DRFM Frequency Spectrum**

g. Figure 4.8a illustrates the frequency spectrum for 1 signal and 4 bits of quantization:

(1) loss = .017934 dB

(2) SNR = 242.659333

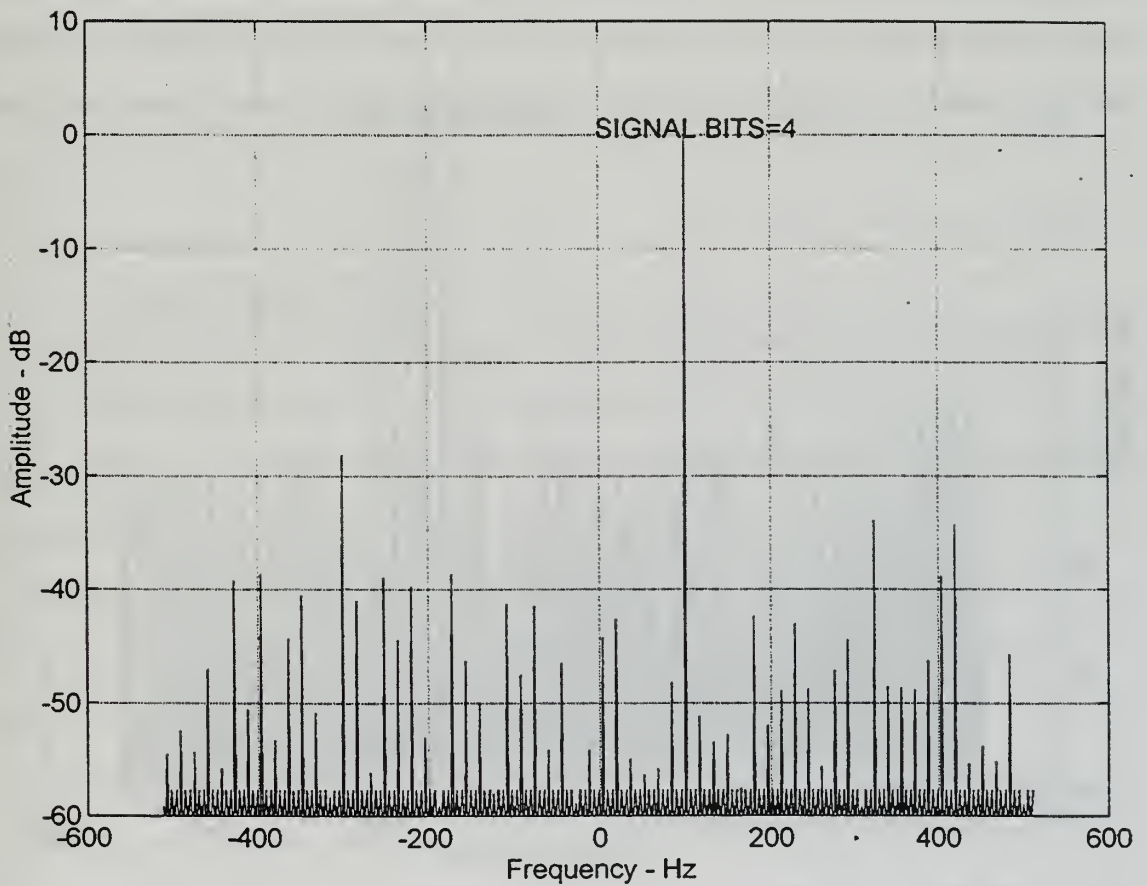


**Figure 4.8a. DRFM Frequency Spectrum**

h. Figure 4.8b illustrates the 4-bit frequency spectrum for 5 signals:

(1) loss = .151675 dB

(2) SNR = 28.136216

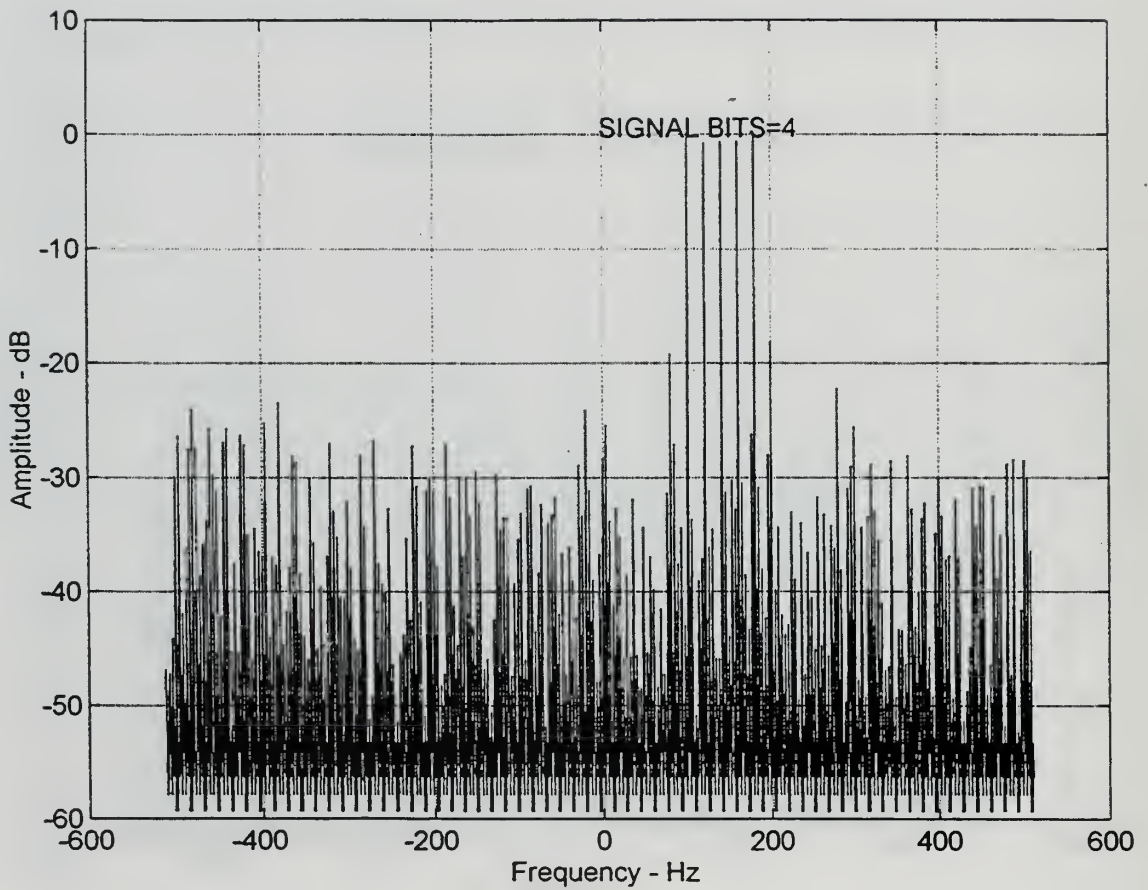


**Figure 4.8b. DRFM Frequency Spectrum**

We can make several observations. First, it is apparent that the quantization process per se produces spurious signals; furthermore, harmonics of the fundamental frequency also produce spurious signals as intermodulation products. Secondly, we observe that the more signals that we try to store, the more degraded will be the performance of our DRFM. In contrast, we observe, perhaps just as importantly, that the more bits of quantization that we apply, the better is the performance of our DRFM; it is apparent that with uniform quantization levels, we achieve about 6 dB improvement in the signal-to-quantization-noise ratio for each additional bit used. Hence, if multiple signals were stored in a DRFM and a 1 to 4 bit quantizer were used, the losses derived from Figure 4.9 would add to the effective jamming spot size

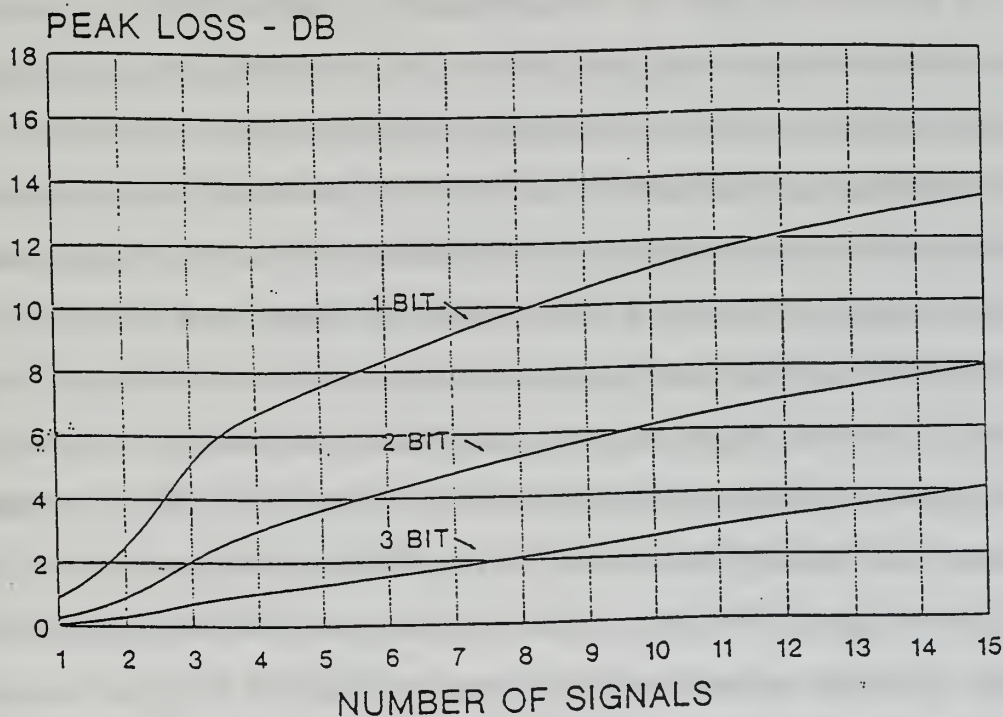


Figure 4.9. DRFM Signal Efficiency

(Figure 4.9 depicts the average loss incurred in the DRFM due to multiple signal storage and quantization). Thirdly, we observe the degree to which quantization noise is decorrelated by the presence of additional input signals and the spurious signals due to demodulation errors; and overall and striking effect is the extent to which the noise floor is raised. Again, as we increase the number of quantization bits, the effect is to stabilize the noise floor -- this is arguably as dramatic an effect as the increasing noise due to multiple signals. Fourthly, we observe that the industry "rule-of-thumb" for DRFMs, as outlined by Kerins, generally does apply to the ideal case, which is what we tested; that is, the highest spur is approximately nine times the number of bits (in dB) down from the fundamental. Of course, we expect non-ideal approximations to produce larger spurs.

In summary, we have observed in this section that the DRFM is not without its own unique challenges which must be taken into consideration if we are to employ it as a DEA technique against state-of-the-art radar systems such as the TPS-70. The greatest challenge we must consider is the production of spurious responses. We observed that these spurs are primarily produced with respect to two effects -- namely, quantization and intermodulation effects. There are other causes which are worth mentioning; these include local oscillator leakage, phase error between I and Q channels(which creates image responses), dc offsets in the I and Q, and out-of-band signals aliased into the system bandwidth. We examined the effects empirically, testing and then evaluating the results of varying the number of quantization bits and the number of signals. We conclude that the challenge of DRFM employment is to overcome (or at least reduce) the effects of spurious responses. In the next section we examine some developments currently in progress to accomplish this task.

## **D. DRFM SPUR REDUCTION DEVELOPMENTS**

There has been extensive development in response to the challenge of maximizing the effectiveness of the DRFM. This is in part a reflex action due to the design of much smarter radar systems; the TPS-70 is well-equipped to handle current EA technology, with the exception of noise jamming. But noise jamming requires excessive amounts of ERP to be effective. The DRFM smart noise jamming technique, like the DDS, becomes a very attractive tool with respect to power management considerations. Techniques for improving the DRFM performance -- particularly for reducing spurious effects -- have met with a reasonable degree of success. In this section, we examine three approaches: 1) LO adjustment, 2) the Gallium Arsenide (GaAs)-based DRFM, and 3) the superconducting DRFM.

### **1. 1-Bit DRFM Spur Reduction**

In the case of the 1-bit DRFM, some manufacturers have attempted to dither the LO with random noise; basically, by adjusting the duty cycle and generating even harmonics, we can eliminate any harmonic spur  $N$ . This modulation of the duty cycle causes energy to be transferred from the odd harmonics to the even harmonics, and the even harmonics are phased out by the reversed duty cycle. This approach has the effect of dispersing the spurs over the entire instantaneous bandwidth. Unfortunately, this is only a cosmetic solution, since the actual spurs are not reduced, but redistributed in such a manner as to make the spurs more difficult to observe on a spectrum analyzer. Another disadvantage is that the total spur power is not reduced [Ref. 17]. In general, what is required to reduce individual spurs and the total spur power is a multiple bit DRFM. These are currently in development, but according to Schneider, the price of the multi-bit DRFM, in terms of increased bandwidth and increased size, as well as weight to accommodate added memory, may be too high for many applications [Ref. 14].

## 2. The GaAs-Based DRFM

High-speed GaAs circuitry is proving increasingly important as an upgrade to current DRFM technology, particularly as a solution to the spurious response problem. The combination of speed and the application of multiple bit ADCs (i.e., 4 bit and 8 bit converters) represents a virtually ideal solution to the spur problem; this is because multi-bit converters restrict bandwidth and expand the storage requirements for multiple signals. GaAs memory technology takes advantage of the RAM-with-logic configuration presently employed with DRFMs, and essentially the need for large numbers of control lines and the associated buffer circuitry can be avoided by integrating memory and logic on the same chip. This chip is called a programmable delay-line element (PDLE), and it is what implements the basic DRFM storage and delay functions for the GaAs-based DRFM [Ref. 18].

The PDLE merits some elaboration (see Figure 4.10). It functions according to what is termed a distributed control concept, and it is basically a clocking scheme.

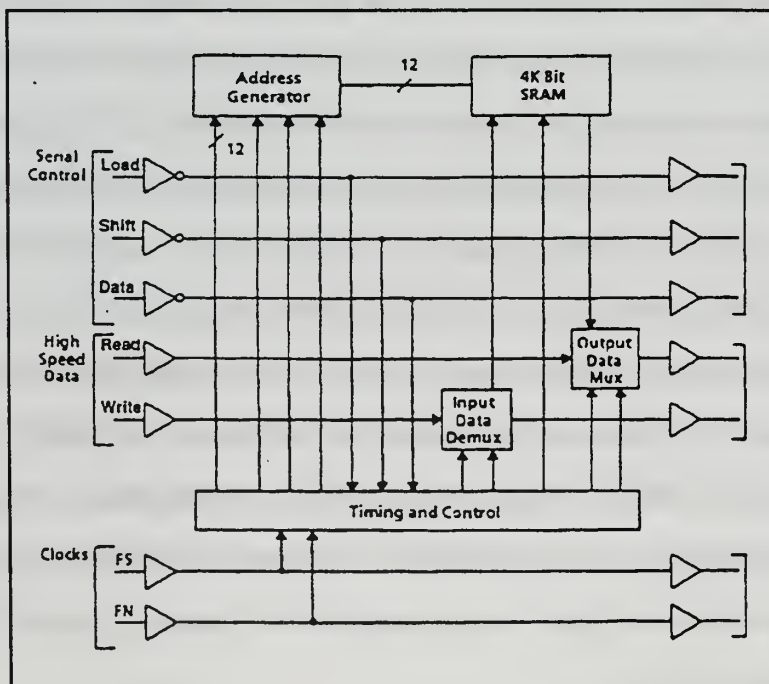


Figure 4.10. Simplified PDLE [Ref. 18]

In simple terms, this is a chip-to-chip interconnectivity process where the outputs of one chip act as the inputs for an identical succeeding chip; the signals are passed across a series of these chips which represent the equivalent of a variable length delay line (where otherwise we would be talking about the successive stages of a shift register). This distributed control concept eliminates the need for a complicated network of globally distributed timing and control signals. Each PDLE chip integrates all of the DRFM's digital logic functions, including multiplexing, demultiplexing, address generation, and control circuitry; these chips are strung together, and the chips within a string correspond to segments of a partitioned plane (memory bank with mux and demux), but they also contain address and memory circuitry to avoid the need for off-chip distribution of the signals. In general, this arrangement allows the DRFM to expand its memory length simply by increasing the number of chips per string.

The RAM-logic configuration also merits some elaboration. We have previously examined the RAM concept as applied to the general DRFM. This concept directly applies to the GaAs-based DRFM with some modifications. The integrated circuitry of our PDLE takes WRITE (reception data) and READ (transmission data) data streams and clocks them through single-stage demultiplex and multiplex circuits, respectively, at the sampling frequency rate. Input (WRITE) and output (READ) data are demultiplexed and multiplexed across the number of chips ( $N$ ) in a string. In regards to data storage, one of every  $N$  input samples from the WRITE data stream is latched and held for one period, during which time it is written to the on-chip RAM. In the recall mode, samples are retrieved from the on-chip RAM and strobed into every  $N$ th output position into the READ data stream.

Next, we make two important observations. Firstly, the PDLE chip is designed to operate with four modes: reset, receive, transmit, and delay. In reset, the addresses

are set and held at zero, data storage is inhibited, and data retrieval along with the resulting data output stream are inhibited. In the receive mode, the input data are stored in sequential memory locations, but the output data stream remains inhibited. In the transmit mode, input data storage is inhibited, but previously stored data are read and output from sequential memory locations. And in the delay mode, data are simultaneously received and transmitted with a programmable delay. Secondly, we observe some limitations; specifically, the PDLE chip will be limited by one of the following four factors: memory access time, counter update time, adder update time, or the time required to toggle the flip-flop cells in the high-speed shift register stages (demultiplex, multiplex, and timing circuitry). [Ref. 18]

In summary, GaAs technology holds great potential for DRFM development. The GaAs memory/logic chip is a fast chip which requires less demultiplexing and multiplexing to match high-speed data streams; furthermore, it results in a very simple DRFM architecture in which memory length can be expanded simply by increasing the number of chips in a string. Ultimately, this may prove very valuable for producing DRFMs which are custom designed to reduce spurious outputs to insignificant levels. The U.S. Department of Defense has expressed a great deal of interest in this technology, as evidenced by the fact that under the Defense Advanced Research Projects Agency sponsorship, technology insertion efforts were awarded to demonstrate the potential of GaAs circuits for upgrading existing programs; in fact, the feasibility of a GaAs-based DRFM has been explored by the U.S. Army for use in the ALQ-136 airborne jammer [Ref. 12].

### **3. The Superconducting DRFM (S-DRFM)**

A superconducting DRFM is under development at Wright-Patterson Air Force Base's Wright laboratory. The S-DRFM is being developed with the objective of high-speed performance and faster memory access than can be obtained with current

large volume memories. In fact, DRFMs presently in use are relatively narrow band devices (up to 500 MHz) which can process only one signal in the band; also, to date, no technology has successfully handled the speed and volume required for superconducting digital EW receiver systems [Ref. 19]. Herein lies the challenge for S-DRFM engineers; specifically, the S-DRFM is being designed (in two phases) as a hybrid superconductor/semiconductor memory system, which will provide a high-speed memory to match the speeds of the gigasample rate of the A/D and D/A converters. It will be developed to be able to process frequency bandwidths of 3 to 5 GHz.. using A/D converters of 4 to 8 bit resolution, one of which with multi-port memory structure can cover multiple bands (i.e., H,I bands) and process multiple threats simultaneously -- affording high dynamic range capabilities and negligible spurious response. Development of the S-DRFM is to be accomplished in two phases, which we briefly describe.

Phase I involves the choice of superconducting materials and the choice of logic family. The following list of superconducting materials is under consideration: niobium, niobium nitrate, and high temperature superconductors (most commonly Yttrium-Barium-Copper Oxide, YBCO). These materials were chosen because they can easily fabricate superconducting circuits with 200 - 400 logic gates, and because they allow for reliable operation within the operating temperature range of practical refrigerators. Presently niobium nitrate circuitry seems to be the most logical choice for meeting the S-DRFM's ADC, demux, mux, and DAC high speed data requirements. Three different logic families are applied in combination to produce the S-DRFM: single flux quantum (SFQ), latching logic, and complementary monolithic semiconductor (CMOS)/cryogenic CMOS. These work in combination because no one logic family can serve all of the functions required by the S-DRFM; in general, it relies upon the SFQ to handle the high-speed data stream -- which it

does while consuming only minimum power, the latching logic family allows for smooth coupling between the SFQ and the semiconductor logic, and finally, the S-DRFM relies upon the CMOS for data storage because of the lack of high density superconducting memory required for DRFM applications. CMOS technology is quite developed, with multi-megabit RAM chips readily available.

The primary technical objective of Phase II is to custom design, build, and test a 1-bit DRFM that can be expanded into a high dynamic multi-bit system that can handle multiple signals. The memory will be able to READ while WRITING on command. In the WRITE cycle, the data from the ADC will be demultiplexed into 32 bit words for storage in the CMOS memory at a 100 megasample rate. The ADC and demultiplexer will utilize both SFQ and Modified Voltage Threshold Logic (latch logic) superconducting technologies. This combination of superconducting logic elements complement each other in processing digital bits and converting into logic levels that allow for translation into CMOS logic levels. In the READ cycle, the data from the CMOS RAM at the 100 megasample rate is multiplexed back to the 3.2 gigasample rate and then converted back to analog waveform by a 1-bit DAC. The 1-bit ADC was selected so that more effort in the development would be placed upon the superconducting elements of the demultiplexer/multiplexer, and more importantly, the 1-bit demux/RAM/mux module which follows the ADC also serves as the building block for the ultimate N-bit S-DRFM. Finally, the memory will have I and Q channels for eventual Doppler shift implementation, and will be capable of processing signals with a sampling bandwidth up to 3.2 GHz. with pulse durations up to 20 microseconds. And this will accomplish the ultimate objective of the S-DRFM technology, which is to produce a multi-port synchronous RF memory system for EW SIGINT and EAs, whose memory can accurately store digital waveforms and hold the information for later recall [Ref. 19].

## **E. SUMMARY**

In this chapter, we analyzed the DRFM technique. We began by examining the technique from a purely conceptual perspective, emphasizing the aspects of the DRFM which qualify it as a viable DEA option. We then broadened our scope by progressing from the theoretical idea of the DRFM to the actual architecture of the DRFM; specifically, we examined the actual process of how the DRFM generates a smart noise jamming waveform. We highlighted the primary challenge of this technique, which is to overcome the effects of spurious outputs. We used data obtained from a MATLAB program to actually observe what these spurious responses look like in spectrum analysis. Finally, we examined techniques which are currently under development to combat these effects, ultimately affording the DRFM the ability to effectively accommodate multiple signal storage. In the following chapter, we weigh some of the advantages and disadvantages of the DRFM technique against the DDS technique.



## V. COMPARATIVE ANALYSIS

### A. INTRODUCTION

Modern radar system technology has greatly increased the challenge for current support jamming systems. The ability to meet this challenge lies largely in the expertise, creativity, and stubbornness of the EA designer. Effectiveness requires that a number of issues be considered from both operational and technical perspectives. In this thesis we have identified the challenge to EA designers with respect to the stand-off jamming mission. The challenge is that radars such as the TPS-70 have become much "smarter". Effective measures of combating these modern radars has resulted in the advent of "smart noise" jamming waveforms, which we have shown, can be generated by two techniques: DDS and DRFM. In this chapter, we weigh each of the two techniques against the other -- focusing on advantages and disadvantages of using either one in light of smarter radars.

### B. SMARTER RADARS

In chapter two of this thesis, we examined modern radar technology from the perspectives of both the radar and EA designers, using the AN/TPS-70 as the paradigm for the modern radar threat environment. The first comparison that we need to make concerns the evolution of the radar threat challenge, because DDS and DRFMs were designed in response to "smarter" radars. Four areas of improvement, spanning three decades (1970, 1980, and 1990), provide us with a comprehensive comparison of developments: pulse density, frequency range, pulse repetition interval (PRI), and some radar system features.

Pulse density and frequency range have been markedly improved over the three decade span. In the 1970s, the typical pulse density for a 40,000 ft altitude -- with receiver sensitivity at -60 dBm -- was about 40,000 pps. Today, a typical pulse

range runs from 1 million to 10 million pulses per second; this represents a tremendous improvement. Similarly, the range of frequencies has been notably extended. In the 1970s, operating frequencies ranged from selected portions of 2 through 12 GHz., to the current 40 GHz.. The ability to operate at ranges in excess of 40 GHz. is possible, but practical applications for these frequencies remain limited.

Smarter radars have been designed to vary their pulse repetition intervals in order to respond to a number of situational changes. In the 1970s, the PRI basically was set for stable condition operation. This improved during the 1980s, allowing for operations in both staggered and jittered pulse modes. Today, we add one other mode which is the pseudorandom-generated pulse mode.

Radar systems have probably seen the most pronounced improvement in the area of special features; in short, radar flexibility has increased geometrically. During the 1970s, a conventional radar system was very limited in what it could do, operating at a single frequency and having the ability to do standard inter-pulse processing. Over the course of the last two decades, the range of features has expanded to include the following: digital processing, multiple frequency operation, spread spectrum, frequency hopping, intra-pulse phase shift, multiple agile antenna beams, coded modulations, improved power management, larger time bandwidth product radar signals, increased duty cycles with lower peak power, bistatic operations, and weapon systems using multi-mode seekers (IR,RF,LASER).

As a subcategory of modern radar systems, search radars have become much smarter -- from the EPs in the transmitter, to the EPs in the data processor. EPs at the transmitter include frequency agility, burnthrough, low probability of intercept (LPI), pulse compression, and jitter. Beam networks are designed with ULSA, CSLC, SLB, and jam strobing technologies. The receiver has some interesting EPs built into it such as automatic gain control (AGC) and the STC -- not to mention developments

in non-linear and guard-based receiving. The most critical component, the signal processor, is a unique EP package in itself; features include coherent processing, non-coherent processing, adaptive CFAR, intra-pulse processing, and poly-phase coded waveforms. Finally, data processors have contributed to the smartness of radar technology with improvements such as track-while-scan (TWS).

Smarter radar systems can be dealt with by smarter EA systems. Smart noise jammers have been in development since the 1970s (DRFMs), and, therefore, have a history commensurate with that of modern radar systems with the improvements we highlighted above. We next weigh the effectiveness of DDS against that of the DRFM with respect to these improvements.

## **C. SMARTER JAMMERS**

### **1. The Digital Advantage**

Conceptually, both the DDS and the DRFM are fascinating methods of performing EA, particularly because they employ digital technology. In both cases, we require some knowledge of the victim radar in order to duplicate his signal and use it to deceive him; furthermore, both methods are designed to handle multiple threats simultaneously. The idea of custom-designing a jam signal is even more intriguing when considering that the primary alternative -- noise jamming -- is basically a brute force method.

The option of digital rather than analog implementation adds considerable viability to the notion of employing DDS and DRFM techniques as DEAs. Current exciter technology relies heavily upon voltage controlled oscillators (VCO) and uses analog modulation techniques to generate a wide variety of jamming waveforms. These types of systems tend to be hardware intensive and use dedicated hardware solutions to jamming requirements. This approach limits the effectiveness of fielded EW systems in the constantly changing threat environment. In general, systems

which rely on analog circuitry do offer simplicity, relatively high speed, and generally low cost solutions to many design problems; also, analog systems produce outputs more in line with naturally occurring phenomena, and as such must work over wide dynamic ranges. Limitations of resolution and accuracy are related to interference, signal magnitudes, component tolerances, and degradations with time. But the employment of digital technology completely changes the rules of the game, as it were.

Digitally-based technology, is generally characterized by higher speed operation, and markedly higher resistance to noise. This technology has also afforded both techniques with the capability of reaching output frequencies into the hundreds of megahertz, with increased frequency tuning, precision, and resolution accuracy. [Ref. 20]

## **2. Spurious Response Performance**

Spectral purity is an area where both DDS and DRFM face the most significant performance limitation. The generation of spurs is common to both techniques, as we have already discussed in great detail.

Spurs are generated in the DDS mainly due to the accuracy of both the ROM and the DAC. The ROM acts as a phase-to-amplitude converter, where the conversion process maps a sequence of instantaneous binary phase values provided by the phase accumulator through corresponding phase values into the quantized amplitude time samples of the generated waveform [Ref. 21]. A ROM, which has instantaneous amplitude values that deviate from the ideal, results in periodic distortion and spurs; the deviations are inevitable, but an increase in the number of ROM bits will cause a decrease in the error and reduce the amplitude of the quantization spurs. Basically, the size, speed, accuracy, and configuration of the

phase-to-amplitude converter (the ROM) influence the DDS performance in terms of spurs, total harmonic distortion, and bandwidth.

The DAC is the performance bottleneck of the DDS [Ref. 21]. The DAC is a considerable contributor of spurious responses due to the non-linearities which are inherent in any D/A converter design. These non-linearities result in degradation of the ideal instantaneous sine amplitude, and produce error signals at every sample the DDS takes. As mentioned, in addition to quantization errors and high-frequency spurs associated with the DAC, we also incur some dynamic problems due to settling time, glitch energy, and jitter.

The DDS spur problem is mitigated by the fact that spurs are located at specific frequencies and can be mathematically predicted. Prediction requires a careful analysis of the associated error function in both time and frequency domains. Quantizing error spurs produced by the ROM and the DAC fall under two categories: 1) those produced when the DDS output frequency is an integer ratio of the clock, and 2) those produced when the DDS output frequency is a non-integer ratio of the clock. In the first category, the sine waveform is sampled at the same point cycle after cycle; consequently, quantization error voltages occur at a constant high frequency periodic rate and, hence, the energy will be concentrated in only a few discrete (identifiable) spurious signals. In the second category, the sampling process occurs at low periodic rates and, consequently, the error period will be very long, producing very closely spaced discrete spurs (not altogether identifiable).

The DRFM is prone to spurious responses on two levels; spurs caused by quantization, as with the DDS, and spurs due to intermodulation. Quantization-generated spurs are the same digitization processes as with the DDS, except in this case the prime generator is not a DAC, but an ADC. The effects are equally significant. Accuracy of sampling degrades as the sampling rate increases, and the

coarseness of quantization increases as the time available for each A/D conversion decreases. In this context, we can make a few generalizations regarding conversion -- whether digital to analog, or vice versa: 1) conversion processes are bottlenecks in both cases, and 2) differential non-linearity results in quantization error, and subsequent production of high frequency spurs, in both cases.

DRFM spurs due to intermodulation effects represent a unique challenge. As we discussed and experimentally examined (Figures 4.5 to 4.9), these spurs -- generated as harmonic responses of signals stored in the RAM -- increase exponentially with the number of signals added. This is a significant disadvantage for the DRFM; we have discussed two corrective actions which are in current development: GaAs technology and Superconducting DRFMs.

In general, we can compare the degree to which spurs are generated in both DDS and DRFM techniques. Quantization effects are incurred in either the DAC or the ADC, and can be mitigated in part due to the fact that they are generally predictable. We can infer, however, that in this particular area, the technique that is *less* disadvantaged is the DDS. This is because the DRFM spur problem is compounded by the fact that intermodulations occur in addition to the general quantization effects, and the only foreseeable solutions are reliant upon developing solid state technology. We caveat this by noting that this technology promises increase the quantization bit level significantly, and as our experimentation showed, a 4-bit DRFM with multiple signals stored in it will potentially be very effective.

### **3. Synthesis Versus Memory**

Duplication of a threat radar waveform to produce a jamming waveform represents the most interesting challenge of all the considerations in this thesis. In both the DDS and the DRFM, we shall use pulse compression is used to generate the jamming waveform, but at this point serious contrasts begin to surface, depending on

the radar system we are targeting. In this respect, the victim radar will make the decision for us (figuratively) regarding the form of DEA to use.

Coherence is the first and most obvious contrast that surfaces. As we have determined, coherence pertains to a radar's treatment of phase; with fully coherent radars, the phase of the illumination signal is derived from stable internal sources and is constant and predictable. A coherent system "knows" the phase of each illumination pulse prior to transmission, and can compare the phase of any returning signal. Also, coherence allows the radar to provide large processing gains against interfering noise-like signals, such as non-coherent jamming waveforms. The effect of this increased processing gain (as determined by the pulse compression factor) is the dilution of the effective jamming power with respect to the available target power. We note, then, that both the DDS and the DRFM can produce the same processing gain if they are tuned to the radar carrier frequency. The contrast that results concerns frequency set-on; basically, coherence (with respect to frequency set-on) is better with the DRFM.

There are two implications resulting from the lack of coherence of the DDS. The most important implication is the that in order to be effective as a DEA, particularly since frequency set-on tends to be a disadvantage, the DDS must maintain a very accurate, constantly updated threat library -- that is, an accurate database of threat radar parameters. The second implication concerns intra-pulse processing gain. DDS jamming waveforms are quasi-coherent (coherent over the intra-pulse processing period), and consequently, this kind of jamming has the effect of mitigating the intra-pulse processing gain advantage of the radar, even though the jammer is forced to spread its energy over a wider frequency range in order to jam the radar [ Ref. 2].

The next contrast is also in relation to coherence, but refers more directly to the claim that we made earlier that the victim radar might make the decision for us

regarding the type of DEA to employ; this claim regards the type of phase coded waveform -- biphasic versus quadriphase. Specifically, the DEA chosen must be able to adapt to the waveform generated by the radar. Earlier 3D surveillance radars such as the TPS-43 use a biphasic (Barker) coded waveform. This is a predictable and relatively easily synthesized waveform; that is, a rectangular pulse with a rectangular amplitude spectrum. We analyzed the mismatches we can expect to encounter, based upon our ability to account for Doppler shifting in our synthesized waveform. These mismatches are determined via the autocorrelation function, which represents a pulse compressed waveform after being passed through a matched filter. In general, we observed that both biphasic and quadriphase coded waveforms are equally tolerant to frequency mismatches.

But the TPS-70 no longer uses a biphasic-coded waveform! The introduction of the quadriphase coded waveform favors the DRFM. Quadriphase codes with half-cosine shaped subpulses significantly outperform phase codes which use rectangular subpulses in a number of critical areas. We begin with the subpulse geometry. Quadriphase codes produce subpulses with a half-cosine shape; the complex coded pulse produced is extremely difficult to duplicate without an extremely comprehensive database of threat radar parameters. For practical purposes, the amount of information required to jam this radar system using DDS makes this a difficult application. A memory which can store coherent signals may be a better way of generating the complex half-cosine waveform, particularly in a fast moving, dense jamming environment.

In summary, factors such as frequency set-on and the type of radar waveform employed will determine what kind of jamming we must perform. We can infer, for conventional radars which are not relatively sophisticated or which use biphasic coded pulses (i.e., the TPS-43), the DDS is the best option; it may be less costly and produce

the desired effect for minimal effort. The challenge lies in the fact that a quadriphase coded half-cosine subpulse places demands on a DEA that require great precision in terms of threat parameters, and a memory may be more attractive in this case.

#### **4. DEAs Versus Sidelobe EPs**

Both the DDS and the DRFM (ideal) can be equally effective in injecting smart noise against sidelobe outputs, particularly for conventional radars such as the TPS-43. Radar systems employing ULSAs and CSLCs pose a more interesting problem. The TPS-70 employs a state-of-the-art ULSA. Its principal application is to sense the presence of active EA within the radar band. As mentioned, this antenna system is part of the JATS function of the radar signal processor.

On the average, ULSAs have sidelobe levels on the order of -20 dBi (which implies that only one percent of the radiated power is within the sidelobes). State-of-the-art technology allows the TPS-70 to achieve azimuth sidelobe levels of better than 45 dB down. The CSLC has also proven effective against sidelobe jamming; currently, CSLCs can reduce sidelobe noise jamming by 20 to 30 dB [Ref. 5].

In general, control of sidelobe jamming using either the ULSA or the CSLC, will be moderately effective, but will not completely protect a surveillance radar against sidelobe jamming. The DDS and DRFM smart noise jammers have been specifically designed with devices such as the ULSA and the CSLC in mind. It is fair, then, to conclude that employing either the ULSA or the CSLC as stand-alone sidelobe EPs favors the DEA (DDS or DRFM). However, employment of the ULSA and the CSLC in combination swings the advantage back to the radar in effectively suppressing jamming effects.

#### **5. Systems Engineering Considerations**

Jamming assets, regardless of how advanced the design technology is, may not be able to jam all the target threat transmissions. DDS and DRFM smart noise

jamming techniques have been designed to allow for discriminate, precise jamming so as to effect enemy command and control to the maximum possible extent. More importantly, shrinking military budgets have resulted in many support jammer upgrade programs being canceled. The bottomline is that having technology for technology's sake is no longer acceptable. Systems engineering factors such as cost, complexity, and power management of EW hardware all have to be factored into the proverbial equation.

Systems engineering factors play a large role in the current plans regarding the installation of DEA technology in Army attack helicopters. The first consideration is cost; to the credit of both the DDS and the DRFM, both are considered low cost technologies, especially with the incorporation of digital technology. Analog-based systems tend to be very hardware intensive, using dedicated hardware solutions to jamming requirements. Though not expensive on the surface, analog techniques offer less capability for the amount of hardware involved, and in the long run tend not to be as cost effective as digital technology. Another key factor is that both DDS and DRFM technology has become available commercially-off-the-shelf (COTS).

Complexity depends upon the degree of performance we expect to attain. Currently, the DDS architecture is less complex than the DRFM architecture; but, as we observed, the level of complexity of modern radar systems is pressing DDS designers to demand more of their systems in terms of precision. The DRFM may be generally more complex, but in relative terms, complexity is balanced out by performance. Specifically, the DRFM is better suited to handle complex radar systems in terms of the waveforms they generate.

Finally, the area of power management represents both an advantage and a disadvantage for both DEA techniques. The advantage lies in the fact that as smart noise jammers, each can operate at a duty cycle which is consistent with that of the

victim radar, rather than the 100 percent duty factor associated with the noise jammer; this results in a significant reduction in average power which it must *generate*. The disadvantage, however, lies in the fact that both techniques exhibit relatively high power *consumption*, largely due to the power generation in the spurs. Overall, neither technique can be considered very power efficient.

#### **D. SUMMARY**

In this chapter, we performed a comparative analysis, not just of the DDS versus the DRFM, but also of how current technology has developed over the years since the 1970s. As modern radars have increased in sophistication and capability, demands on EAs to combat these systems have also increased. This problem is compounded by the fact that advanced technology is being exported globally, and poses a very serious potential threat. The focus of our analysis was on comparisons and contrasts between the DDS and the DRFM; we examined the following areas: 1) the importance of using digitally-based technology, 2) spurious output performance, 3) waveform synthesis versus memory, 4) potential for effective sidelobe jamming, and 5) systems engineering considerations. Ultimately, the mission and the threat will dictate which DEA should be applied.



## VI. CONCLUSION

As the threat changes, so changes the mission. In this thesis, we presented a comparative analysis of the effectiveness of "smart noise" jamming waveforms as generated by two different digital techniques: Direct Digital Synthesis and Digital Radio Frequency Memory. The premise for performing such analysis is founded upon the changing threat, shrinking budgets, and how the Department of Defense might conform the stand-off jamming mission in order to support the Commander's priority requirements.

The current stand-off jamming challenge is defined in terms of advancements in modern radar system technology. The rapid development in design features such as digital signal processing, pulse compression, and the generation of complex phase-coded waveforms has led to a reconsideration of how we accomplish the stand-off jamming mission; Northrop Grumman's AN/TPS-70 3D surveillance radar stands as a paradigm of what EA designers must contend with in the near future. In a world of custom-designed radar systems, it stands to reason that a jammer that produces custom-designed waveforms must be developed to respond in kind.

We examined in detail the methods of generating custom-designed jamming waveforms. DDS was introduced, both in theory and actual technique, with a concentration on the type of phase coding required in waveform synthesis, and the associated problems. We then introduced the DRFM in both theory and technique, with a concentration on its associated problems. In essence, both techniques represent viable DEAs, and our analysis described advantages and disadvantages associated with each.

Upon weighing one technique against the other, comparison revealed one important advantage that the techniques have in common -- namely, the use of

digitally-based technology. In this respect, each technique fares well, especially in light of vast improvements in speed and fidelity that are attainable, in contrast to analog techniques.

Two important areas stand out to give EA designers, program managers, and, indeed, commanders considerable reason for thought. In the area of spurious response output, the advantage appears to be with the DDS; the primary source for error for DDS is frequency mismatch, while the DRFM produces spurs due to quantization error and intermodulation (which increase geometrically with storage of multiple signals). In the area of coherence, the advantage swings to the DRFM, which produces coherent jamming waveforms, in contrast to the DDS which is quasi-coherent; modern radar systems are being designed to be very discriminating of any interference, especially jamming.

The DDS and DRFM are both equally viable as stand-off DEAs. However, the threat should dictate whether we employ the DDS, the DRFM, or neither! We submit, conventional search radars, such as the AN/TPS-43, will require less complicated applications, and hence, the DDS is better. But with systems which use complex coded waveforms and Gaussian filters the DRFM is a very attractive option.

## APPENDIX A. PCMISS PROGRAM

```
%Pulse Compression Mismatch
%Program called pcmiss.m
clear
%Enter Barker Code
xx=[1 1 1 1 1 -1 -1 1 1 -1 1 -1 1];
%Form input signal
r= input('fd/bw=');
dp=2*pi*r;
for n=1:13;
    y(n)=xx(n)*exp(j*n*dp);
end;
%Form cross correlation
yy=conv(y,xx);
z=abs(yy);
%plot cross correlation
t=1:25;
plot (t,z),grid
title('Figure 3.7 Biphas Coded PC, fd/BW=0.0');
xlabel('Time');
ylabel('Amplitude');
['Magnitude=', num2str(z(13))]
z(13)=0;
m=max(z);
['Peak Sidelobe=',num2str(m)]
end
```



## APPENDIX B. QUADRIPHASE PROGRAM

```
% Program called quadriphase.m

% COMPUTE OVERSAMPLE RATE
rg=0.5;
osamp=4;
samp=rg/osamp;

% ENTER BARKER BIPHASE CODE (13)
xx=[1 1 1 1 1 -1 -1 1 1 -1 1 -1 1];

% CONVERSION TO QUADRIPHASE
quad=xx.*(j.^(1:length(xx)-1));

% DESIGN GAUSSIAN FILTER
gaussf=exp(-(2*pi*2.*[-(6*rg):samp:(6*rg)]).^2/11.09);

% OVERSAMPLE OUTPUT
quosamp=reshape([1 zeros(1,osamp-1)]*quad,1,length(quad)*osamp);

% HALF-COSINE SUBPULSE MODULATION
subpulse=cos(pi*[-.5:.5/(osamp):.5]);

% TRANSMIT PULSE
tpulse=conv(quosamp,subpulse);
```

```

% PLOT TRANSMIT PULSE SIGNAL
txmit=samp*(1:length(tpulse));
axis([min(txmit) max(txmit) -1 4.0])
plot(txmit,real(tpulse),'w'),hold on
plot(txmit,imag(tpulse),'--')
plot(txmit,abs(tpulse)+2,'w'),grid,hold off
xlabel('Time - usec')
ylabel('Amplitude')
text(txmit(length(txmit)/2),3,'Signal Envelope')
index=find(max(real(tpulse))==real(tpulse));
text(txmit(index(1)),real(tpulse(index(1))),'Real Part')
index=find(min(imag(tpulse))==imag(tpulse));
text(txmit(index(1)),imag(tpulse(index(1))),'Imag Part')
title('Figure 3.6 Uncompressed Transmit Pulse Signal Modulation')
pause

```

```

% DECODER PROCESSING
decquad=quad(length(quad):-1:1);decquad=conj(decquad);
decquad=(quad(length(quad):-1:1));

```

```

% DECODER OVERSAMPLE OUTPUT
odex=zeros(osamp,length(quad));
odex(1,1:length(quad))=decquad;
qdox = odex(:)';

```

```

% PASS UNCOMPRESSED TRANSMIT PULSE THROUGH GAUSSIAN FILTER
gausup = conv(tpulse,gaussf);

```

```
% PASS FILTERED PULSE THROUGH PULSE COMPRESSOR
```

```
decup=conv(gausup, qdox);
```

```
% SCALE COMPRESSED PULSE
```

```
[scale, rngind]=max(abs(decup));
```

```
t=samp*(1:length(decup))-samp*rngind;
```

```
% PLOT OF COMPRESSED PULSE RESPONSE
```

```
axis([t(1) t(length(t)) -30 0 ])
```

```
plot(t,(abs(decup/scale)+1e-15),'w');grid
```

```
xlabel('Time - usec')
```

```
ylabel('Relative Amplitude')
```

```
title('Figure 3.20 Compressed Pulse Response')
```

```
end
```



## APPENDIX C. DRFMBITS PROGRAM

```
% Program Plots Output Spectrum of DRFM
```

```
% Program called drfmbits.m
```

```
clear;
```

```
% Sample Input Signal
```

```
N = input('Samples=');
```

```
t = (1:N)/N;fs=100;
```

```
j = sqrt(-1);
```

```
% Generate input signals
```

```
z = exp(j*2*pi*fs*t);
```

```
num = input('Number of Input Signals=');
```

```
for k=1:num-1;
```

```
    zz=exp(j*2*pi*fs*(1+.2*k)*t);
```

```
    z = z+zz;
```

```
end;
```

```
B = input('Quantizing Bits=');
```

```
M = 2^(B-1);
```

```
% Quantize Input Signal
```

```
for i=1:N;
```

```
    xx(i)=(M*real(z(i)))/num;
```

```
    yy(i)=(M*imag(z(i)))/num;
```

```
    if xx(i)>0;x(i)=ceil(xx(i))/M;
```

```

        else x(i)=floor(xx(i))/M;end;
    if yy(i)>0;y(i)=ceil(yy(i))/M;
        else y(i)=floor(yy(i))/M;end;
end;
w = x+j*y;

% Find Spectrum
X = fft(w,N);
X = fftshift(X);
Pxx = X.*conj(X);
Pxx = Pxx/max(Pxx);
Pz = 10*log10(Pxx+1e-6);
f = (-N/2:N/2-1);
plot(f,Pz);
title(['FIGURE 4.8b  DRFM FREQUENCY SPECTRUM']);
xlabel('Frequency - Hz');
ylabel('Amplitude - dB');grid;
%text(.4, .80,['SAMPLES=',num2str(N)],'sc');
text(.1,.75,['SIGNAL BITS=',num2str(B)],'sc'),pause
zy=sort(Pxx);
pwr=sum(Pxx);
for kk=N+1-num:N;sy(kk)=zy(kk);
zy(kk)=0;end;
spur=sum(zy);
sig=pwr-spur;
snr=sig/spur;

```

```

loss=-10*log10(sig/pwr);
fprintf('snr= %f \n',snr)
fprintf('spur= %f \n',spur)
fprintf('sig= %f \n',sig)
fprintf('loss= %f db\n',loss)
sy(N+1-num:N)
for jj=1:num;
    ww(jj)=Pxx(613+20*(jj-1));
end;
siga=sum(ww);lossa=-10*log10(siga/pwr);
spura=pwr-siga;snra=(siga/spura);
fprintf('lossa= %f db\n',lossa)
fprintf('spura= %f \n',spura)
fprintf('siga= %f \n',siga)
fprintf('snra= %f \n',snra)
%ppplot
end

```



## LIST OF REFERENCES

1. Army Field Manual 34-10, Division intelligence and *Electronic Warfare Operations*, November 1986.
2. Schleher, D.C. and Pace, P.E., "Support Jamming Effectiveness: Comparison of Direct Digital Synthesis and RF Memory Exciter Techniques", Joint Electronic Warfare Conference, Naval Postgraduate School, Monterey, CA, May 1996.
3. Edde, Byron, RADAR, Englewood Cliffs, NJ, Prentice Hall, Inc., 1993.
4. Barton, David K., "Principles of Pulse Compression", Pulse Compression, Vol. 3, pp. 109-116, April 1961.
5. Schleher, D.C., Introduction to Electronic Warfare, Norwood, MA, Artech House, Inc., 1986.
6. Hoisington, D.B., Electronic Warfare, Naval Postgraduate School, Monterey, CA, 1995.
7. "AN/TPS-70 System Description", Information Release, Northrop Grumman Corporation, Baltimore, MD, 1996.
8. Widrow, B., "Adaptive Noise Canceling: Principles and Applications", Proc. IEEE, Vol. 69, pp. 1692-1719, December 1975.
9. Lewis, Bernard L., Kretschmer, Frank K., Schelton, Wesley W., Aspects of Radar Signal Processing, Norwood, MA, Artech House, Inc., 1986.
10. Proakis, John G., and Manolakis, Dimitris G., Digital Signal Processing, New York, NY, Macmillan Publishing Company, 1992.
11. Taylor, J.W., Jr., and Blinchikoff, Herman J., "Quadriphase Code - A Radar Pulse Compression Signal With Unique Characteristics", IEEE Transactions on Aerospace and Electronic Systems, Vol. 24, pp. 156- 70, March 1988.

12. "Digital RF Memories", Journal of Electronic Defense Supplement, pp. 19-20, January 1994.
13. Roome, S.J., "Digital Radio Frequency Memory", Electronics & Communication Engineering Journal, pp. 147-153, August 1990.
14. Schneider, W.J., "Digital Countermeasures Measures: New Techniques Possible", ICH, pp. 367-373, 1986.
15. Eaves, Jerry L., and Reedy, Edward K., Principles of Modern Radar, New York, NY, Van Nostrand Reinhold, 1987.
16. Pring, PCJ, James, G.E., Hayes,D., "The Phase Performance of Digital Radio Frequency Memories", IEEE Conference Publication No.393, pp. 18-23, 1994.
17. Kerins, William, "Spur Levels In Multiple-Bit DRFMs", Journal of Electronic Defense, pp. 49-54, January 1991.
18. White, William A., Taddiken, Albert H., Shichijo, Hisashi, Vernon, Michael A., and Whitmire, David A., "Design and Application of a GaAs Digital RF Memory Chip", "IEEE Journal of Solid-State Circuits", Vol. 25, No.4, pp. 961-969, August 1990.
19. Lao, Binneg Y., and Zeiger, Kenneth, Superconducting Digital RF Memory, Business Innovation Report, Sierra Monolithics, February 1994.
20. Lauria, Vincent, "Direct Digital Synthesizers In Modern Electronic Warfare Systems", Topics in Engineering, Vol. 3, pp. 2-49 - 2-63, 1990.
21. Noel, P.P., and Kwasniewski, T.A., Frequency Synthesis: A Comparison of Techniques, Carleton University, Ottawa, Ontario, pp. 535-537, 1991.
22. Jane's: Radar and Electronic Warfare Systems, Alexandria, VA, Jane's Information Group Ltd., 1996.
23. Smith, Ralph J., Circuits Devices and Systems, New York, NY, John Wiley and Sons, Inc., 1984.

## INITIAL DISTRIBUTION LIST

1. Defense Technical Information Center ..... 2  
8725 John J. Kingman Road, Suite 0944  
Fort Belvoir, VA 22060-6218
2. Dudley Knox Library ..... 2  
Naval Postgraduate School  
411 Dyer Road  
Monterey, CA 93943-5101
3. Prof. Phillip E. Pace (Code EC/Pc) ..... 3  
Naval Postgraduate School  
Monterey, CA 93943-5100
4. Prof. D. Curtis Schleher (Code IW/Sc) ..... 1  
Naval Postgraduate School  
Monterey, CA 93943-5100
5. Charles J. Watson ..... 2  
c/o Louise D. Watson  
645 Main St., Apt. 1113  
Bethlehem, PA 18018



DUDLEY KNOX LIBRARY  
NAVAL POSTGRADUATE SCHOOL  
MONTEREY CA 93943-5101

DUDLEY KNOX LIBRARY



3 2768 00327395 4